Eddy transport, wave-mean flow interaction, and Eddy forcing during the 2013 Uttarakhand extreme event in the reanalysis and S2S retrospective forecast data

Article

Accepted Version

International Journal of Climatology

RMetS Royal Meteorological Society

Eddy transport, Wave-mean flow interaction, and Eddy forcing during the 2013 Uttarakhand Extreme Event in the Reanalysis and S2S Retrospective Forecast Data

Journal:	*International Journal of Climatology*
Manuscript ID	JOC-21-0894.R1
Wiley - Manuscript type:	Research Article
Date Submitted by the Author:	14-Mar-2022
Complete List of Authors:	Kalshetti, Mahesh; Indian Institute of Tropical Meteorology, Extended Range Prediction Chattopadhyay, Rajib; Indian Institute of Tropical Meteorology, Extended Range Prediction Hunt, Kieran ; University of Reading, Meteorology Phani, M. K.; Indian Institute of Tropical Meteorology, Pune, Seasonal Prediction Joseph, Susmitha; Indian Institute of Tropical Meteorology, Extended Range Prediction Pattanaik, Dushmanta; India Meteorological Department, Numerical Weather Prediction Division Sahai, A. K.; Indian Institute of Tropical Meteorology, Extended Range Prediction
Keywords:	Dynamic/Processes < 1. Tools and methods, Forecasting (methods) < 1. Tools and methods, Climate < 2. Scale, Synoptic < 2. Scale, Rainfall < 3. Physical phenomenon, Severe weather < 3. Physical phenomenon, Atmosphere < 4. Geophysical sphere, Monsson < 5. Geographic/climatic zone
Country Keywords:	India

Eddy transport, Wave-mean flow interaction, and Eddy forcing during the 2013 Uttarakhand Extreme Event in the Reanalysis and S2S Retrospective Forecast Data

Mahesh Kalshetti[1,3], Rajib Chattopadhyay[1,2], Kieran M R Hunt[4], R Phani[1], Susmitha Joseph[1], DR Pattanaik[2], AK Sahai[1]

1. Indian Institute of Tropical Meteorology, Pune-411008, India
2. India Meteorological Department, India
3. Savitribai Phule Pune University, Pune-411007
4. Department of Meteorology, University of Reading, UK

Corresponding Author

Rajib Chattopadhyay
India Meteorological Department, Pune 411005, India
Email: rajib@tropmet.res.in

Keywords

Extreme events; Extratropical-Tropical teleconnection; Indian monsoon, subseasonal forecasts

Abstract

In this study, to explore the wave-mean interaction during the monsoon season, we investigate (a) the potential role of transient eddy forcing and the wave-mean interaction on the monsoon weather during the June 2013 heavy rainfall event over the Himalayan regions (especially the Uttarakhand State of India and the nearby regions) and, (b) how they are captured in a set of operational models. Some studies have pointed out how prolonged breaks can occur due to extratropical trough incursions. However, there is a lack of clarity on how transient eddy forcing associated with such interactions can lead to modulation of monsoonal circulation or whether such interaction can lead to heavy rainfall events.

E-vector fields are analyzed to quantify the eddy forcing from extratropical transient eddies and the feedback mechanism between transient eddies and the mean flow during June 2013. Analysis reveals that along with local factors (orography, moisture convergence), the large-scale heavy rainfall event over the Uttarakhand region during 16-17 June 2013 was influenced by eddy forcing due to the intrusion of extratropical Rossby waves over the Indian region. The location of eddy affects the location of regional occurrence of the eddy-mean interaction. Model hindcast analysis results suggest that operational models cannot forecast the upper-level eddy forced circulation patterns, and the improper representation of the E-vector divergence field leads to the underestimation of intensity and the spatial pattern of rainfall.

1. *Introduction*

It is well known that extratropical-tropical (E2T) interaction can cause prolonged *breaks* (low rainfall spells) over the Indian region due to intrusion of extratropical troughs and ridges during the monsoon season (Ramaswamy, 1962; Raman and Rao, 1981; Krishnan *et al.*, 2009; Fadnavis and Chattopadhyay, 2017). However, in recent years, studies have shown that high-intensity rainfall events over the Himalayan region are sometimes associated with the coexistence of low-frequency monsoon intraseasonal oscillations and extratropical eddies (or Rossby waves or Western Disturbances). The eddy transport and fluctuations are evident through the associated heat and momentum transport towards or out of the tropics during the summer monsoon, as shown in Kalshetti et al. (2021). Disturbances originating in the extratropics can locally shift the jet stream equatorward and thus disturb the synoptic setup of the Indian summer monsoon. These intrusions are supposedly linked to high-intensity rainfall events like the 2010 Pakistan and 2013 Uttarakhand floods (Hong *et al.*, 2011; Lau and Kim, 2011; Joseph *et al.*, 2015; Vellore *et al.*, 2016a; Sooraj *et al.*, 2020) and many similar weather events.

How does the extratropical wave intrusion create high-intensity rainfall over Northern India, especially over the Himalayan region? The high-intensity rainfall event can be dynamically defined as zones of strong vertical velocities with ample moisture supply from

the boundary layer or lower troposphere (such as during monsoon time), which is likely due to strong ageostrophic components (Bohlinger *et al.*, 2019). Can a Rossby wave intrusion cause this high-intensity rainfall or other types of extreme events, e.g., heatwaves? Classic numerical experiments such as from Hoskins and Karoly (1981) and some recent case studies based on Eurasian blocking suggests that the 2010 western Russian heatwave was forced by downstream Rossby wave propagation (Trenberth and Fasullo, 2012), with high-frequency Rossby waves also propagated southward during the end of July (Lau and Kim, 2011). Thus, Rossby waves are often a precursor of extreme heatwave events. Similarly, the leading trough of the Rossby wave train triggered upward motion to the east, favoring deep convection leading to extreme rainfall event-related flooding over Pakistan during 2010 (Hong *et al.*, 2011; Lau and Kim, 2011). Likewise, extratropical Rossby wave-linked convection is also reported in the tropical Pacific (Kiladis, 1998). Heavy rainfall, especially extreme events, is associated with mesoscale convective systems. Several studies on midlatitude convection showed that midlatitude Rossby waves are reinforced by mesoscale systems (Lillo and Parsons, 2017; Parsons *et al.*, 2019), which create downstream forced response. Some studies have also shown how mesoscale convective systems over the Pacific warm pool region get reinforced by Rossby-kelvin waves(Houze *et al.*, 2000), indicating the role of large-scale waves in local mesoscale precipitating systems. In addition to waves, studies have also identified thermal forcing and background moist processes over the arid

region of Indo-Pakistan in the 16 to18 days prior and have shown them to be precursors for extreme rainfall events over the monsoon core zone (Sooraj *et al.*, 2020).

As mentioned in the last paragraph, the state of Uttarakhand in India witnessed heavy rainfall during 15-17 June 2013 with widespread reporting of a "cloudburst"-like scenario over the Kedarnath region in Uttarakhand. Some studies have demonstrated the role of mesoscale convective systems in cloudburst situations(Parida *et al.*, 2017). Other studies suggest high-intensity rainfall events such as those that occurred over the Uttarakhand region during June 2013 result from an occluded frontal system that developed in response to a western disturbance and monsoon low (Chevuturi and Dimri, 2016). The validity of the frontal theory of ageostrophic uplift requires the validity (i.e., finiteness) of the ratio NH/f ($\boldsymbol{N}$ is Brunt-Väisälä frequency, $\boldsymbol{f}$ is the Coriolis parameter, and $\boldsymbol{H}$ is the depth of the fluid) as described in Hoskins (1982). In the tropics, the validity of this ratio is not well defined due to the smallness of f. Also, as (Charney 1969) suggested, such large-scale lifting in the stably stratified tropical climate is not easily (or generally) possible due to lack of vertical coupling unless it occurs in the regions of active tropical deep cumulus convection.

In addition to such localized extreme events during 16-17 June, heavy to very heavy rainfall occurred during this time over larger regions (in the synoptic scale, e.g., refer fig.2 of Joseph et al., (2015) or **Fig.12**). The coexistence of synoptic-scale heavy rainfall and Rossby wave intrusion may indicate that the transient eddies may be a dominant factor in comparison

98 with other factors like local destabilization due to latent heating, which is already reported
99 (e.g., Fig. 9b of (Wills and Schneider, 2018).

100 This eddy (i.e., transient synoptic disturbance) perspective has also been explored in
101 several studies. Vellore et al. (2016b) and Hunt et al. (2018a, 2018b), using cluster composite
102 analysis, looked into several extratropical intrusions of western disturbances in a detailed
103 manner and described the presence of monsoon low-pressure systems and western
104 disturbance as a necessary condition for heavy events. Another recent study (Hunt *et al.*,
105 2021) explained the extreme events in terms of the coexistence of monsoon low-pressure
106 systems and western disturbances. They found that high-intensity precipitation occurs as a
107 result of their interactions, but their analysis uses the perspective of Hanley et al. (2001),
108 which assumes the pre-existence of an intense cyclonic storm (with substantial azimuthal
109 eddy flux transfer, EFCs which is a measure of local eddy forcing) co-located with the jet
110 stream and that this storm interacts with the upper-level troughs when the eddy-induced
111 azimuthal flux transfer measured by EFCs cross certain thresholds and provide necessary
112 eddy forcing. This EFC-based criterion is, however, not quantitatively verified in these
113 studies.

114 The studies described above indicate that the orography, monsoonal moisture flow,
115 stability, and waves/eddies can contribute to the extreme as well as heavy rainfall event, but
116 do not go into explaining this monsoon midlatitude eddy interaction scenario as an eddy

forcing problem on the mean flow (i.e., eddy-mean interaction perspective), and hence, though the earlier analysis highlights exchanges, they neglect a transient wave forcing perspective (e.g., refer eq. 1 in sec.3). In the current analysis, we will focus on how (or whether) wave-mean interaction can be used to explain ageostrophic vertical velocities and rainfall that occurs during such events. Such interactions perspective are often useful to study the mid-latitude low-frequency oscillations (Jin, 2010).

Models fail to predict the rainfall pattern and amplitude over Uttarakhand with sufficient lead-time **Fig.1** shows that several operational dynamical models lack skill in predicting the rainfall event over Uttarakhand even at a one-week lead-time. Several models have these problems with events related to Rossby waves (e.g., forecast bursts as referred in (Lillo and Parsons, 2017). In addition to understanding the eddy-mean interaction during the intrusion, the eddy forcing approach can be useful if we want to know why the dynamical models fail to forecast such events at sufficient lead times for issuing alerts, especially in the weather to the extended-range forecast time scale. We hypothesize that the eddy-mean interaction perspective can be helpful in understanding the skill (or lack of it) in dynamical models.

The Uttarakhand extreme event of 2013 and the high-intensity rainfall over large regions has been studied by many researchers and is a well-known event in which tropical-extratropical interaction is well documented (Dube *et al.*, 2014; Vellore and Jayant, 2014; Joseph *et al.*, 2015; Pattanaik *et al.*, 2015; Singh and Chand, 2015; Vellore *et al.*, 2016a; Kaur and Gupta, 2017). Hence, owing to the good documentation of linear perspective, the

current paper selects this event and discusses the eddy-mean interaction perspective. We elaborate on two aspects: (a) whether wave-mean interaction was significant during this event in addition to the earlier linear theories used to explore such events and (b) based on this transient eddy wave mean interaction formulation, whether such steps can be retraced or evaluated in the dynamical models to understand the lack of skill in these models when forecasting such events. The study is arranged as follows: Sec.2 describes the study area, data used, and formal methodology. In sec.3, we computed the transient eddy forcing during the extreme event using the ***E-vector*** approach (Andrews and McIntyre, 1976; Hoskins *et al.*, 1983), which explains the eddy dynamical pathway for such events near subtropical jet streams. Sec.4 describes the application of the E-vector approach while describing the life cycle of tropical-extratropical interaction while describing the intrusion event during the Uttarakhand heavy rainfall event (June 2013). Sec.5 describes the operational forecasts of the event, and the results are discussed, summarized, and concluded in Sec.6.

2. Study area, Data, and Methods

2.1. Study area

The natural disaster, in the form of landslides and flash flooding, occurred due to heavy precipitation over the Uttarakhand region (29°-31°N, 78°-81°E), India on 16-17 June 2013. Uttarakhand is part of the region of complex orography along the Western Himalayas. The Western Himalaya region surrounds snow-covered peaks, crest, glaciers, valleys, and perennial river basins (Parida *et al.*, 2017).

2.2. Observation Data

The atmospheric (retrospective) reanalysis dataset from the fifth-generation European Centre for Medium-Range Weather Forecasts (ECMWF) Atmospheric Reanalysis of the global climate (ERA5) is used as a proxy for observation of dynamical variables. ERA5 data are produced by the Copernicus Climate Change Service (C3S) at ECMWF. ERA5 climate data is available in a 0.25° × 0.25° grid from 1979 to within five days of real-time (Hersbach *et al.*, 2020). The primary data used in this study are zonal (***u***, ms^{-1}), meridional (***v***, ms^{-1}), vertical (ω Pa s^{-1}) wind, temperature (K) at 200hPa, and geopotential height (m) at 500hPa. The observed precipitation is obtained from Tropical Rainfall Measuring Mission (TRMM) Multi-satellite Precipitation Analysis (TMPA, 3B42) (Huffman *et al.*, 2007). 3B42 data contains a gridded, satellite-based merged infrared precipitation data (mm/hr), with a 3-hour temporal resolution and a 0.25-degree spatial resolution. We have converted the sub-daily data to daily data.

2.3. Models

The Indian Institute of Tropical Meteorology (IITM) extended range forecast (IITM-ERPAS) runs (Abhilash *et al.*, 2014; Sahai *et al.*, 2019), UKMO (United Kingdom Met Office), and ECMWF (European Centre for Medium-range Weather Forecasts*)* forecast runs are the S2S reforecast model runs used in this study. All the observed and model data set regridded to 1° ×1° spatial resolution and daily temporal resolution with appropriate pre-

processing. Except for IITM-ERPAS (Abhilash *et al.*, 2014), the UKMO and ECMWF forecast data were accessed through the S2S "*instantaneous and accumulated"* database maintained by ECMWF (Vitart *et al.*, 2017). ERPAS data is obtained from the IITM-IMD operational database maintained at IITM. Each S2S model has a control member (using unperturbed initial conditions) and several perturbed members produced for sampling uncertainty in the initial conditions**.** In the present study, the model forecast is taken from the closest available initial condition on 9th June 2013 for ERPAS and UKMO and for 10th June 2013 for ECMWF when the forecast of 16-17 June lies in the synoptic range. Spatial plots are shown for the ensemble mean (IITM-ERPAS-16-member mean; UKMO-7 member (including one control member); ECMWF-11 member (including one control member) unless stated otherwise.

3.0 A schematic description of the life cycle of extratropical intrusion

The extratropical eddies are associated with colder extratropical air masses and stronger westerly momentum in the upper levels than tropical monsoonal flow. The transport of this eddy momentum and heat flux over the Indian region in the presence of low-frequency monsoonal background (monsoon intraseasonal oscillations and low-pressure systems (Goswami, 2012)) can significantly impact the local flow as it imparts additional heat and momentum in the local budget terms (cf. eq. one and eq.2 in sec.3.2). The event life cycle can thus be hypothesized to have three major stages: (i) southward *digging* (or intrusion with amplification) of troughs associated with a meandering of the subtropical jet stream, (ii)

196 transient eddy forcing onto the mean flow, and (iii) reversal of jet stream (or weakening of
197 southward intrusion) position with the restoration of monsoon flow. These are described
198 below.

199 ***3.1 Linear Process: Intensification of digging trough over the Indian Region***
200 ***during the monsoon season***

201 Rossby waves show meridional propagation, but the southward intrusion of the Rossby wave
202 in the tropical region is generally restricted due to the presence of critical latitudes where the
203 phase velocity of the wave approaches the zonal (westerly) wind speed, and the waves are
204 absorbed along the critical latitudes as it propagates equatorward (Karoly and Hoskins, 1982).
205 Normally Rossby waves break, and mixing of potential vorticity (PV) occurs with the decay
206 of the wave leading to mid-latitude to tropical exchange (Homeyer and Bowman, 2013).
207 However, Rossby waves can dig deep south into the tropical region due to the ducting effect
208 or southward extension of westerlies over a certain region (Webster and Holton, 1982). The
209 southward shifting/meandering of the westerly jet stream due to the presence of the blocking
210 high can provide such ducts where Rossby waves can propagate into the tropics. At the same
211 time, cyclonic Rossby wave breaking can be prevented, and it can intensify over the Indian
212 region in the presence of monsoonal instabilities. It can be seen as follows:

213 Consider the conservation of PV in the absence of diabatic heating: $\frac{\zeta + f}{\frac{\partial p}{\partial \theta}} \approx Const$

If a cyclonic phase Rossby wave (positive vorticity) comes into a region of higher thickness ($\frac{\partial p}{\partial \theta}$) and f decreases, relative vorticity has to increase. For more detailed explanations of the PV aspects of synoptic developments, the reader refers to case studies discussed in Hoskins (1997). Thus, the cyclonic vorticity induced by the Rossby wave can intensify (or at least its amplitude does not decay) depending on the strength of the denominator, as a southward extension means a decrease in f. Typically such thickness would increase in the presence of strong heating. Hence the Rossby wave would strengthen and not break or weaken in the presence of background instability that modifies. Such increased background thickness can be provided by latent heat release associated with modes of subseasonal variability when the organized convection stays over the foothills of the Himalayas.

The intruded (or possibly intensified) Rossby wave can create a digging trough, leading to indirect ageostrophic circulation with the high vertical velocity at the jet exit region (e.g., Chapter 2.3 and Fig. 2.7 of Lackmann (2012). In addition to such direct effects, the strengthening or weakening of the westerly or the Rossby wave depends on the growth of eddy instability, which can extract energy from the mean flow (Held and Phillips, 1989). The response of the mean state due to transient eddy forcing is essential to control the growth or decay of the Rossby wave. This nonlinear process is discussed next.

3.2 Nonlinear process: the transient eddy forcing of the mean flow and Monsoon time mean background

There are numerous studies demonstrating empirical evidence of the role of the transient eddies in maintaining the time-mean flow and how eddies extract energy from the mean flow or give energy to the mean flow (Lau and Holopainen, 1984; G. Branstator, 1995; Jin, 2010; Tan *et al.*, 2014). In particular, a recent study (Wills and Schneider, 2018) showed transient eddy feedback for Rossby waves over the orographic region is more important than latent heating. The eddy mean interaction for the horizontal momentum equations, assuming zonal wind *(u)* and meridional wind *(v)* compartmentalized into mean and transient eddy components: ($\boldsymbol{\mathcal{V}} = \overline{\boldsymbol{\mathcal{V}}} + \boldsymbol{\mathcal{V}}', \boldsymbol{\mathcal{V}} = (u,v)$) (Hoskin et al. 1983; James 1994; Williams et al. 2007) is given by:

$$\frac{\overline{D}\overline{u}}{Dt} = f + \nabla.E \text{----------(1a)}$$

$$\frac{\overline{D}\overline{v}}{Dt} = -fu_{am} - (\overline{u'v'})_x \text{----------(1b)}$$

$\frac{\overline{D}}{Dt} = \overline{u}\frac{\partial}{\partial x} + \overline{v}\frac{\partial}{\partial y}$, $(\,)_x = \frac{\partial}{\partial x}$, ∇ is the horizontal gradient operator and f is the Coriolis parameter. $\boldsymbol{V_{am}} = (u_{am},v_{am})$ is the "*modified ageostrophic*" wind given by $\overline{\boldsymbol{v_{am}}} = \overline{\boldsymbol{v}} - \boldsymbol{f^{-1}k} \times \nabla(\overline{\boldsymbol{\phi}} + \overline{\boldsymbol{v'^2}})$. Refer to Appendix A of Hoskins et al. (1983) for more details.

$\boldsymbol{E}$ in the equation. (1a) is the so-called E-vector defined as:

$$\boldsymbol{E} = \left(\overline{\boldsymbol{v'^2} - \boldsymbol{u'^2}}\,,\ \overline{-\boldsymbol{u'v'}}\ \right) \text{.....(2)}$$

Where $\overline{v'^2 - u'^2}$ *= Ex, Eddy anisotropy or asymmetry,* $\overline{-u'v'}$ *= Ey, eddy momentum flux transport (EMF)*

The E-vector is a generalized form of Eliassen-Palm flux (Andrews and McIntyre, 1976) and can be used to estimate the local impact of transient eddies (Hoskins *et al.*, 1983; Trenberth, 1986; James, 1994).

The above relations suggest that the E-vector flux divergence can change zonal and meridional wind (assuming other factors like friction are negligible in the upper level), i.e., eddies can force the mean flow. Divergence of the E-vector can cause acceleration of mean flow, and convergence can decelerate the mean flow. In a monsoonal setting, if we take the terms in the LHS of Eq.1 as representing the mean monsoonal quasi-stationary background, the second term in the RHS can be interpreted as the eddy forcing term arising due to extratropical intrusions or similar low-pressure systems. Depending on the sign of the eddy convergence, the eddy can either grow (or extract energy from mean flow) or they can dissipate by supplying energy to the monsoonal mean flow (also refer to (Held and Phillips, 1989). To understand and estimate the impact of this eddy forcing during the Uttarakhand event, we will use this E-vector formalism.

The E-vector is also related to transient eddy vorticity flux convergence and divergence. It can be shown (Hoskins *et al.*, 1983) that:

$$\nabla.\overline{\boldsymbol{u}'\boldsymbol{\zeta}'} \approx \frac{\boldsymbol{d}}{\boldsymbol{dy}}(\nabla.\boldsymbol{E}) \quad \ldots\ldots\ldots\ldots\ldots\ldots\ldots\ldots(\mathbf{3})$$

Then, from Eq.1 and Eq.3, we can see that an E-vector framework provides a first-hand idea of the transient eddy forcing and zonal asymmetries imparted by the *transient* eddies (Hoskins *et al.*, 1983; Trenberth, 1986) in the momentum and the vorticity equations.

Also, plotting of E-vectors, i.e. (Ex, Ey), can give an idea about the direction and location of eddy convergence. The E-vector approach can be used to study both zonally asymmetric tropical (Leroux *et al.*, 2010) and extratropical transport patterns (Novak *et al.*, 2015). The above discussion is only based on the mechanical effects of eddies. A complete quasigeostrophic discussion including the thermal effects of eddies by defining a third component in E-vector using temperature (T) and meridional wind ($\sim\overline{v'T'}$) can also be made analogously but is beyond the scope of our study.

3.3 *Extratropical intrusion and heavy rainfall events*

The next question is, how are the extratropical intrusions or the eddy forcing are linked to the high-intensity rainfall events? We can have two possibilities based on the above two sections (3.1 and 3.2). First, a convergence of eddy flux can be interpreted as a positive, i.e., cyclonic curl directly introduced in the mean flow (eq.12 and 13 of Williams et al., (2007). In a monsoon environment, this can invigorate the existing monsoonal convergence directly over a region where the curl is created (such as when a monsoon trough exists over the foothills of the Himalayas). The second possibility is through an ageostrophic secondary circulation mechanism. The generation of cyclonic (anticyclonic) vorticity in the lower troposphere (transverse circulation dynamics) is associated with the formation of surface lows and indirect circulation (e.g., Fig.2 of Hoskins 1982). Such circulation will lead to the generation of ageostrophic vertical velocity, and depending on local factors (like orography

and moisture), dramatic intensification can occur over the elevated topographies (Uccellini and Johnson, 1979; Vellore *et al.*, 2016a; Hunt *et al.*, 2021), leading to extreme precipitation, as a result of a jet streak excitation as shown by Hunt *et al.*, (2021). This ageostrophic motion associated with the indirect circulation can extract kinetic energy from the mean flow in the downstream region of the jet exit, where it is super-geostrophic (Lau, 1979). Extreme precipitation can result from strong ageostrophic vertical upward motion restoring static stability. Based on Orlansky and Sheldon (1995), the quasigeostrophic omega equation can be written as:

$$f_0{}^2\frac{\partial}{\partial z}\left(\frac{1}{\rho}\frac{\partial}{\partial z}\rho w\right) + N^2\nabla^2 w = s_g + s' \text{----------(4)}$$

Where w is the vertical velocity, ρ is the density, f_0 is the Coriolis parameter, N^2 is the Brunt-Vaisalla frequency and s' is the source term involving friction, diabatic heating, and meridional gradient of Coriolis parameter. s_g is the source term involving geostrophic quantities (denoted by $\boldsymbol{g}$ indicated in the suffix), which Sutcliffe approximated as:

$$s_g = 2|\mathrm{f}\,\partial \boldsymbol{V}_g/\partial \mathrm{z}|\frac{\partial \zeta_g}{\partial l}\text{ ,---------(5)}$$

where $\boldsymbol{l}$ is a unit coordinate aligned along the thermal wind direction and v_g is the geostrophic wind. From Eq (4), (5), (3), and (1), it is clear that ζ_g as well as $\partial \boldsymbol{V}_g/\partial \mathrm{z}$ can be forced/modulated by eddy forcing through the generation of vertical velocities. $\nabla.\boldsymbol{E}$ forces the zonal mean wind, which then changes the vertical shear, subsequently changing the source term s_g. A

large increase in vertical shear due to E-vector divergence would then lead to a proportional increase in vertical velocity. Under the right conditions (e.g., moisture supply), increased vertical velocity can result in an increase in rainfall. The jet will move back to the original position after the Rossby wave has propagated out (or dissipated). The cloud-free conditions restore the horizontal meridional (north-south) gradients of temperature, forcing the jet to move back to its normal position. The mechanisms explained in this section are summarized in **Fig.2**. The theoretical mechanism proposed here can be verified by diagnosing the direct (mean flow modification, cf eq. 1) and indirect (transverse circulation) mechanism based on the E-vector field will be explored in the next session.

4.0 The lifecycle of extratropical intrusion during the 2013 Uttarakhand extreme event

In the context of the sequence of events described in sec.3, the following section describes the precipitation and circulation plots to quantify the linear and nonlinear perspectives during this event. To understand the nature of the extratropical intrusion, we plot the first two components of E-Vectors (eddy asymmetry term $\left(\overline{u'^2} - \overline{v'^2}\right)$and the eddy momentum flux transfer term $(\overline{u'v'})$ or the EMF term) area averaged over a domain north of the Uttarakhand (30°-40°N;75°-82°E) region in **Fig.3a.** The primes are defined with respect to the monthly mean for June 2013. The plot shows that there is strong eddy asymmetry $\overline{v'^2} \gg \overline{u'^2}$ during 16-17 June 2013 and strong northward transfer of EMF. Such meridional elongation is significant and consistent with theory in the sense that it indicates southward

phase propagation associated with northward momentum transfer (e.g., sec. 3b of (Waterman and Hoskins, 2013) A similar EMF flux but weak eddy asymmetry amplitude are seen during 7-9 June. This implies that both flux transfer and eddy asymmetry could play an essential role during this event. This meridional intrusion will be further discussed in detail in sec.4.2. Next, we will see the synoptic situations during this time.

4.1 Precipitation and circulation during the event: synoptic-scale nature of the event

Fig.3a shows the strengthening of the eddy asymmetry and EMF index (first and the second components of the E-vector), which helps to understand the low-frequency intrusion over the Indian region (Kalshetti *et al.*, 2021). To understand the synoptic situation, we first analyze the precipitation during June 2013. **Fig. 3b** shows the northward propagation based on 20-80 days Lanczos-filtered TRMM precipitation data during June 2013. It shows clear intraseasonal northward propagation in this band. Around 13-17 June, the rainfall band strengthened due to the expected monsoon progression after the onset phase (also refer to **Fig.1)**. Similarly, **Fig.4** shows the evolution of the rainfall and the 200hPa wind pattern. The meandering contours confirm the deeper southward movement of the jet stream staying southward of its climatological mean position during summer (~35°N). The temporal evolution plots in **Fig.4** show how the blob of precipitation evolves and decays over the Uttarakhand region. It is clear from this plot that the rainfall band spans over larger areas

spanning a few thousand square kilometers, indicating that the event which caused the high-intensity rainfall is not a purely local extreme event phenomenon and is likely to be correlated with large-scale structures. This large-scale nature is further confirmed from the vorticity plots in **Fig.5**. The temporal evolution on 16th June and 17th June shows cyclonic vorticity advection with strong vorticity bands moving eastward with the additional formation of jet streaks (on 16th June, the strongest vorticity shading is in the southward descending branch west of 75°E and on 17th June it is east of 7°5E in the northward ascending branch). The contours of EMF terms show strong northward (i.e., positive contours) transport of eddy momentum. Thus, cyclonic vorticity advection could be responsible for creating anomalous eddy momentum fluxes, and hence the Uttarakhand region shows more substantial eddy forcing during this period as compared to other days in June 20013.

In addition to the extratropical system, as shown in **Fig. 3**, a low-pressure system was also propagating over the Indian region. The low-level circulation and the sea-level pressure pattern are shown in **Fig.6.** The strong low-level circulation is associated with strong moisture inflow. Also, the surface pressure shows negative anomalies over northwest India and positive anomalies over the eastern part along the Bay of Bengal. Strong northerlies and anomalous high pressure and low-pressure regions are also visible over the Afghanistan region, indicating the existence of upper-level waves. How is the moisture transported in the upper level? We plot the 500-200hPa averaged moisture transport (***uq***, ***vq***) and see the strong moisture outflow from the southern side, particularly from the Bay of Bengal low-pressure

system towards the Uttarakhand region in **Fig.7a-d**. The north-westerly moisture transport is strong in the upper level, with the dominant source of moisture being the Bay of Bengal. The static stability plots **(Fig.7e-h)** also show a strong meridional gradient with stability decreasing northwest to southeast over the location of the extreme rainfall during 16-17th June 2013 (blue shading). Thus, **Figs.3-7** confirm the presence of both the extratropical system and the tropical system during this period with adequate monsoonal and extratropical influence over the Uttarakhand region. In the next section, we will elaborate on the southward extension of the extratropical intrusion.

4.2 Southward digging of extratropical troughs

To understand the southward digging of the trough, which faces decreased stability over the Indian region, we plot ***Fig.8***. The plot has multiple variables, all averaged for the days 15-17 June 2013, which are described below: (a) the shading shows the vertical velocity (***w***) with positive shading indicating upward motion, (b) the magenta curve shows the streamlines at 200hPa, (c) blue contours shows the (positive only) relative vorticity at 200hPa, (d) the black contours show zonal winds at 200hPa (positive values are contoured) (e) the green curve shows the 1 PVU contour. The black contours show that the mean jet is shifted over the Indian region and is highly meandering. This meandering indicates trough intrusion, confirmed by the blue vorticity contour in the northern part of Pakistan and Indian region over Kashmir and Leh-Ladakh region. The jet is pushed southward with the southward

extending intensified Rossby wave trough. Two anticyclones are formed on the southern side of the jetstream, which is evident by the streamlines (magenta color). The deep cyclonic curvature over the northern flank of India shows that the southward extension is deep with an intense Rossby wave trough. The green-coloured 1PVU curve shows that the Rossby wave did not break over the Indian region during this period as the breaking of the Rossby wave induces higher PV (~1-2PVU or higher) over the Indian region (below 30°N(Fadnavis and Chattopadhyay, 2017). The strong amplitude of anomalous relative vorticity (blue contours showing positive only values) indicates that the Rossby wave is intense, with no sign of weakening and breaking with jet pushed southward. At the same time, however, there is upward vertical velocity (red shading)) and rainfall (**Fig.4**) over both the central and the north Indian regions. It is interesting to note that the Rossby wave vorticity structure does not directly reach the region where the heavy rainfall event occurred and does not show much tilt in the zonal vertical direction until 600hPa (plot not shown). Hence, none of the above discussions would indicate the rainfall over the Uttarakhand region occurs as the end product of simple in-situ linear processes such as Rossby waves or monsoon low pressure-induced local convergence (e.g., the linear part in **Fig.2**). Can this widespread rainfall be explained if we assume that the ageostrophic vertical velocity is generated due to a nonlinear conversion process related to downstream amplification associated with baroclinic conversion (Orlanski and Sheldon, 1995) or a downstream wave-mean interaction or a combination of both over the Uttarakhand region? Such nonlinear conversion processes and wave mean interaction can

lead to the conversion of zonal mean to eddy kinetic energy or vice versa and generate ageostrophic vertical velocity.

To highlight the strong vertical velocity and the ageostrophic component, the vertical velocity over a region including Uttarakhand is plotted in **Fig. 9** as a height-latitude plot**.** The plot clearly shows large vertical velocity developing over the Indian region. The development of vertical velocity at this scale can be contributed to by two components, one coming from orographically-forced ascent and the other from wave-induced ascent associated with shears (Teixeira, 2014; Cohen and Boos, 2017). As the upper-level flow is predominantly westerly and largely baroclinic (i.e., $\partial u/\partial z>0$), having developed from barotropic easterlies (i.e., predominantly easterlies at all levels) before 16th June, the plot shows the development of strong vertical velocity that is associated with strong vertical shear (zonal wind contours). Such shear development would give rise to unstable waves and vertical velocities (contained in the term $sg\ and\ s'$ in eq.4). We also examine (not shown) the bulk Richardson index (the ratio of Brunt Vaisala frequency to vertical shear). This index and also **Fig.7d-f** show troposphere above the southern Himalayas slowly becomes unstable as the westerly shear zone develops over the slopes. This generation of ageostrophic vertical velocity also indicates the conversion of mean flow to eddy kinetic energy, as we demonstrate in the next section.

4.3 Transient Eddy Mean Interaction

Fig.10 shows the E-vector divergence, i.e. $\nabla.(\overrightarrow{E})$ (shaded) and the E-vectors. The mean is defined as the 21-day average from 9th June to 30th June, and the daily transient is defined accordingly as a departure from this mean. Components of E-vectors and the divergence are computed after that. The divergence plot is averaged for the period 14-18 June 2013. Divergence is very strong for the period 15-17 June 2013 (not shown). Also, we superimposed the contour of zonal wind averaged during 15-17 June to show the location of the jetstream during this period. The $\nabla.$ E-vector shadings indicate that over the Uttarakhand region, $\nabla.$E is positive, and hence the mean flow gains energy (cf. equation 1a). The vector plot shows the convergence pattern of the E vector (Ex, Ey). There are two zones of convergence-divergence patterns around 40°N, which are consistent with the locations of blocking ridges (east and west Asian ridges). This transfer of energy is further confirmed from the plot of the local transient eddy kinetic energy (EKE given by $1/2(u'^2 + v'^2)$) in **Fig.11**. The black bar plot from ERA5 shows the growth of EKE during that period, which reduces afterward. The growth of EKE and the increased eddy forcing on the mean can lead to an increase in the upper level zonal flow and vertical shear, as shown in **Fig.8**. This can lead to the development of vertical velocity over the forcing region (eq.5), and with the appropriate feedback of moisture supply from monsoon intraseasonal oscillations (**Fig.7**), the condition may then be more favorable for the development of heavy rainfall episodes over this region. This analysis demonstrates that the wave-mean flow interaction in the presence of

moisture can create favorable conditions for high-intensity precipitation events, depending on the potential of wave-mean interaction during the intrusion event.

5.0 Operational Model Forecast

It is clear from **Fig.1** that the operational models (IITM-ERPAS, UKMO, and the ECMWF have failed to capture the event. Among the three models, ECMWF performs the best. It is natural to evaluate model performance in the light of the above discussion and see if the relative success or failure is linked to the inability to capture the intrusion or not. The verification of rainfall is plotted in ***Fig. 12.*** The plot shows that all three models underestimated the rain over the Uttarakhand region. IITM-ERPAS shows low-intensity rainfall over the whole of north India; the UKMO rainfall shows a high-intensity rainfall blob over the Pakistan region but has very little over the Uttarakhand region. The ECMWF model, however, shows some success in capturing the rainfall, but it started one day later than the actual event. Thus, rainfall shows a spatial and temporal shift, which could indicate either improper eddy forcing onto the mean flow resulting in improper vertical velocity or improper moisture transport or a combination of both. The spatial pattern of moisture transport averaged between 500-200hPa is shown in **Fig. 13,** which shows that the models fail to forecast the low pressure-induced moisture transport. Improper moisture transport means the moisture is not available for conversion to rainfall. During 15-16 June 2013, IITM-ERPAS has the cyclonic circulation shifted towards the Bay of Bengal, while for UKMO, it has

shifted more towards the Arabian Sea, both missing the Indian landmass, which could cause rainfall over the Pakistan region. The ECMWF model shows two anticlockwise cyclonic circulations over the Arabian Sea and the Bay of Bengal during 15-16 June 2013. Finally, we show $\nabla.(\overrightarrow{E})$ in **Fig.14** to determine how well the models have forecasted the eddy mean interaction by comparing it with the reanalysis data. The top left panel is shown for reanalysis, as in **Fig. 10**. The reanalysis plots show that $\nabla.(\overrightarrow{E})$ is positive (red shading) over the Uttarakhand and Kashmir regions, implying acceleration of the zonal mean wind. The hindcast from the models shows weaker E-vector divergence (red shades) over the Uttarakhand region. Hence, the plot indicates that the eddy E-vector convergence and divergence are not correctly simulated in the model forecasts over the Uttarakhand region, which is also indicated by the yellow vectors (Ex, Ey). Also, the isotachs are much less dense with a less wavy and intruding pattern over Kashmir, Uttarakhand, and Punjab (between 25°-35°N and 70°-80°E) in the model than the reanalysis over the Indian region, implying that the mean flow is also not correctly simulated in the model. Thus, the location of eddy-transient forcing is also not correctly simulated in the model. Due to inappropriate eddy forcing, the zonal wind height longitude profile also does not show the development of appropriate zonal wind acceleration at the upper level (not shown). Inappropriate zonal wind acceleration at the upper level weakened the vertical shear, thus weakening the Sutcliffe term in equation (5), indicating weaker ageostrophic vertical velocity, resulting in reduced precipitation amplitude. The result, therefore, suggests that the model did not capture the Uttarakhand event because

of inappropriate moisture transport from the monsoon flow and forecast of the wrong location of eddy transport leading to a spatial phase shift of eddy flux divergence (north and south of Uttarakhand region), resulting in improper eddy forcing over the Uttarakhand region. This is also confirmed from the eddy kinetic energy (EKE) plot in **Fig.11**, which shows EKE plots for the model forecasts. From **Fig.11**, it may be seen that the ECMWF model captured this time sequence of EKE evolution more effectively than either the IITM-ERPAS or the UKMO models. Thus, the analysis suggests that inappropriate eddy forcing and improper representation of EKE in the model could be a reason for erroneous rainfall forecast in the model.

6.0 Discussion and Conclusion

This case study examines the life cycle of the extratropical intrusion event over Uttarakhand (India) during June 2013 to understand the role of anisotropic shape, meridional propagation of extratropical eddies, and their feedback onto the monsoon mean flow during the 2013 Uttarakhand event. Previous studies of extreme events such as those over the Uttarakhand region during June 2013 neglect the role of eddy-mean interaction in the monsoonal region**.** The study reveals a potential role of underlying eddy dynamics and the inadequacy in the operational forecast models to capture the eddy dynamics. The E-vector-based approach that is adopted here gives a first-hand idea about the eddy forcing

mechanism, both in the observation and in the model forecast for the 2013 Uttarakhand heavy rainfall event.

On the synoptic scale, extratropical Rossby wave intrusion influenced the June 2013 heavy rainfall event over the Uttarakhand region through the southward extension of troughs and associated southward shift in the subtropical jet pattern. Such synergistic evolutions are documented earlier also (Raman and Rao, 1981; Kalshetti *et al.*, 2021). At a local scale, along with western Himalayan orography and moisture convergence associated with monsoon lows during this time, the upper-level extratropical trough intrusion imparted a strong eddy forcing, which is evident through the existence of E-vector divergence (**Fig. 10**) and the conversion of mean kinetic energy to eddy kinetic energy (**Fig.11**). Thus, on 16-17 June, upper-level eddy forcing accelerated the eddy circulation dynamics and developed an additional shear flow that leads to the high-intensity rainfall event by amplifying the Sutcliff source term (equation 5). In some locations, the mesoscale circulation can develop through feedback from the large-scale flow. It can lead to cloudburst-type situations by forming a super-convective system, as discussed in Houze et al. (2000). However, we have not focused on this large scale to mesoscale connection in this study as we emphasized the quantification of eddy forcing. The current analysis, unlike earlier studies, differentiates the eddy and mean flow over the monsoonal region during this period. Our analysis only assumes the mean flow and background instability associated with extratropical modes and does not assume tropical depressions as a precondition. During the intrusion event, if there is background instability

518 (which can be provided by eddies of extratropical origin), wave-mean interaction can develop
519 ageostrophic velocity leading to high-intensity rainfall events.

520 The analysis presented here is based on a single extreme event. Does every extreme
521 event over the north Indian region require extratropical intrusion? It is found that high-
522 intensity rainfall events over northern India (along the Himalayan belt and adjoining foothills
523 and plains) can occur in the absence of extratropical eddy forcing. Extreme events can occur
524 purely due to monsoon flow over the Indian region and are common during monsoon season
525 over different areas of India. Is there any apparent difference in the spatial pattern of rainfall
526 when an extratropical intrusion occurs? We have checked for two situations when the
527 standardized anomaly of rainfall over the north Indian region (area averaged over a box of
528 25°-40°N & 65°-90°E) is more than two standard deviations (i.e., the rainfall is high
529 intensity). In the first situation, we computed rainfall, 200-hPa wind vectors, and eddy flux
530 divergence composites in the presence of strong low frequency southward EMF transfer, and
531 in the second situation, when there is negligible EMF transfer. The low-frequency eddy
532 transfer band is defined by taking a 30-60 day filtered EMF index (F_L) area averaged over a
533 box (30°-45°N & 70°-95°E) which is then standardized. Strong southward transfer cases are
534 selected by identifying days when the standardized anomaly is less than -1. This plot is
535 shown in **Fig.15.** The figure compares the rainfall, wind vector at 200hPa, the divergence of
536 E vector, and E-vector components for the two extreme rainfall scenarios: with or without
537 eddy forcing. The composite is based on 24 selected cases. The plot shows that there are

indeed certain regions in the Himalayas and the foothills of the Himalayas, starting from Uttarakhand and extending towards the east, where high-intensity rainfall occurs when there is southward momentum transfer (**Fig.15a**). High-intensity precipitation also occurs when there is negligible eddy transfer (**Fig.15b**). The rainfall bias plot (**Fig.15c**) in the last row shows a positive rainfall anomaly in Uttarakhand. Although there are regional variations, many locations over the foothills of the Himalayas in the eastern side of Uttarakhand show positive rainfall anomalies. The wind vector plot shows that the cyclone-anticyclone pattern is much closer and stronger over the north Indian region in the strong low-frequency eddy transfer case. The E-vector and its divergence $\nabla.(\overrightarrow{E})$ are shown for the two corresponding scenarios in **Fig.15d** and **Fig.15e**. Strong positive values of $\nabla.(\overrightarrow{E})$ indicate substantial divergence in the low-frequency band and strong forcing on the zonal wind over the Indian region (in the Kashmir region). The bias plot for divergence in **Fig.15(f)** also shows that these extreme events associated with momentum flux transfer require strong E-vector divergence above the Kashmir region. Although we have highlighted the role of EMF and its southward transfer in the low-frequency mode only, all E-vector components can generate extreme events. A detailed analysis for all the bands is required to understand the full implications and it will be reported in a later study. Our initial results based on a case study and a composite analysis in the low-frequency band suggests the usefulness of the E-vector approach in understanding extratropical intrusion event.

The above explanation, based on the E-vector approach, was then verified in operational model forecasts. Results suggest that ECMWF, ERPAS, and UKMO operational models simulated upper-level circulation patterns but that the E-vector divergent field and their impact on underlying atmospheric states were not correctly simulated. E-vector divergence and local eddy kinetic energy are captured with varying accuracy, suggesting improper eddy forcing in S2S forecast models. Also, the moisture transport in the upper level is also not captured adequately (**Fig.13**). Thus, inappropriate eddy forcing leads to improper ageostrophic and mean flow adjustment in the forecast, and inappropriate moisture transport weakens moisture support, leading to a lack of skill in the model forecast. Although previous analyses provided a description of the event as a Rossby wave intrusion process, the exact role of Rossby wave dynamics and the eddy-mean interaction was not very clear. Our analysis uncovers a series of dynamic steps to understand the reason why the rainfall is underestimated in operational models during the Uttarakhand heavy rainfall event. Our study also provides a diagnostic basis for evaluating the model skill using the E-vector approach and can be used for model skill evaluation.

Acknowledgments

MK acknowledges Ph.D. research fellowship from the Indian Institute of Tropical Meteorology, Pune (IITM), an autonomous Institute under the Ministry of Earth Sciences, Govt. of India. The authors acknowledge the research and funding support from IITM and India Meteorological Department(IMD). All the computations and plots are carried out using

577 the freely available NCL-NCAR software and XmGRACE. The forecast data for the UKMO
578 and ECMWF models are downloaded from the S2S project website hosted by ECMWF
579 (https://apps.ecmwf.int/datasets/data/s2s/levtype=sfc/type=cf/). S2S, a sub-seasonal to
580 seasonal prediction project, is a WWRP/THORPEX-WCRP joint research project established
581 to improve forecast skill and understanding on the sub-seasonal to seasonal time scale and
582 promote its uptake by operational centers and exploitation by the applications community.
583 IITM CFS model extended forecast runs are available in the IITM data server and would be
584 made available on request (https://www.tropmet.res.in/monsoon/). KMRH is funded through
585 Weather and Climate Science for Service Partnership (WCSSP) India, a collaborative initiative
586 between the Met Office, supported by the UK Government's Newton Fund, and the Indian
587 Ministry of Earth Sciences (MoES). The authors would like to acknowledge Dr. Gill Martin,
588 UKMO, Program Manager Indo-UK WCSSP India project (UK side), for providing detailed
589 comments and suggestions in this version of the manuscript.

590 ## *References*

591

592 Abhilash S, Sahai AK, Pattnaik S, Goswami BN, Kumar A. 2014. Extended range prediction of active-
593 break spells of Indian summer monsoon rainfall using an ensemble prediction system in NCEP
594 Climate Forecast System. *International Journal of Climatology*, 34(1): 98–113.
595 https://doi.org/10.1002/joc.3668.

596 Andrews DG, McIntyre ME. 1976. Planetary Waves in Horizontal and Vertical Shear: The Generalized
597 Eliassen-Palm Relation and the Mean Zonal Acceleration. *Journal of the Atmospheric Sciences*,
598 33(11): 2031–2048. https://doi.org/10.1175/1520-0469(1976)033<2031:PWIHAV>2.0.CO;2.

599 Bohlinger P, Sorteberg A, Liu C, Rasmussen R, Sodemann H, Ogawa F. 2019. Multiscale characteristics
600 of an extreme precipitation event over Nepal. *Quarterly Journal of the Royal Meteorological Society*.
601 John Wiley & Sons, Ltd, 145(718): 179–196. https://doi.org/10.1002/qj.3418.

Charney JG. 1969. A Further Note on Large-Scale Motions in the Tropics. *Journal of Atmospheric Sciences*. American Meteorological Society: Boston MA, USA, 26(1): 182–185. https://doi.org/10.1175/1520-0469(1969)026<0182:AFNOLS>2.0.CO;2.

Chevuturi A, Dimri AP. 2016. Investigation of Uttarakhand (India) disaster-2013 using weather research and forecasting model. *Natural Hazards*. Springer Netherlands, 82(3): 1703–1726. https://doi.org/10.1007/s11069-016-2264-6.

Cohen NY, Boos WR. 2017. The influence of orographic Rossby and gravity waves on rainfall. *Quarterly Journal of the Royal Meteorological Society*. John Wiley & Sons, Ltd, 143(703): 845–851. https://doi.org/10.1002/qj.2969.

Dube A, Ashrit R, Ashish A, Sharma K, Iyengar GR, Rajagopal EN, Basu S. 2014. Forecasting the heavy rainfall during Himalayan flooding-June 2013. *Weather and Climate Extremes*. Elsevier, 4(June 2013): 22–34. https://doi.org/10.1016/j.wace.2014.03.004.

Edmon HJ, Hoskins BJ, McIntyre ME. 1980. Eliassen-Palm Cross Sections for the Troposphere. *Journal of the Atmospheric Sciences*. American Meteorological Society, 37(12): 2600–2616. https://doi.org/10.1175/1520-0469(1980)037<2600:EPCSFT>2.0.CO;2.

Fadnavis S, Chattopadhyay R. 2017. Linkages of Subtropical Stratospheric Intraseasonal Intrusions with Indian Summer Monsoon Deficit Rainfall. *Journal of Climate*, 30(13): 5083–5095. https://doi.org/10.1175/JCLI-D-16-0463.1.

G. Branstator. 1995. Organization of storm track anomalies by recurring low-frequency circulation anomalies. , 52: 207–226.

Goswami BN. 2012. South Asian monsoon. *Intraseasonal Variability in the Atmosphere-Ocean Climate System*. Springer, Berlin, Heidelberg, 21–71.

Hanley D, Molinari J, Keyser D. 2001. A Composite Study of the Interactions between Tropical Cyclones and Upper-Tropospheric Troughs. *Monthly Weather Review*. American Meteorological Society: Boston MA, USA, 129(10): 2570–2584. https://doi.org/10.1175/1520-0493(2001)129<2570:ACSOTI>2.0.CO;2.

Held IM, Phillips PJ. 1989. A Barotropic Model of the Interaction between the Hadley Cell and a Rossby Wave. *Journal of the Atmospheric Sciences*, 47(7): 856–869. https://doi.org/10.1175/1520-0469(1990)047<0856:ABMOTI>2.0.CO;2.

Hersbach H, Bell B, Berrisford P, Hirahara S, Horányi A, Muñoz-Sabater J, Nicolas J, Peubey C, Radu R, Schepers D, Simmons A, Soci C, Abdalla S, Abellan X, Balsamo G, Bechtold P, Biavati G, Bidlot J, Bonavita M, De Chiara G, Dahlgren P, Dee D, Diamantakis M, Dragani R, Flemming J, Forbes R, Fuentes M, Geer A, Haimberger L, Healy S, Hogan RJ, Hólm E, Janisková M, Keeley S, Laloyaux P, Lopez P, Lupu C, Radnoti G, de Rosnay P, Rozum I, Vamborg F, Villaume S, Thépaut J-N. 2020. The ERA5 global reanalysis. *Quarterly Journal of the Royal Meteorological Society*. John Wiley & Sons, Ltd, 146(730): 1999–2049. https://doi.org/10.1002/qj.3803.

Homeyer CR, Bowman KP. 2013. Rossby Wave Breaking and Transport between the Tropics and Extratropics above the Subtropical Jet. *Journal of the Atmospheric Sciences*. American Meteorological Society: Boston MA, USA, 70(2): 607–626. https://doi.org/10.1175/JAS-D-12-0198.1.

Hong CC, Hsu HH, Lin NH, Chiu H. 2011. Roles of European blocking and tropical - extratropical interaction in the 2010 Pakistan flooding. , 38(May): 1–6. https://doi.org/10.1029/2011GL047583.

Hoskins B. 1997. A potential vorticity view of synoptic development. *Meteorological Applications*. John Wiley & Sons, Ltd, 4(4): 325–334. https://doi.org/10.1017/S1350482797000716.

Hoskins BJ. 1982. The Mathematical Theory of Frontogenesis. *Annual Review of Fluid Mechanics*. Annual Reviews, 14(1): 131–151. https://doi.org/10.1146/annurev.fl.14.010182.001023.

Hoskins BJ, James IN, White GH. 1983. The Shape, Propagation and Mean-Flow Interaction of Large-Scale Weather Systems. *Journal of the Atmospheric Sciences*. American Meteorological Society: Boston MA, USA, 40(7): 1595–1612. https://doi.org/10.1175/1520-0469(1983)040<1595:TSPAMF>2.0.CO;2.

Hoskins BJ, Karoly DJ. 1981. The Steady Linear Response of a Spherical Atmosphere to Thermal and Orographic Forcing. *Journal of the Atmospheric Sciences*, 38(6): 1179–1196. https://doi.org/10.1175/1520-0469(1981)038<1179:TSLROA>2.0.CO;2.

Houze RA, Chen SS, Kingsmill DE, Serra Y, Yuter SE. 2000. Convection over the Pacific Warm Pool in relation to the Atmospheric Kelvin-Rossby Wave. *Journal of the Atmospheric Sciences*. American Meteorological Society: Boston MA, USA, 57(18): 3058–3089. https://doi.org/10.1175/1520-0469(2000)057<3058:COTPWP>2.0.CO;2.

Huffman GJ, Adler RF, Bolvin DT, Gu G, Nelkin EJ, Bowman KP, Hong Y, Stocker EF, Wolff DB. 2007. The TRMM Multisatellite Precipitation Analysis (TMPA): Quasi-global, multiyear, combined-sensor precipitation estimates at fine scales. *Journal of Hydrometeorology*, 8(1): 38–55. https://doi.org/10.1175/JHM560.1.

Hunt KMR, Turner AG, Schiemann RKH. 2021. How Interactions between Tropical Depressions and Western Disturbances Affect Heavy Precipitation in South Asia. *Monthly Weather Review*. American Meteorological Society: Boston MA, USA, 149(6): 1801–1825. https://doi.org/10.1175/MWR-D-20-0373.1.

Hunt KMR, Turner AG, Shaffrey LC. 2018a. The evolution, seasonality and impacts of western disturbances. *Quarterly Journal of the Royal Meteorological Society*, 144(710): 278–290. https://doi.org/10.1002/qj.3200.

Hunt KMR, Turner AG, Shaffrey LC. 2018b. Extreme Daily Rainfall in Pakistan and North India: Scale Interactions, Mechanisms, and Precursors. *Monthly Weather Review*, 146(4): 1005–1022. https://doi.org/10.1175/MWR-D-17-0258.1.

James IN. 1994. *Introduction to Circulating Atmospheres*. *Cambridge Atmospheric and Space Science Series*. Cambridge University Press: Cambridge.

Jin F-F. 2010. Eddy-Induced Instability for Low-Frequency Variability. *Journal of the Atmospheric Sciences*. American Meteorological Society: Boston MA, USA, 67(6): 1947–1964. https://doi.org/10.1175/2009JAS3185.1.

Joseph S, Sahai AK, Sharmila S, Abhilash S, Borah N, Chattopadhyay R, Pillai PA, Rajeevan M, Kumar A. 2015. North Indian heavy rainfall event during June 2013: diagnostics and extended range prediction. *Climate Dynamics*, 44(7): 2049–2065. https://doi.org/10.1007/s00382-014-2291-5.

680 Kalshetti M, Chattopadhyay R, Phani R, Joseph S, Sahai AK. 2021. Climatological patterns of
681 subseasonal eddy flux transfer based on the co-spectral analysis over the Indian region and the
682 derivation of an index of eddy transfer for operational tracking. *International Journal of Climatology*.
683 John Wiley & Sons, Ltd, 41 (Suppl. 1)(n/a): E1906–E1925. https://doi.org/10.1002/joc.6821.

684 Kalshetti M, Chattopadhyay R, Phani R, Joseph S, Sahai AK. 2021. Climatological patterns of
685 subseasonal eddy flux transfer based on the <scp>co-spectral</scp> analysis over the Indian region
686 and the derivation of an index of eddy transfer for operational tracking. *International Journal of*
687 *Climatology*, 41(S1): E1906–E1925. https://doi.org/10.1002/joc.6821.

688 Karoly DJ, Hoskins BJ. 1982. Three Dimensional Propagation of Planetary Waves. *Journal of the*
689 *Meteorological Society of Japan. Ser. II*, 60(1): 109–123. https://doi.org/10.2151/jmsj1965.60.1_109.

690 Kaur S, Gupta PK. 2017. Devastating rainstorm of June-2013 in Uttarakhand. *Mausam*, 68(4): 633–
691 642.

692 Kiladis GN. 1998. Observations of Rossby Waves Linked to Convection over the Eastern Tropical
693 Pacific. *Journal of the Atmospheric Sciences*. American Meteorological Society: Boston MA, USA,
694 55(3): 321–339. https://doi.org/10.1175/1520-0469(1998)055<0321:OORWLT>2.0.CO;2.

695 Krishnan R, Kumar V, Sugi M, Yoshimura J. 2009. Internal Feedbacks from Monsoon–Midlatitude
696 Interactions during Droughts in the Indian Summer Monsoon. *Journal of the Atmospheric Sciences*,
697 66(3): 553–578. https://doi.org/10.1175/2008JAS2723.1.

698 Lackmann G. 2012. *Midlatitude Synoptic Meteorology Dynamics, Analysis, and Forecasting*. American
699 Meteorological Society: Boston (US).

700 Lau N-C. 1979. The Structure and Energetics of Transient Disturbances in the Northern Hemisphere
701 Wintertime Circulation. *Journal of Atmospheric Sciences*. American Meteorological Society: Boston
702 MA, USA, 36(6): 982–995. https://doi.org/10.1175/1520-0469(1979)036<0982:TSAEOT>2.0.CO;2.

703 Lau N-C, Holopainen EO. 1984. Transient Eddy Forcing of the Time-Mean Flow as Identified by
704 Geopotential Tendencies. *Journal of the Atmospheric Sciences*, 41(3): 313–328.
705 https://doi.org/10.1175/1520-0469(1984)041<0313:TEFOTT>2.0.CO;2.

706 Lau WKM, Kim K-M. 2011. The 2010 Pakistan Flood and Russian Heat Wave: Teleconnection of
707 Hydrometeorological Extremes. *Journal of Hydrometeorology*, 13(1): 392–403.
708 https://doi.org/10.1175/jhm-d-11-016.1.

709 Leroux S, Hall NMJ, Kiladis GN. 2010. A climatological study of transient-mean-flow interactions over
710 West Africa. *Quarterly Journal of the Royal Meteorological Society*, 136(SUPPL. 1): 397–410.
711 https://doi.org/10.1002/qj.474.

712 Lillo SP, Parsons DB. 2017. Investigating the dynamics of error growth in ECMWF medium-range
713 forecast busts. *Quarterly Journal of the Royal Meteorological Society*. John Wiley & Sons, Ltd,
714 143(704): 1211–1226. https://doi.org/10.1002/qj.2938.

715 Novak L, Ambaum MHP, Tailleux R. 2015. The life cycle of the North Atlantic storm track. *Journal of*
716 *the Atmospheric Sciences*, 72(2): 821–833. https://doi.org/10.1175/JAS-D-14-0082.1.

Orlanski I, Sheldon JP. 1995. Stages in the energetics of baroclinic systems. *Tellus A: Dynamic Meteorology and Oceanography*. Taylor & Francis, 47(5): 605–628. https://doi.org/10.3402/tellusa.v47i5.11553.

Parida BR, Behera SN, Bakimchandra O, Pandey AC, Singh N. 2017. Evaluation of satellite-derived rainfall estimates for an extreme rainfall event over Uttarakhand, Western Himalayas. *Hydrology*, 4(2): 1–18. https://doi.org/10.3390/hydrology4020022.

Parsons DB, Lillo SP, Rattray CP, Bechtold P, Rodwell MJ, Bruce CM. 2019. The Role of Continental Mesoscale Convective Systems in Forecast Busts within Global Weather Prediction Systems. *Atmosphere*, 10(11). https://doi.org/10.3390/atmos10110681.

Pattanaik DR, Pai DS, Mukhopadhyay B. 2015. Rapid northward progress of monsoon over India and associated heavy rainfall over Uttarakhand: A diagnostic study and real time extended range forecast. *Mausam*, 66(3): 551–568.

Raman CR V, Rao YP. 1981. Blocking highs over Asia and monsoon droughts over India. *Nature*. Nature Publishing Group, 289: 271.

Ramaswamy C. 1962. Breaks in the Indian summer monsoon as a phenomenon of interaction between the easterly and the sub-tropical westerly jet streams. *Tellus*. Taylor & Francis, 14(3): 337–349. https://doi.org/10.3402/tellusa.v14i3.9560.

Sahai AK, Chattopadhyay R, Joseph S, Krishna PM, Pattanaik DR, Abhilash S. 2019. Chapter 20 - Seamless Prediction of Monsoon Onset and Active/Break Phases. In: Robertson AW and Vitart F (eds) *Sub-Seasonal to Seasonal Prediction*. Elsevier, 421–438.

Singh C, Chand R. 2015. Exceptionally heavy rainfall over Uttarakhand during 15-18 June, 2013 - A case study. *Mausam*, 66(4): 741–750.

Sooraj K, Terray P, Shilin A, Mujumdar M. 2020. Dynamics of rainfall extremes over India: A new perspective. *International Journal of Climatology*, (February): joc.6516. https://doi.org/10.1002/joc.6516.

Tan G-R, Jin F-F, Ren H-L, Sun Z-B. 2014. The role of eddy feedback in the excitation of the NAO. *Meteorological Applications*. John Wiley & Sons, Ltd, 21(3): 768–776. https://doi.org/10.1002/met.1415.

Teixeira MAC. 2014. The physics of orographic gravity wave drag. *Frontiers in Physics*, 2: 43. https://doi.org/10.3389/fphy.2014.00043.

Trenberth KE. 1986. An Assessment of the Impact of Transient Eddies on the Zonal Flow during a Blocking Episode Using Localized Eliassen-Palm Flux Diagnostics. *Journal of the Atmospheric Sciences*, 43(19): 2070–2087. https://doi.org/10.1175/1520-0469(1986)043<2070:AAOTIO>2.0.CO;2.

Trenberth KE, Fasullo JT. 2012. Climate extremes and climate change: The Russian heat wave and other climate extremes of 2010. *Journal of Geophysical Research: Atmospheres*. John Wiley & Sons, Ltd, 117(D17). https://doi.org/10.1029/2012JD018020.

Uccellini LW, Johnson DR. 1979. The Coupling of Upper and Lower Tropospheric Jet Streaks and Implications for the Development of Severe Convective Storms. *Monthly Weather Review*, 107(6): 682–703. https://doi.org/10.1175/1520-0493(1979)107<0682:TCOUAL>2.0.CO;2.

Vellore RK, Jayant RK. 2014. On the anomalous precipitation enhancement over the Himalayan foothills during monsoon breaks. , 2009–2031. https://doi.org/10.1007/s00382-013-2024-1.

Vellore RK, Kaplan ML, Krishnan R, Lewis JM, Sabade S, Deshpande N, Singh BB, Madhura RK, Rama Rao MVS. 2016a. Monsoon-extratropical circulation interactions in Himalayan extreme rainfall. *Climate Dynamics*. Springer Berlin Heidelberg, 46(11–12): 3517–3546. https://doi.org/10.1007/s00382-015-2784-x.

Vellore RK, Kaplan ML, Krishnan R, Lewis JM, Sabade S, Deshpande N, Singh BB, Madhura RK, Rama Rao MVS. 2016b. Monsoon-extratropical circulation interactions in Himalayan extreme rainfall. *Climate Dynamics*, 46(11): 3517–3546. https://doi.org/10.1007/s00382-015-2784-x.

Vitart F, Ardilouze C, Bonet A, Brookshaw A, Chen M, Codorean C, Déqué M, Ferranti L, Fucile E, Fuentes M, Hendon H, Hodgson J, Kang HS, Kumar A, Lin H, Liu G, Liu X, Malguzzi P, Mallas I, Manoussakis M, Mastrangelo D, MacLachlan C, McLean P, Minami A, Mladek R, Nakazawa T, Najm S, Nie Y, Rixen M, Robertson AW, Ruti P, Sun C, Takaya Y, Tolstykh M, Venuti F, Waliser D, Woolnough S, Wu T, Won DJ, Xiao H, Zaripov R, Zhang L. 2017. The subseasonal to seasonal (S2S) prediction project database. *Bulletin of the American Meteorological Society*, 98(1): 163–173. https://doi.org/10.1175/BAMS-D-16-0017.1.

Waterman S, Hoskins BJ. 2013. Eddy Shape, Orientation, Propagation, and Mean Flow Feedback in Western Boundary Current Jets. *Journal of Physical Oceanography*. American Meteorological Society: Boston MA, USA, 43(8): 1666–1690. https://doi.org/10.1175/JPO-D-12-0152.1.

Webster PJ, Holton JR. 1982. Cross-Equatorial Response to Middle-Latitude Forcing in a Zonally Varying Basic State. *Journal of Atmospheric Sciences*. American Meteorological Society: Boston MA, USA, 39(4): 722–733. https://doi.org/10.1175/1520-0469(1982)039<0722:CERTML>2.0.CO;2.

Williams RG, Wilson C, Hughes CW. 2007. Ocean and Atmosphere Storm Tracks: The Role of Eddy Vorticity Forcing. *Journal of Physical Oceanography*. American Meteorological Society: Boston MA, USA, 37(9): 2267–2289. https://doi.org/10.1175/JPO3120.1.

Wills RCJ, Schneider T. 2018. Mechanisms Setting the Strength of Orographic Rossby Waves across a Wide Range of Climates in a Moist Idealized GCM. *Journal of Climate*. American Meteorological Society: Boston MA, USA, 31(18): 7679–7700. https://doi.org/10.1175/JCLI-D-17-0700.1.

Figure Caption

Figure 1 The daily time series of rainfall from observation (TRMM) and s2s model forecasts(ERPAS, UKMO, ECMWF) area averaged over a box 29°-31°N 78°-81°E surrounding Uttarakhand region. The 95th percentile of TRMM rainfall for this box is also shown as a grey horizontal line. The ensemble spread (± 1SD) for the models is indicated by the shaded regions. ERPAS and UKMO model forecasts are from 09June2013 initial conditions(ICs) and the ECMWF forecast is from 10June2013 IC.

Figure 2 A schematic diagram describing the proposed sequence of events during the extratropical wave intrusions over the monsoonal region. Panel A shows a non-intruding situation (described as normal situaion in the figure). Panel B shows an intruding situation resulting in linear and non-linear responses, which are shown in panels C1 and C2 repectively. The resultant ageostrophic upward motion (which is forced convection in presence of monsoonal moisture background) is shown in the right side. The nonlinear effects can modulate (i.e. increase or decrease)the ageostrophic vertical velocity generation and thereby can cause flaring up of extreme rainfall events(refer text for more details).

Figure 3 (a) The eddy momentum flux (EMF) and the eddy assymetry factor averaged over a northern box (30°-40°N;75°-82°E;) showing strong flux transfer. The eddy terms are anomaly from monthly means. Positive (negative) sign indicats anomalous northward (southward) transfer during June 2013. (b) Rainfall hovmöller plot from the 20-80 day filtered TRMM data during June 2013 averaged over longitude bands(70°-80°E) over Indian region. (Units: EMF and Eddy Assymetry term: m^2 s^{-2} per unit area; Rainfall: mm day^{-1})

Figure 4 Panels showing rainfall(shaded) patterns and vector winds at 200 hPa during 15-18June 2013. The red contours shows the zonal winds.Dates are mentioned at the top of each panels.(units: Precipitation mm day^{-1}; winds m s^{-1})

Figure 5 Same as last figure but showing evolution of ERA5 relative vorticity pattern (shaded) and standardized eddy momentum fluxes (u′v′, EMF)as contours during 15-18th June 2013. The northward (southward) transport is positive (negative). The primes and anomalies are computed with respect to the monthly mean of June 2013. The Kedarnath region of Uttarakhand state(India) which received heavy rainfall is represented as balck dots.(Units: *vorticity* $10^{-5} \times s^{-1}$; *EMF* m^2 s^{-2})

Figure 6 Same as last figure but showing surface pressure anomalies from monthly mean of June 2013 and actual wind at 850 hPa.The dates are mentioned at the top of each panels.The Kedarnath region of Uttarakhand state (India) which received heavy rainfall is represented as red dots. (Units: *pressure* hPa; *wind* m s^{-1})

Figure 7 (a)-(d) Vertically (400-200hPa) averaged moisture transport(vector) moisture divergence(shaded) during 15-18 June 2013 (dates mentioned at the top of each panel). (e)-(h) Upper level (400-200hPa) averaged static stability (Brunt Vaisalla frequency,N, anomalies from monthly mean) for the same period. The Kedarnath region of Uttarakhand state (India) which received heavy rainfall is represented as green dots.(units:div/N s^{-1}; transport vector ms^{-1})

Figure 8 Plots shwoing vertical velocity (shaded, upward positive *units hPa* s^{-1}), zonal wind (black contour), relative vorticity anomaly from monthly mean(blue contour, *units* 10^{-6} $\times$ s^{-1}) and streamlines (magenta, *units* ms^{-1})) at 200hPa averaged for the period 15-17 June 2013. The green contour shows the potential vorticity of magnitude 1PVU.

Figure 9 Height latitude profile evolution of vertical velocity (omega as shaded, upward positive *units hPa* s^{-1}) and zonal wind (contours,*units* m s^{-1})) for the days between 13-18June 2013. The plot is shown for longitudinal average range 75°E-85°E.

Figure 10 E-Vector divergence (shaded,$\nabla \cdot \mathbf{E}$), E-Vectors (yellow) for the period averaged between 10-30June 2013. The zonal wind contours for the days averaged between 14-18 June 2013 are also plotted to show the average jet position during the extreme event days. The eddies are defined by taking average for the period 10-30 June 2013.

Figure 11 The time evolution of area averaged (28°-35°N;78°-82°E) eddy kinetic energy (EKE) from ERA5 reanalysis, UKMO model(green), ECMWF model (blue) and ERPAS model (red). For ERPAS and UKMO the ICs are 09June while for ECMWF the IC is 08June. Plots are shown from 10June 2013 onwards. (*Units:*$m^2 s^{-2}$)

Figure 12 A comparison of rainfall evolution (shaded) for the period 15-18 June 2013 for different operational models and TRMM observation data. (unit: mm day^{-1})

Figure 13 Plot showing the comparison of mositure transport vectors and moisture divergence (shaded) based on ERA5 reanalysis and different s2s model runs (mentioned in top of each panels).(units: div s^{-1}; transport vector m s^{-1})

Figure 14 Plot showing the verification of E-vectors and E-vector divergence (shaded,$\nabla \cdot \mathbf{E}$) for different model runs with respect to observation for the days averaged between 14-18 June 2013.

Figure 15 Rainfall and wind anomaly composites when (a) the standardized rainfall anomaly over north-Indian region is more than 2 standard deviation and the standardized EMF index area-averaged over a northern box (30°-45°N , 70°-95°E) is more than 2 standard deviation, (b) same as (a) but when the standardized EMF is close to zero. (c) shows the rainfall and wind vector bias for these two cases i.e. (a)-(b). (d) E-vector divergence composite and plot of E-vector at 200hPa for the same criteria as (a).(e) is same as (b) but for E-vector divergence composite and plot of E-vector at 200hPa. (f) same as (c) but showing the bias in E-vector divergence and E-vectors.

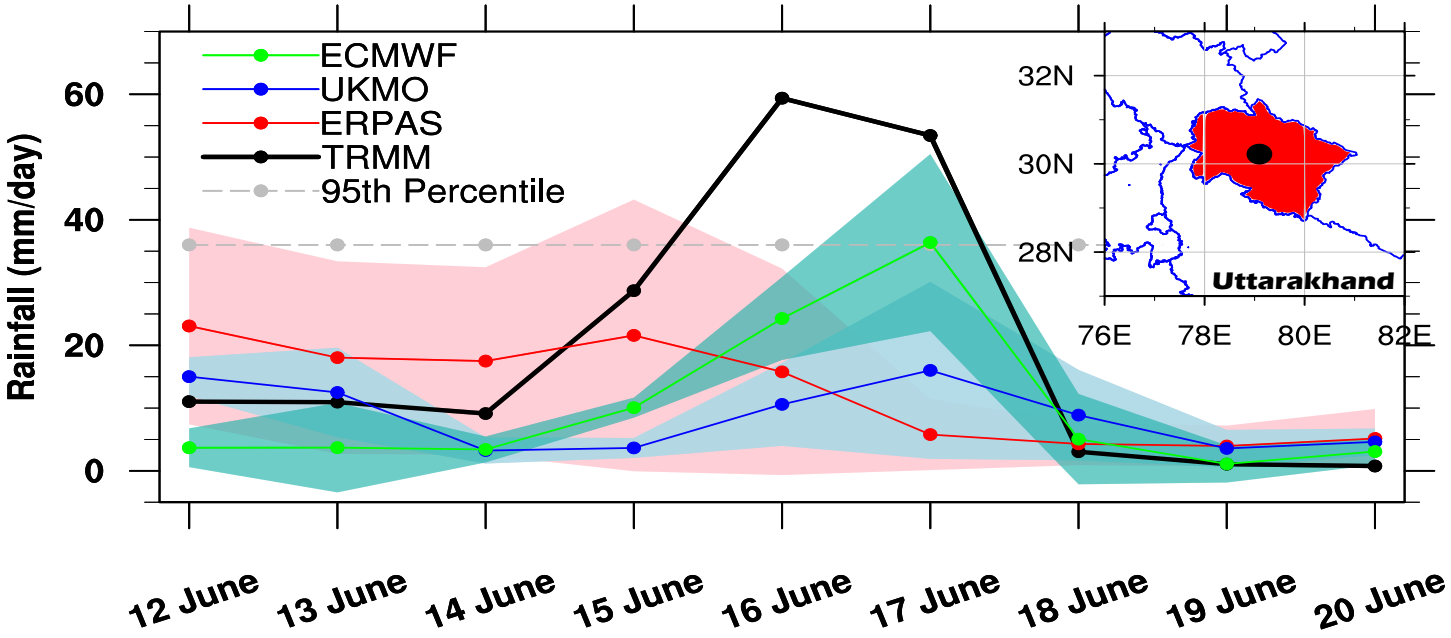

Figure 1: The daily time series of rainfall from observation (TRMM) and s2s model forecasts(ERPAS, UKMO, ECMWF) area averaged over a box 29°-31°N 78°-81°E surrounding Uttarakhand region. The 95th percentile of TRMM rainfall for this box is also shown as a grey horizontal line. The ensemble spread (± 1SD) for the models is indicated by the shaded regions. ERPAS and UKMO model forecasts are from 09June2013 initial conditions(ICs) and the ECMWF forecast is from 10June2013 IC.

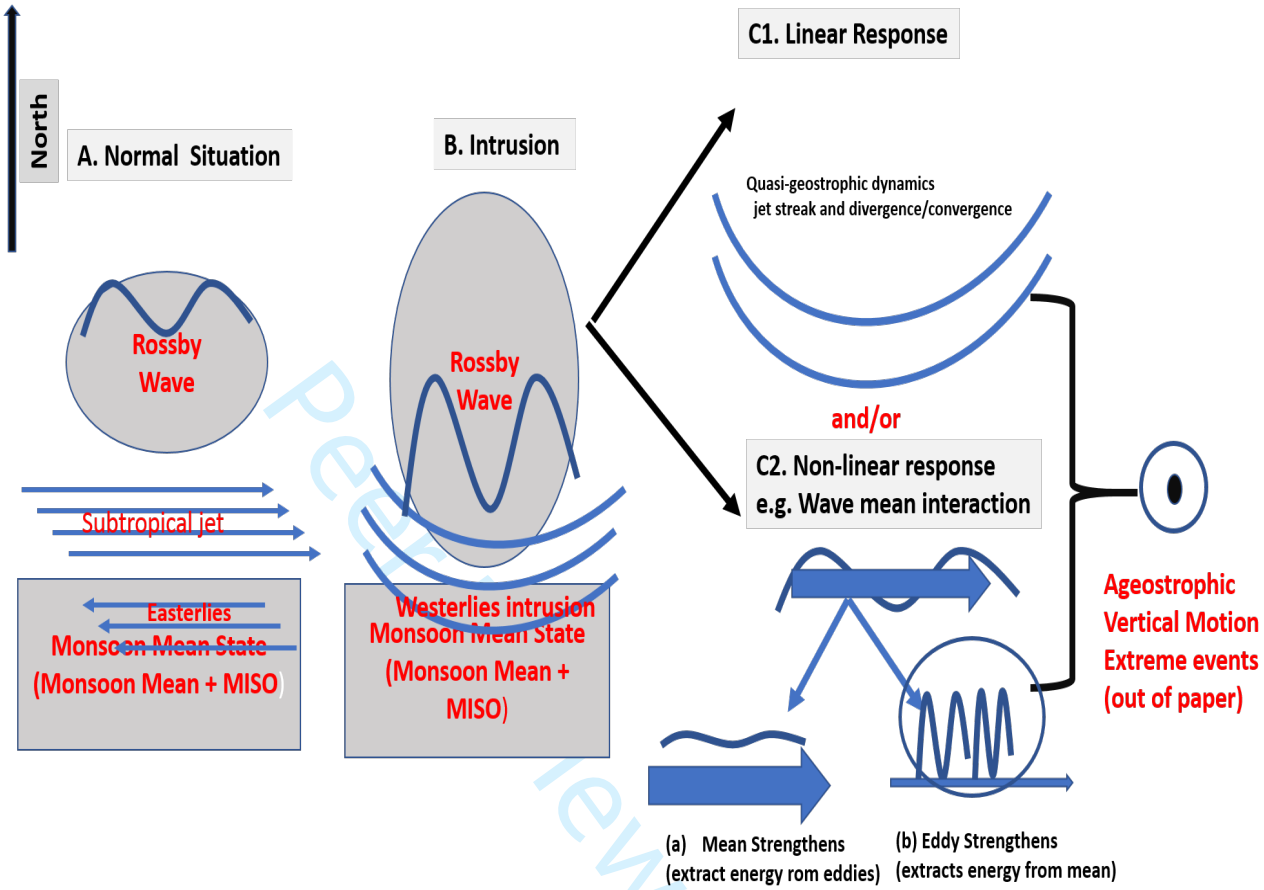

Figure 2: A schematic diagram describing the proposed sequence of events during the extratropical wave intrusions over the monsoonal region. Panel A shows a non-intruding situation (described as normal situaion in the figure). Panel B shows an intruding situation resulting in linear and non-linear responses, which are shown in panels C1 and C2 repectively. The resultant ageostrophic upward motion (which is forced convection in presence of monsoonal moisture background) is shown in the right side. The nonlinear effects can modulate (i.e. increase or decrease)the ageostrophic vertical velocity generation and thereby can cause flaring up of extreme rainfall events(refer text for more details).

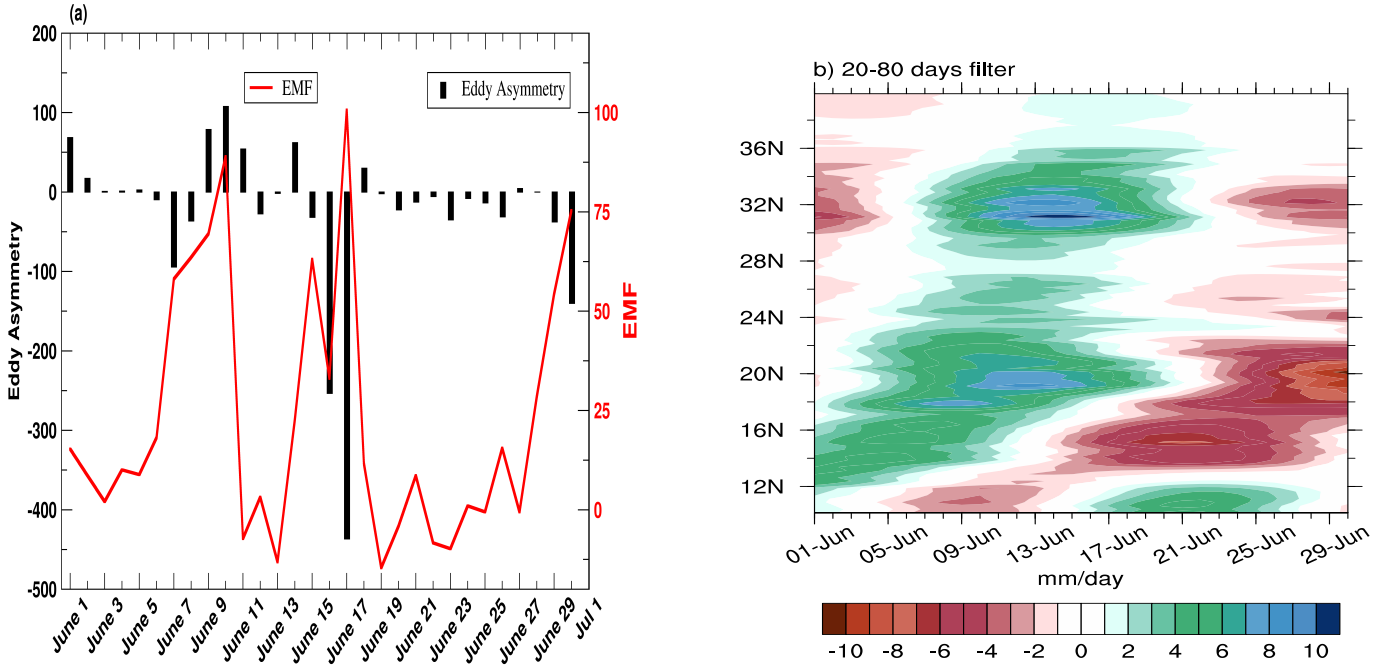

Figure 3: (a) The eddy momentum flux (EMF) and the eddy assymetry factor averaged over a northern box (30°-40°N;75°-82°E;) showing strong flux transfer. The eddy terms are anomaly from monthly means. Positive (negative) sign indicats anomalous northward (southward) transfer during June 2013. (b) Rainfall hovmöller plot from the 20-80 day filtered TRMM data during June 2013 averaged over longitude bands(70°-80°E) over Indian region. (Units: EMF and Eddy Assymetry term: m^2 s^{-2} per unit area; Rainfall: mm day^{-1})

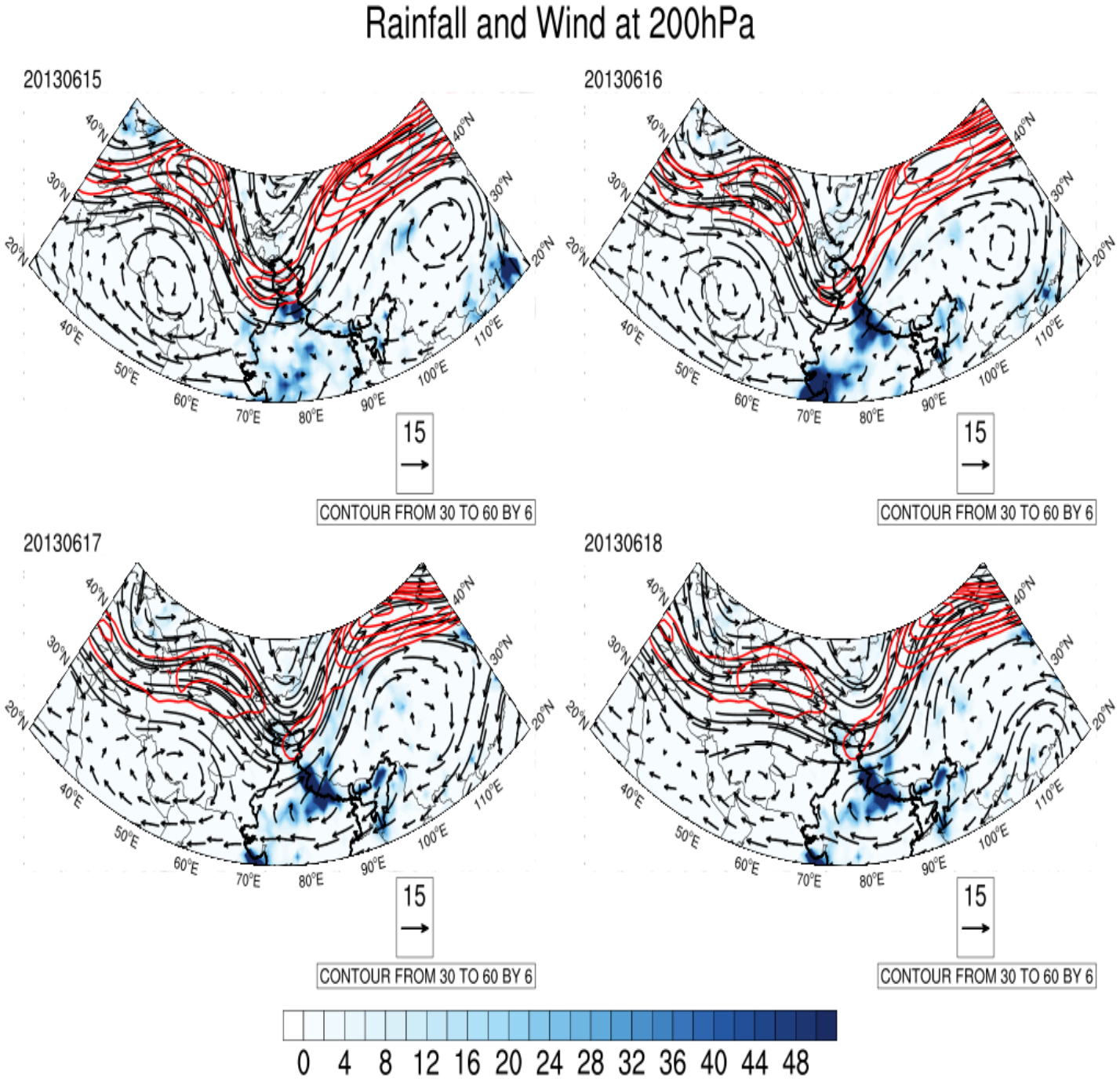

Figure 4: Panels showing rainfall(shaded) patterns and vector winds at 200 hPa during 15-18June 2013. The red contours shows the zonal winds.Dates are mentioned at the top of each panels.(units: Precipitation mm day^{-1}; winds m s^{-1})

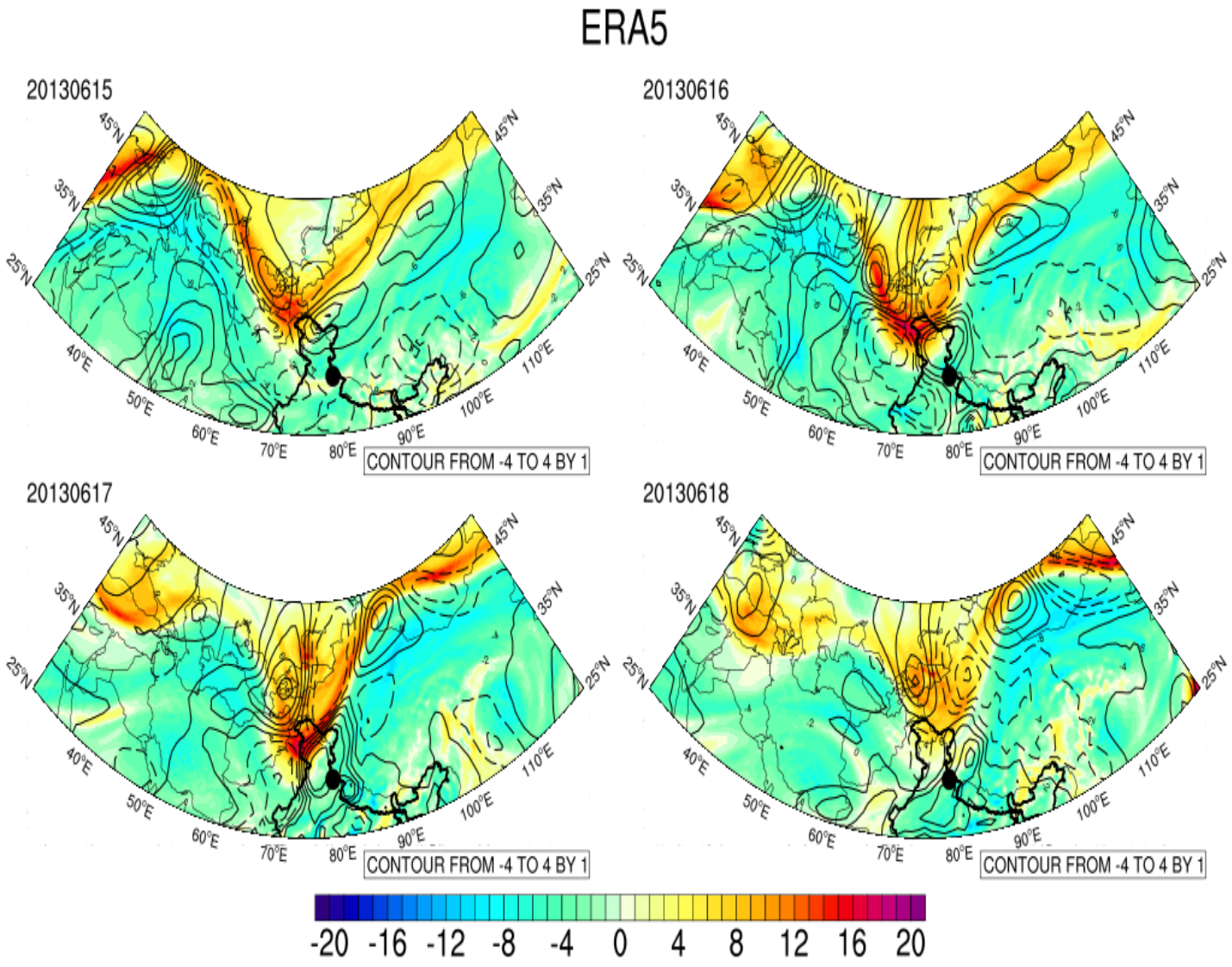

Figure 5: Same as last figure but showing evolution of ERA5 relative vorticity pattern (shaded) and standardized eddy momentum fluxes (u′v′, EMF)as contours during 15-18th June 2013. The northward (southward) transport is positive (negative). The primes and anomalies are computed with respect to the monthly mean of June 2013. The Kedarnath region of Uttarakhand state(India) which received heavy rainfall is represented as balck dots.(Units: *vorticity* $10^{-5} \times s^{-1}$; *EMF* m^2 s^{-2})

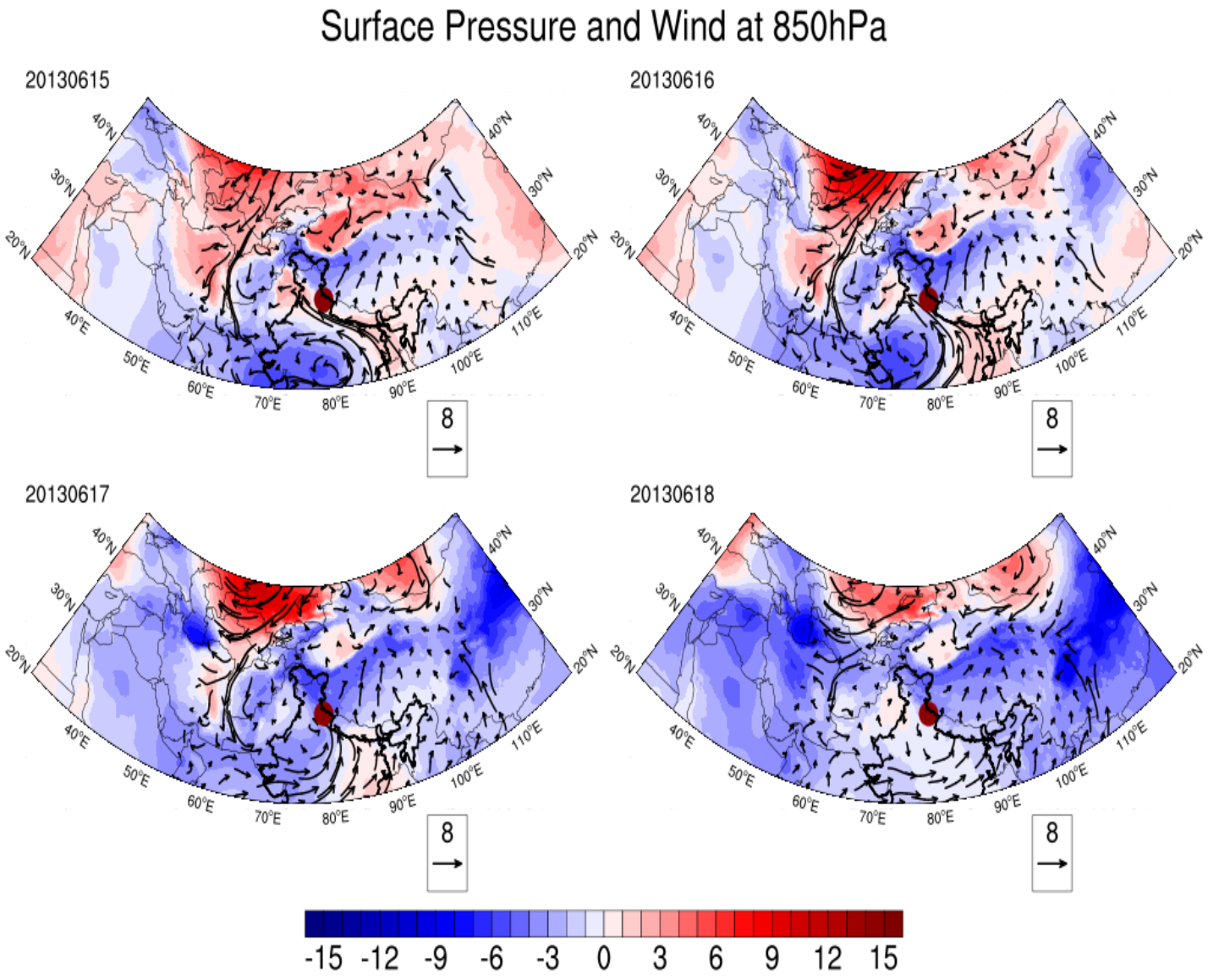

Figure 6: Same as last figure but showing surface pressure anomalies from monthly mean of June 2013 and actual wind at 850 hPa.The dates are mentioned at the top of each panels.The Kedarnath region of Uttarakhand state (India) which received heavy rainfall is represented as red dots. (Units: *pressure* hPa; *wind* $m\ s^{-1}$)

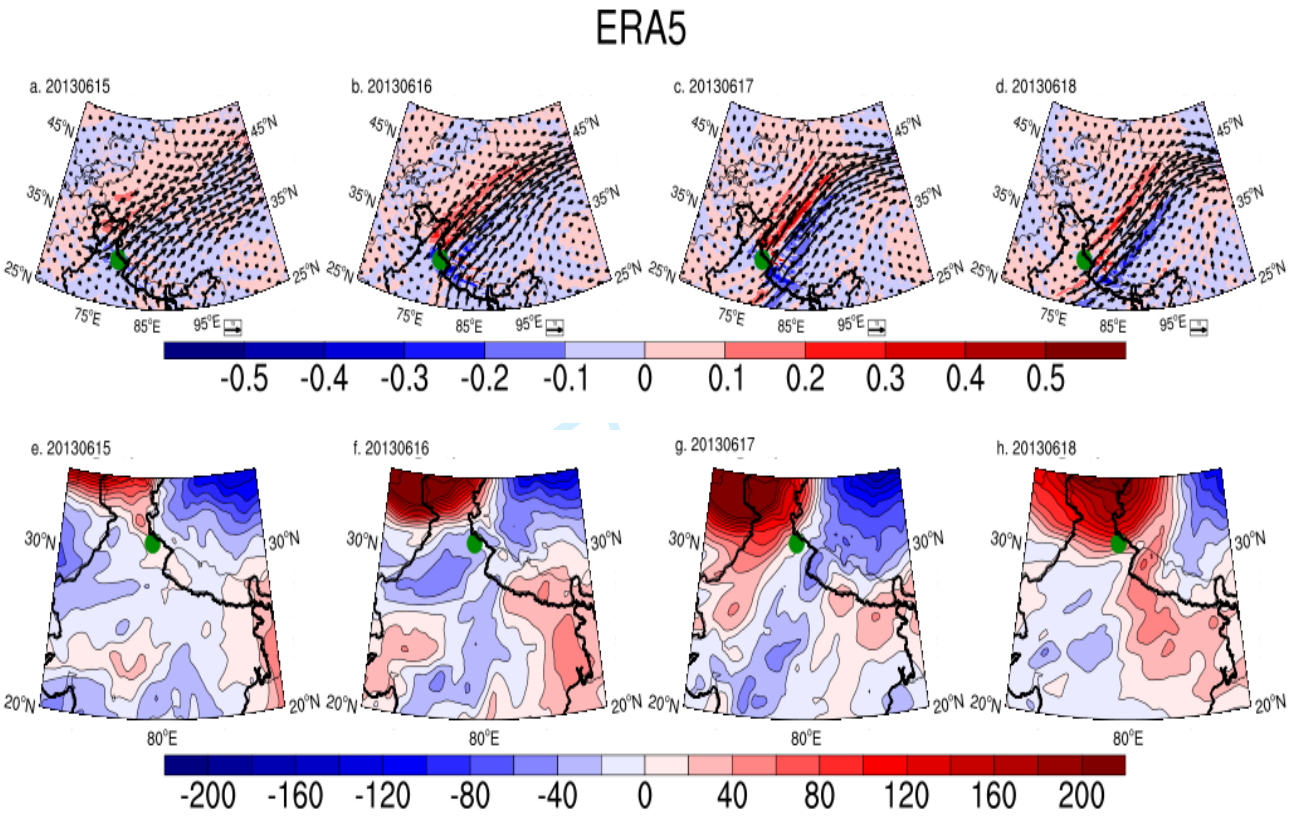

Figure 7: (a)-(d) Vertically (400-200hPa) averaged moisture transport(vector) moisture divergence(shaded) during 15-18 June 2013 (dates mentioned at the top of each panel). (e)-(h) Upper level (400-200hPa) averaged static stability (Brunt Vaisalla frequency,N, anomalies from monthly mean) for the same period. The Kedarnath region of Uttarakhand state (India) which received heavy rainfall is represented as green dots.(units:div/N s^{-1}; transport vector ms^{-1})

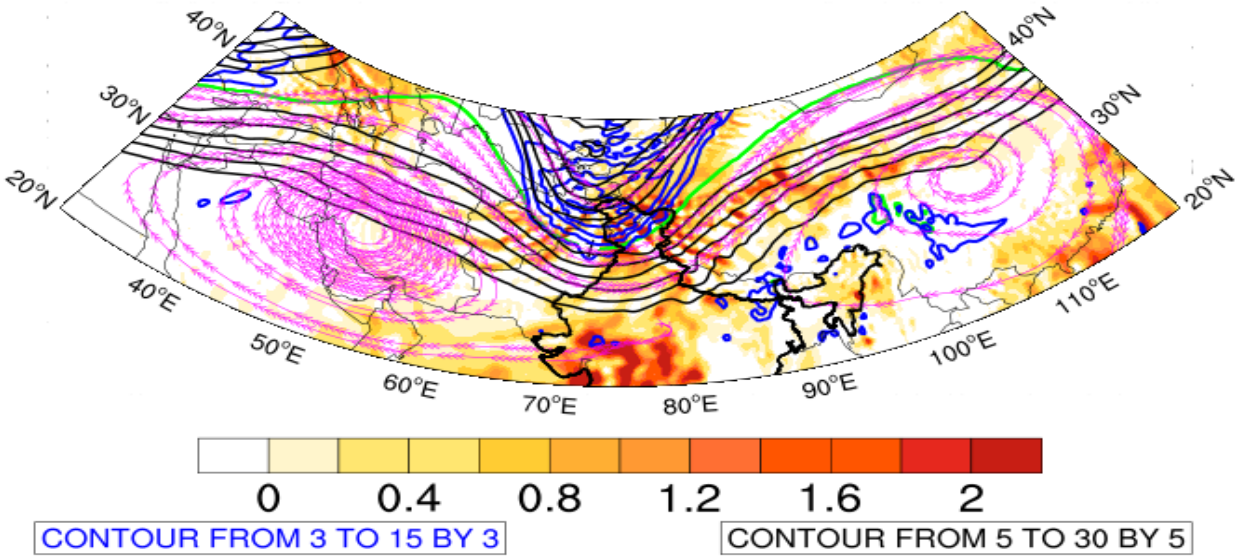

Figure 8: Plots shwoing vertical velocity (shaded, upward positive *units hPa* s^{-1}), zonal wind (black contour), relative vorticity anomaly from monthly mean(blue contour, *units* $10^{-6} \times s^{-1}$) and streamlines (magenta, *units* ms^{-1})) at 200hPa averaged for the period 15-17 June 2013. The green contour shows the potential vorticity of magnitude 1PVU.

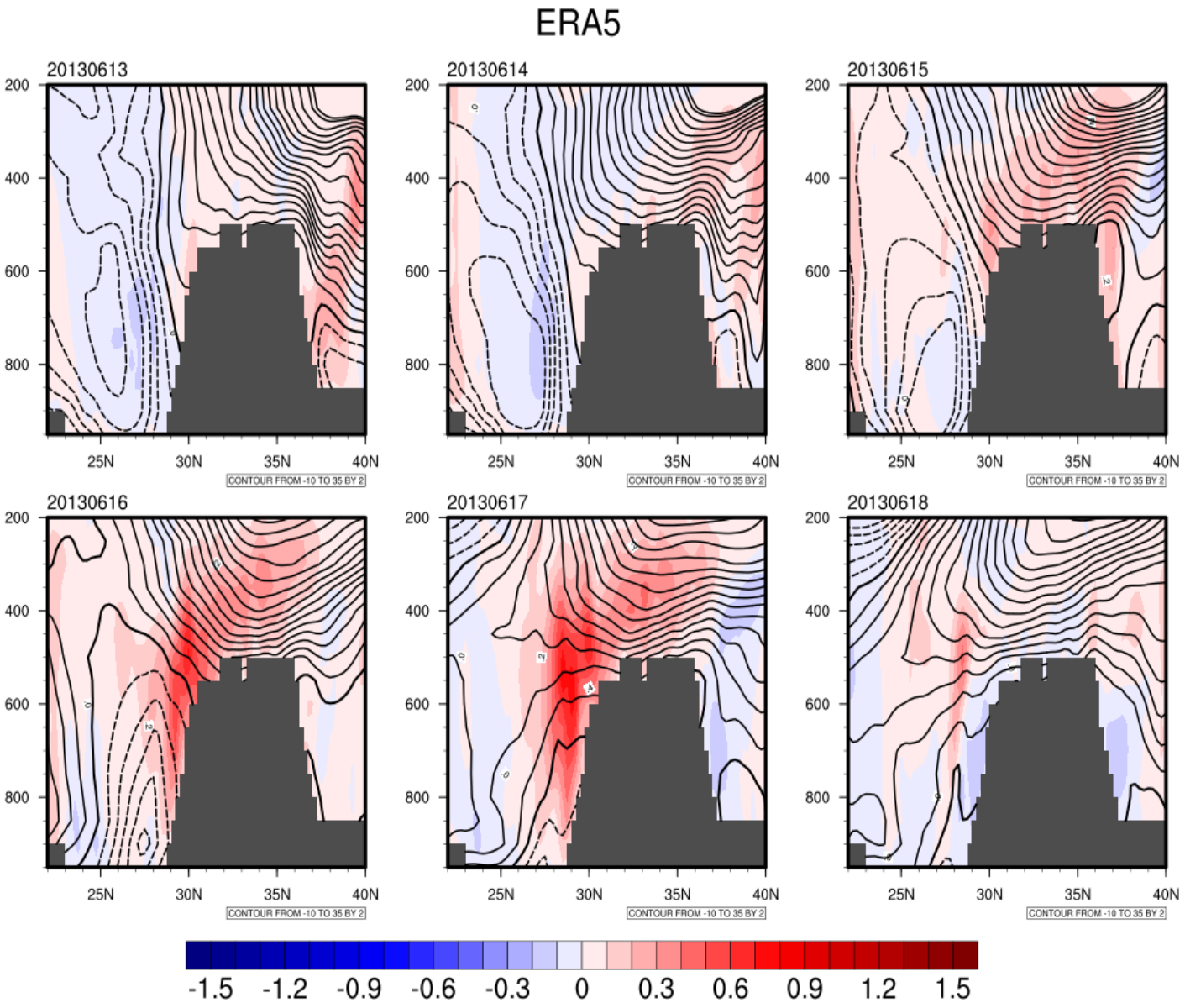

Figure 9: Height latitude profile evolution of vertical velocity (omega as shaded, upward positive *units hPa* s^{-1}) and zonal wind (contours,*units m* s^{-1})) for the days between 13-18June 2013. The plot is shown for longitudinal average range 75°E-85°E.

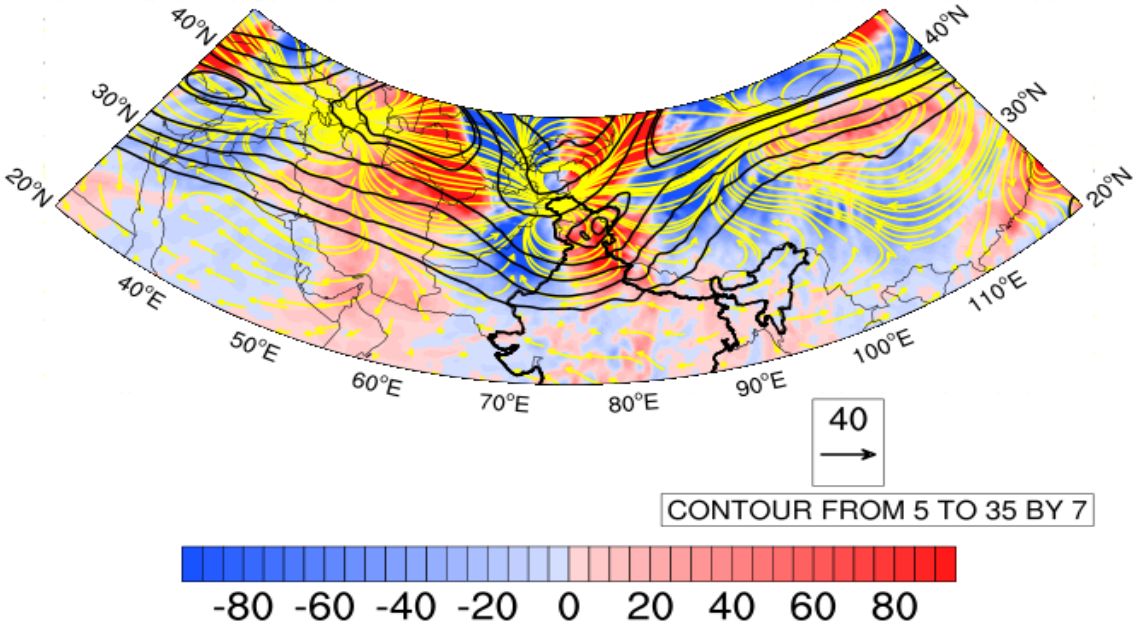

Figure 10: E-Vector divergence (shaded,$\nabla \cdot \mathbf{E}$), E-Vectors (yellow) for the period averaged between 10-30June 2013. The zonal wind contours for the days averaged between 14-18 June 2013 are also plotted to show the average jet position during the extreme event days. The eddies are defined by taking average for the period 10-30 June 2013.

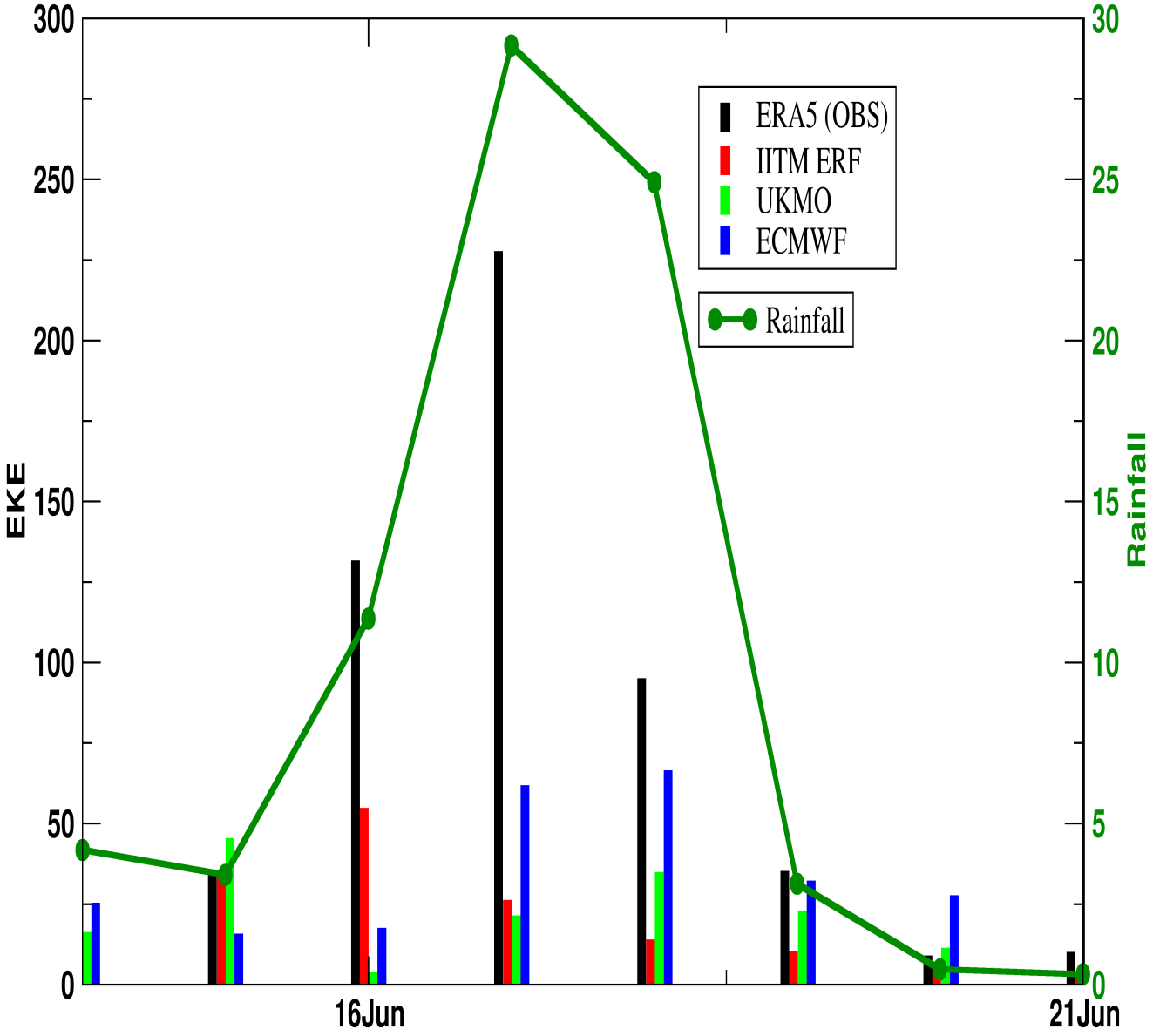

Figure 11: The time evolution of area averaged (28°-35°N;78°-82°E) eddy kinetic energy (EKE) from ERA5 reanalysis, UKMO model(green), ECMWF model (blue) and ERPAS model (red). For ERPAS and UKMO the ICs are 09June while for ECMWF the IC is 08June. Plots are shown from 10June 2013 onwards. ($Units: m^2 s^{-2}$)

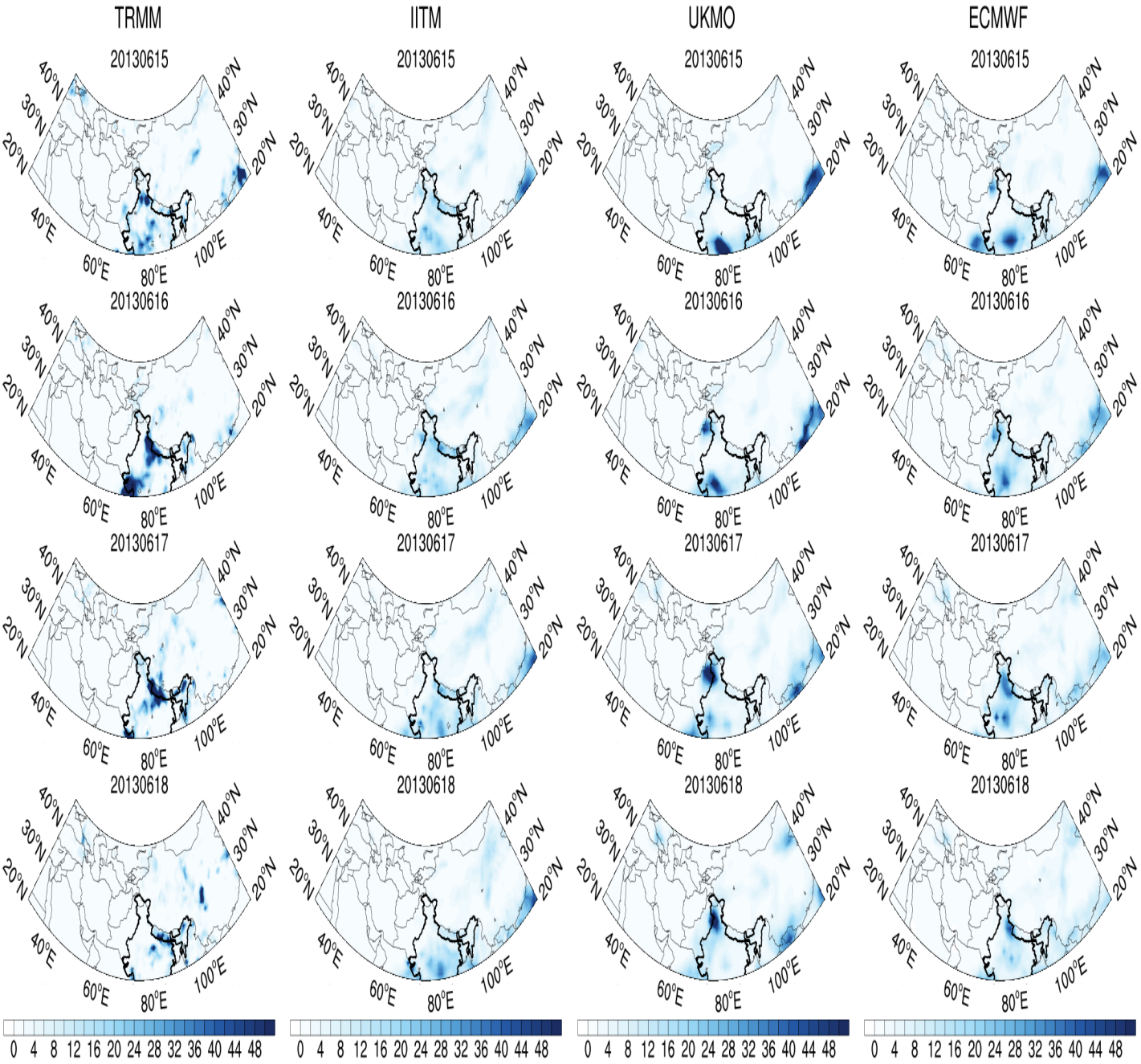

Figure 12: A comparison of rainfall evolution (shaded) for the period 15-18 June 2013 for different operational models and TRMM observation data. (unit: mm day^{-1})

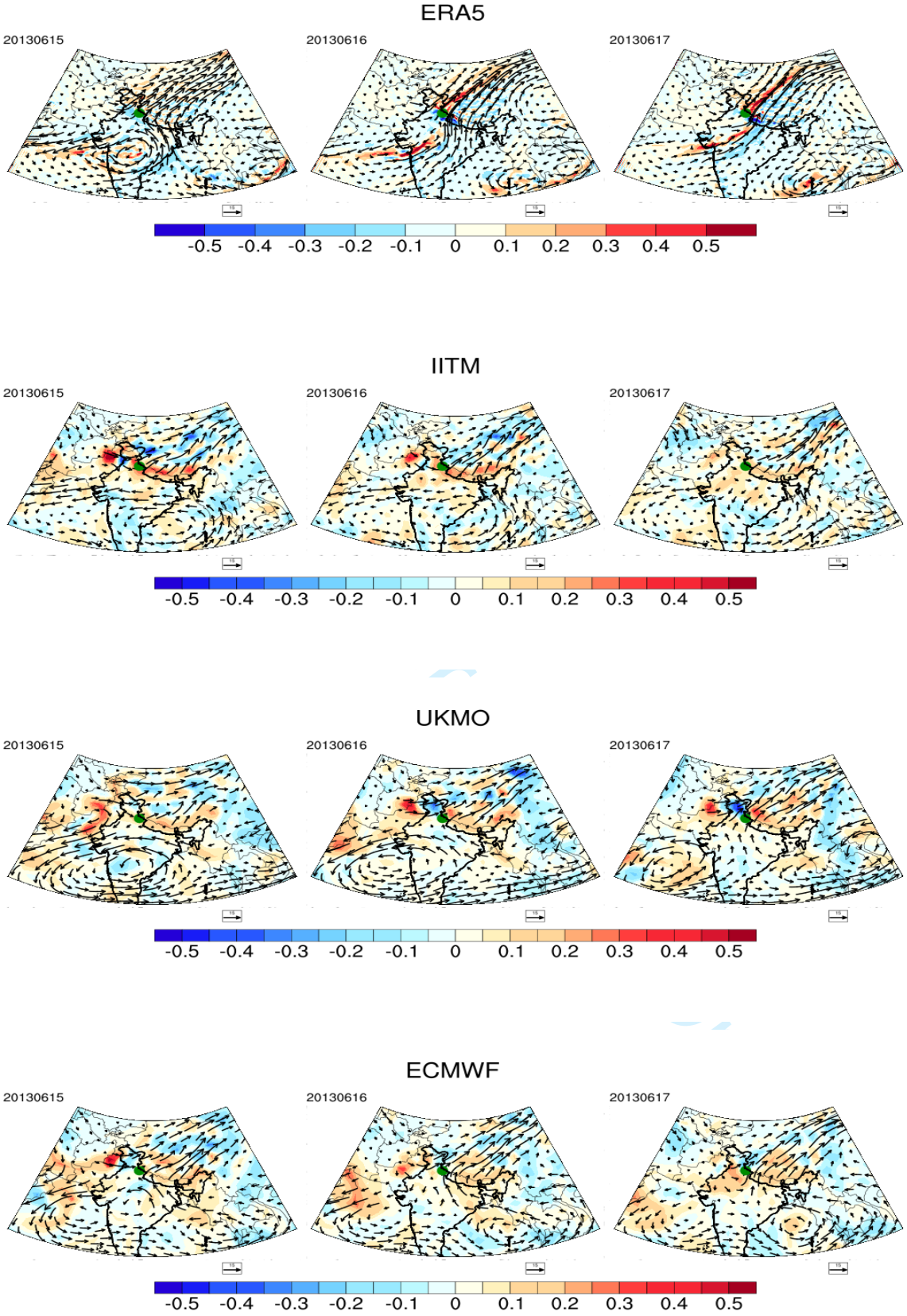

Figure 13: Plot showing the comparison of mositure transport vectors and moisture divergence (shaded) based on ERA5 reanalysis and different s2s model runs (mentioned in top of each panels).(units: div s^{-1}; transport vector m s^{-1})

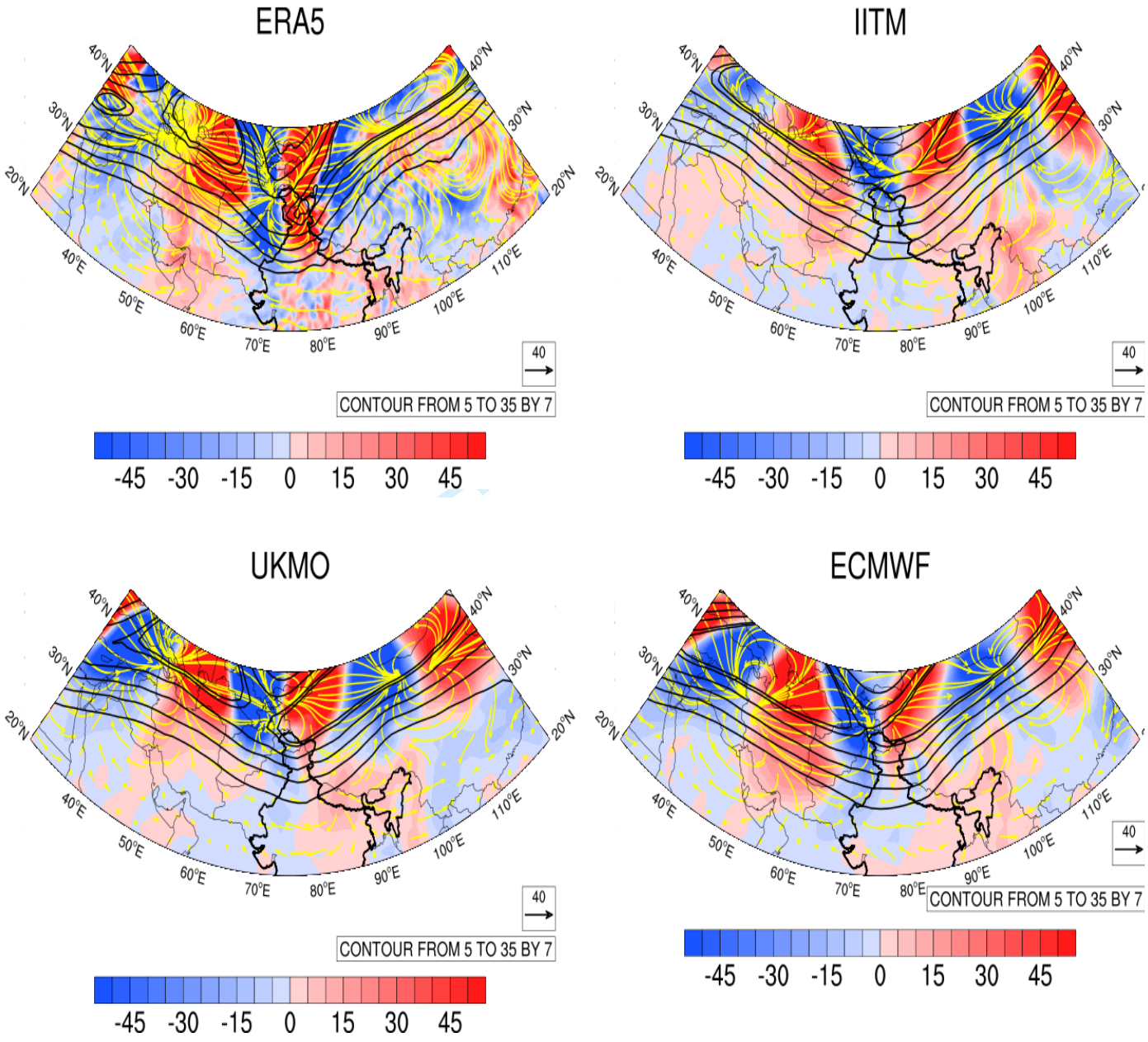

Figure 14: Plot showing the verification of E-vectors and E-vector divergence (shaded, $\nabla \cdot \mathbf{E}$) for different model runs with respect to observation for the days averaged between 14-18 June 2013.

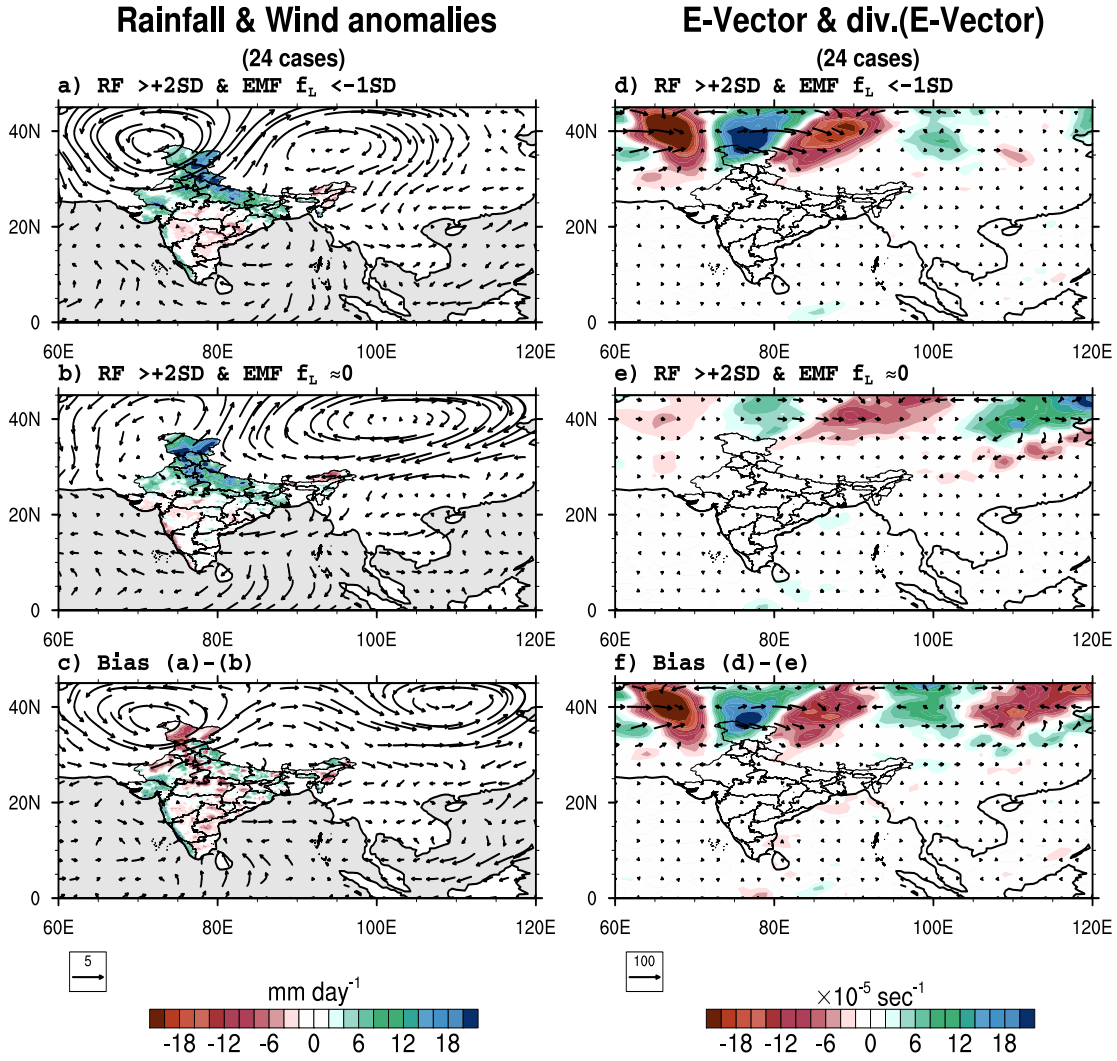

Figure 15: Rainfall and wind anomaly composites when (a) the standardized rainfall anomaly over north-Indian region is more than 2 standard deviation and the standardized EMF index area-averaged over a northern box (30°-45°N , 70°-95°E) is more than 2 standard deviation, (b) same as (a) but when the standardized EMF is close to zero. (c) shows the rainfall and wind vector bias for these two cases i.e. (a)-(b). (d) E-vector divergence composite and plot of E-vector at 200hPa for the same criteria as (a).(e) is same as (b) but for E-vector divergence composite and plot of E-vector at 200hPa. (f) same as (c) but showing the bias in E-vector divergence and E-vectors.

~~Dynamics of Tropical-Extratropical Interactions in the S2S forecast models and observations during the Monsoon Season over the Himalayan regions~~

Eddy transport, Wave-mean flow interaction, and Eddy forcing during the 2013 Uttarakhand Extreme Event in the Reanalysis and S2S Retrospective Forecast Data

Mahesh Kalshetti[1,3], Rajib Chattopadhyay[1,2]~~-~~, Kieran M R Hunt[4], R ~~phani~~[1]Phani[1], Susmitha Joseph[1], DR Pattanaik[2], AK Sahai[1]

1. Indian Institute of Tropical Meteorology, Pune-411008, India
2. India Meteorological Department, India
3. Savitribai Phule Pune University, Pune-411007
~~4.~~4. Department of Meteorology, University of Reading, UK

Corresponding Author

Rajib Chattopadhyay
India Meteorological Department, Pune 411005, India
~~Indian Institute of Tropical Meteorology, Dr. Homi Bhabha Road, Pashan, Pune- 411008.~~

Email: rajib@tropmet.res.in

Keywords

Extreme events; Extratropical-Tropical teleconnection; Indian monsoon, subseasonal forecasts

Abstract

In this study, to explore the wave-mean interaction during the monsoon season, we investigate (a) the potential role of transient eddy forcing and the wave-mean interaction on the monsoon weather during the June 2013 ~~Uttarakhand (India) extreme~~heavy rainfall event over the Himalayan regions (especially the Uttarakhand State of India and the nearby regions) and, (b) how they are captured in a set of operational models. Some studies have pointed out how prolonged breaks can occur due to extratropical trough incursions. However, there is a lack of clarity on how transient eddy forcing associated with such interactions can lead to modulation of monsoonal circulation~~, leading~~ or whether such interaction can lead to heavy rainfall events.

E-vector fields are analyzed to quantify ~~about~~ the eddy forcing from ~~the~~ extratropical transient eddies and the feedback mechanism between ~~the~~ transient eddies and the mean flow during June 2013. Analysis reveals that along with local factors (orography, moisture convergence), the large-scale heavy rainfall event over the Uttarakhand region during 16-17 June 2013 ~~event~~ was influenced by eddy forcing due to the intrusion of extratropical Rossby

waves over the Indian region. The location of eddy affects the location of regional occurrence of the eddy-mean interaction. Model hindcast analysis results suggest that operational models cannot forecast the upper-level eddy forced circulation patterns, and the improper representation of the E-vector divergence field leads to the underestimation of intensity and the spatial pattern of rainfall ~~pattern~~.

~~*1. Introduction*~~

~~It is well known that extratropical-tropical (E2T) interaction can cause prolonged *breaks* (low rainfall spells) over the Indian region due to intrusion of extratropical troughs and ridges during the monsoon season (RAMASWAMY, 1962; Raman and Rao, 1981; Krishnan *et al.*, 2009; Fadnavis and Chattopadhyay, 2017). However, in recent years studies have shown that extreme rainfall events over the Himalayan region are sometimes associated with the coexistence of both low-frequency monsoon intraseasonal oscillations and extratropical eddies (or Rossby waves or Western Disturbances). The eddy transport and fluctuations are evident through the associated heat and momentum transport towards or out of the tropics during the monsoon time, as shown in Kalshetti et al., (2020). Disturbances originating in the extratropics can locally shift the jet stream equatorward and thus disturbs the synoptic setup of the Indian summer monsoon. This intrusion is supposedly linked to extreme rainfall events like the 2010~~

Pakistan and 2013 Uttarakhand flood events (Hong *et al.*, 2011; Lau and Kim, 2011; Joseph *et al.*, 2015; Vellore *et al.*, 2016a; Sooraj *et al.*, 2020) and many similar weather events.

How does the extratropical intrusion create an extreme event? An extreme event can be dynamically defined as zones of strong vertical velocities with ample moisture supply from the boundary layer or lower troposphere (such as during monsoon time), which is likely due to strong ageostrophic components (Bohlinger *et al.*, 2019). Classic numerical experiments such as from (Hoskins and Karoly, 1981) and some recent case studies based on Eurasian blocking suggests that 2010 western Russian heatwave is forced by downstream Rossby wave propagation, with high-frequency Rossby waves also propagate southward. Thus, Rossby waves are often precursor of extreme weather events. The leading trough of the Rossby wave train triggered upward motion to the east, favoring deep convection leading to extreme flooding over Pakistan during 2010(Hong *et al.*, 2011; Lau and Kim, 2011). Studies have identified the thermal forcing and background moist processes over Indo-Pakistan arid region in the 16-18 days prior and are shown to be precursors for extreme rainfall events over the monsoon core zone (Sooraj *et al.*, 2020).

Similarly, some other studies suggest extreme rainfall events such as those that occurred over the Uttarakhand region during June 2013, result from an occluded frontal system developed in response to western disturbance and monsoon low. Occluded fronts caused mechanical lifting, thus the formation of the large organized storm over the study region

(Chevuturi and Dimri, 2016). The validity of the frontal theory of ageostrophic upliftment requires the validity of the ratio NH/f (N is Brunt-Väisälä frequency, f is Coriolis parameter and H being the depth of the fluid) as described in Hoskins (1982). For tropical atmosphere, the validity of this ratio is not well defined due to smallness of f. Also, as (Charney, 1969) suggested, such large scale lifting in the stably stratified tropical climate is not easily (or generally) possible due to lack of vertical coupling unless it occurs in the regions of active tropical deep cumulus convection on a much smaller spatial scale than the Rossby radius. Since the destabilization by latent heating due to moisture supply may be less over the orographic region over the Himalayas (where the event occurred) than the transient eddy forcing on the mean background (Wills and Schneider, 2018), it is possible that alternate eddy-driven theories may be more helpful.

Several studies have explored the eddy (i.e., transient synoptic disturbance) perspectives as mentioned earlier. The observation suggests that such extreme rainfall events occur invariably during monsoon time or, more specifically, due to the presence of low-pressure systems over the Indian subcontinent. Vellore et al. (2016b)and Hunt et al (2018a, 2018b) have looked into the extratropical intrusions of western disturbances in a detailed manner and described the presence of monsoon system and western disturbances as a sufficient condition for extreme events indicating presence of double eddies (western disturbances and monsoonal low pressure systems) during which interaction occurs as a plausible theory. Hunt et al (2018a, 2018b), based on clustering analysis, shows the composite structure, and also, they have described several

~~classes of such events with highlights on such presence of double eddies(western disturbances and monsoonal high frequency disturbances or low pressure systems). Another recent study (Hunt *et al.*, 2021) explained the extreme events in terms of the coexistence of the monsoon system and western disturbances during the extreme event for different classes of situations. They describe that extreme precipitation occurs as a result of their interactions, but their analysis uses the perspective of Hanley et al. (2001), which assumes pre-existence of an intense cyclonic storm (with substantial azimuthal eddy flux transfer, EFCs) co-located with jet stream and that this storm interacts with the upper-level troughs when EFCs cross certain thresholds. In such situations, the vertical coupling would be strong, as shown by Charney (1969) and developments of extreme events are possible. This EFC-based criterion is, however, not quantitatively verified in these studies.~~

~~The studies described above~~

1. Introduction

It is well known that extratropical-tropical (E2T) interaction can cause prolonged *breaks* (low rainfall spells) over the Indian region due to intrusion of extratropical troughs and ridges during the monsoon season (Ramaswamy, 1962; Raman and Rao, 1981; Krishnan *et al.*, 2009; Fadnavis and Chattopadhyay, 2017). However, in recent years, studies have shown that high-intensity rainfall events over the Himalayan region are sometimes associated with the

coexistence of low-frequency monsoon intraseasonal oscillations and extratropical eddies (or Rossby waves or Western Disturbances). The eddy transport and fluctuations are evident through the associated heat and momentum transport towards or out of the tropics during the summer monsoon, as shown in Kalshetti et al. (2020). Disturbances originating in the extratropics can locally shift the jet stream equatorward and thus disturb the synoptic setup of the Indian summer monsoon. These intrusions are supposedly linked to high-intensity rainfall events like the 2010 Pakistan and 2013 Uttarakhand floods (Hong *et al.*, 2011; Lau and Kim, 2011; Joseph *et al.*, 2015; Vellore *et al.*, 2016a; Sooraj *et al.*, 2020) and many similar weather events.

How does the extratropical wave intrusion create high-intensity rainfall over Northern India, especially over the Himalayan region? The high-intensity rainfall event can be dynamically defined as zones of strong vertical velocities with ample moisture supply from the boundary layer or lower troposphere (such as during monsoon time), which is likely due to strong ageostrophic components (Bohlinger *et al.*, 2019). Can a Rossby wave intrusion cause this high-intensity rainfall or other types of extreme events, e.g., heatwaves? Classic numerical experiments such as from Hoskins and Karoly (1981) and some recent case studies based on Eurasian blocking suggests that the 2010 western Russian heatwave was forced by downstream Rossby wave propagation (Trenberth and Fasullo, 2012), with high-frequency Rossby waves also propagated southward during the end of July (Lau and Kim, 2011). Thus, Rossby waves are often a precursor of extreme heatwave events. Similarly, the leading trough of the Rossby

wave train triggered upward motion to the east, favoring deep convection leading to extreme rainfall event-related flooding over Pakistan during 2010 (Hong *et al.*, 2011; Lau and Kim, 2011). Likewise, extratropical Rossby wave-linked convection is also reported in the tropical Pacific (Kiladis, 1998). Heavy rainfall, especially extreme events, is associated with mesoscale convective systems. Several studies on midlatitude convection showed that midlatitude Rossby waves are reinforced by mesoscale systems (Lillo and Parsons, 2017; Parsons *et al.*, 2019), which create downstream forced response. Some studies have also shown how mesoscale convective systems over the Pacific warm pool region get reinforced by Rossby-kelvin waves(Houze *et al.*, 2000), indicating the role of large-scale waves in local mesoscale precipitating systems. In addition to waves, studies have also identified thermal forcing and background moist processes over the arid region of Indo-Pakistan in the 16 to18 days prior and have shown them to be precursors for extreme rainfall events over the monsoon core zone (Sooraj *et al.*, 2020).

As mentioned in the last paragraph, the state of Uttarakhand in India witnessed heavy rainfall during 15-17 June 2013 with widespread reporting of a “cloudburst”-like scenario over the Kedarnath region in Uttarakhand. Some studies have demonstrated the role of mesoscale convective systems in cloudburst situations(Parida *et al.*, 2017). Other studies suggest high-intensity rainfall events such as those that occurred over the Uttarakhand region during June 2013 result from an occluded frontal system that developed in response to a western disturbance and monsoon low (Chevuturi and Dimri, 2016). The validity of the frontal theory

of ageostrophic uplift requires the validity (i.e., finiteness) of the ratio NH/f ($\boldsymbol{N}$ is Brunt-Väisälä frequency, $\boldsymbol{f}$ is the Coriolis parameter, and $\boldsymbol{H}$ is the depth of the fluid) as described in Hoskins (1982). In the tropics, the validity of this ratio is not well defined due to the smallness of f. Also, as (Charney 1969) suggested, such large-scale lifting in the stably stratified tropical climate is not easily (or generally) possible due to lack of vertical coupling unless it occurs in the regions of active tropical deep cumulus convection.

In addition to such localized extreme events during 16-17 June, heavy to very heavy rainfall occurred during this time over larger regions (in the synoptic scale, e.g., refer fig.2 of Joseph et al., (2015) or **Fig.12**). The coexistence of synoptic-scale heavy rainfall and Rossby wave intrusion may indicate that the transient eddies may be a dominant factor in comparison with other factors like local destabilization due to latent heating, which is already reported (e.g., Fig. 9b of (Wills and Schneider, 2018).

This eddy (i.e., transient synoptic disturbance) perspective has also been explored in several studies. Vellore et al. (2016b) and Hunt et al. (2018a, 2018b), using cluster composite analysis, looked into several extratropical intrusions of western disturbances in a detailed manner and described the presence of monsoon low-pressure systems and western disturbance as a necessary condition for heavy events. Another recent study (Hunt *et al.*, 2021) explained the extreme events in terms of the coexistence of monsoon low-pressure systems and western disturbances. They found that high-intensity precipitation occurs as a result of their

interactions, but their analysis uses the perspective of Hanley et al. (2001), which assumes the pre-existence of an intense cyclonic storm (with substantial azimuthal eddy flux transfer, EFCs which is a measure of local eddy forcing) co-located with the jet stream and that this storm interacts with the upper-level troughs when the eddy-induced azimuthal flux transfer measured by EFCs cross certain thresholds and provide necessary eddy forcing. This EFC-based criterion is, however, not quantitatively verified in these studies.

The studies described above indicate that the orography, monsoonal moisture flow, stability, and waves/eddies can contribute to the extreme as well as heavy rainfall event, but do not go into explaining this monsoon midlatitude ~~wave~~eddy interaction scenario as an eddy forcing problem on the mean flow (i.e., eddy-mean interaction perspective), and hence, though the earlier analysis highlights exchanges, they neglect a ~~wave-mean interaction perspective, i.e., interaction terms in vorticity tendency equations obtained by partitioning the fields into the mean and eddy terms(e.g. ef~~transient wave forcing perspective (e.g., refer eq. 1~~). in sec.3).~~ In the current analysis, we will focus on how (or whether) wave-mean interaction can be used to explain ageostrophic vertical velocities and rainfall that occurs during such events. ~~Unlike earlier studies, we will explain the intrusions in terms of transient eddy forcing (such as eddy flux convergence or divergence) associated with the Rossby waves intruding over the Indian region because of large-scale precursors, e.g., circumglobal teleconnection. Such impacts of high and low-frequency eddies (Synoptic Eddy Low-Frequency or SELF feedback) are studied~~

forSuch interactions perspective are often useful to study the mid-latitude low-frequency oscillations (Jin, 2010).

The eddy forcing approach is particularly useful if we want to know why the dynamical models fail to forecast such events at enough lead times for issuing alerts(i.e., whether there is inappropriate eddy forcing in the model), especially in the weather to extended-range forecast time scale. If such events originate due to low frequency (e.g., circumglobal) teleconnection pattern, which is supposed to have better predictability (because they are slowly evolving), why are such events not captured with good fidelity in the dynamical model forecast (e.g., refer **Fig.1**) as they are captured in midlatitude synoptic-scale forecasts? **Fig.1** shows that several operational dynamical models lack skill in predicting the event even at a one-week lead-time. The Uttarakhand extreme event of 2013 is popularly studied by many researchers and is a well-known event in which tropical-extratropical interaction is well documented (Dube *et al.*, 2014; Vellore and Jayant, 2014; Joseph *et al.*, 2015; Pattanaik *et al.*, 2015; Singh and Chand, 2015; Vellore *et al.*, 2016a; Kaur and Gupta, 2017). The question that arises here is that how to explain lack of skill in a dynamical framework. We hypothesize that eddy-mean interaction framework can be useful in understanding the skill (or lack of it) in dynamical models

In the current paper, we focus on the 2013 extratropical intrusion event over Uttarakhand (India). We elaborate on two aspects: (a) whether wave-mean interaction was significant during this event in addition to the earlier linear theories used to explore such events and (b) based on this transient eddy wave mean interaction formulation, whether such steps can be retraced or

~~evaluated in the dynamical models to understand the lack of skills in these models in forecasting these events. We computed the transient eddy forcing during the extreme event using the ***E-vector*** approach (Andrews and McIntyre, 1976; Hoskins *et al.*, 1983), which explains the eddy dynamical pathway for such events near subtropical jet streams (Sec.3).~~

Models fail to predict the rainfall pattern and amplitude over Uttarakhand with sufficient lead-time **Fig.1** shows that several operational dynamical models lack skill in predicting the rainfall event over Uttarakhand even at a one-week lead-time. Several models have these problems with events related to Rossby waves (e.g., forecast bursts as referred in (Lillo and Parsons, 2017). In addition to understanding the eddy-mean interaction during the intrusion, the eddy forcing approach can be useful if we want to know why the dynamical models fail to forecast such events at sufficient lead times for issuing alerts, especially in the weather to the extended-range forecast time scale. We hypothesize that the eddy-mean interaction perspective can be helpful in understanding the skill (or lack of it) in dynamical models.

The Uttarakhand extreme event of 2013 and the high-intensity rainfall over large regions has been studied by many researchers and is a well-known event in which tropical-extratropical interaction is well documented (Dube *et al.*, 2014; Vellore and Jayant, 2014; Joseph *et al.*, 2015; Pattanaik *et al.*, 2015; Singh and Chand, 2015; Vellore *et al.*, 2016a; Kaur and Gupta, 2017). Hence, owing to the good documentation of linear perspective, the current paper selects this event and discusses the eddy-mean interaction perspective. We elaborate on two aspects: (a) whether wave-mean interaction was significant during this event in addition to the earlier

linear theories used to explore such events and (b) based on this transient eddy wave mean interaction formulation, whether such steps can be retraced or evaluated in the dynamical models to understand the lack of skill in these models when forecasting such events. The study is arranged as follows: Sec.2 describes the study area, data used, and formal methodology. In sec.3, we computed the transient eddy forcing during the extreme event using the ***E-vector*** approach (Andrews and McIntyre, 1976; Hoskins *et al.*, 1983), which explains the eddy dynamical pathway for such events near subtropical jet streams. Sec.4 describes the application of the E-vector approach while describing the life cycle of tropical-extratropical interaction while describing the intrusion event during the Uttarakhand heavy rainfall event (June 2013). Sec.5 describes the operational forecasts of the event, and the results are discussed, summarized, and concluded in Sec.6.

2. *Study area, Data, and Methods*

2.1. Study area

~~The natural disaster in the form of landslide and flash flood occurred due to heavy precipitation over Uttarakhand region (29°-31°N, 78°-81°E), India on 16-17 June 2013. The Uttarakhand is part of the region of complex orography along Western Himalaya. The Western Himalaya region surrounds snow-covered peaks, crest, glaciers, valleys, and perennial river basins (Parida *et al.*, 2017).~~

~~*2.2. Observation Data*~~

The atmospheric (retrospective) reanalysis datasets from the fifth-generation European Centre for Medium-Range Weather Forecasts (ECMWF) Atmospheric Reanalysis of the global climate (ERA5) is used as a proxy for observation of dynamical variables. ERA5 data is produced by Copernicus Climate Change Service (C3S) at ECMWF. ERA5 climate data is available in a 0.25° × 0.25° grid from 1979 to within five days of real-time (Hersbach *et al.*, 2020). The primary data used in this study are zonal (u ms^{-1}), meridional (v ms^{-1}), vertical (ω Pa s^{-1}) wind, temperature (K) at 200hPa, and geopotential height (m) at 500hPa. The observed precipitation is obtained from Tropical Rainfall Measuring Mission (TRMM) Multi-satellite Precipitation Analysis (TMPA, 3B42) (Huffman *et al.*, 2007).

2.3. Models

The IITM-ERPAS or ERPAS (**E**xtended **R**ange **P**rediction for **A**pplication to **S**ociety, run at Indian Institute of Tropical Meteorology (IITM), Pune, India and is also the current operational extended range model of India meteorological Department), UKMO (United Kingdom Meteorological Office, Met Office, Devon, United Kingdom), and ECMWF (European Centre for Medium-range Weather Forecasts, ECMWF, Reading, United Kingdom) are the S2S reforecast models used in this study. All these S2S models are used for real-time operational forecasts. All the observed and model data set regridded to 1° ×1° spatial resolution. Except for IITM-ERPAS (Abhilash *et al.*, 2014) the *UKMO,* and ECMWF forecast data access through the S2S database maintained by the ECMWF (Vitart *et al.*, 2017). ERPAS data is obtained

~~from IITM-IMD operational database maintained at IITM. Each S2S model has a control member (using a single unperturbed initial condition) and several perturbed members produced for sampling uncertainty in the initial condition. **Table 1** shows the basic features of S2S models (Vitart *et al.*, 2017). In the present study, the model forecast is taken from the closest available initial condition on 9th June 2013 for ERPAS and UKMO and for 10th June 2013 for ECMWF.~~

The natural disaster, in the form of landslides and flash flooding, occurred due to heavy precipitation over the Uttarakhand region (29°-31°N, 78°-81°E), India on 16-17 June 2013. Uttarakhand is part of the region of complex orography along the Western Himalayas. The Western Himalaya region surrounds snow-covered peaks, crest, glaciers, valleys, and perennial river basins (Parida *et al.*, 2017).

2.2. Observation Data

The atmospheric (retrospective) reanalysis dataset from the fifth-generation European Centre for Medium-Range Weather Forecasts (ECMWF) Atmospheric Reanalysis of the global climate (ERA5) is used as a proxy for observation of dynamical variables. ERA5 data are produced by the Copernicus Climate Change Service (C3S) at ECMWF. ERA5 climate data is available in a 0.25° × 0.25° grid from 1979 to within five days of real-time (Hersbach *et al.*, 2020). The primary data used in this study are zonal (***u***, ms^{-1}), meridional (***v***, ms^{-1}), vertical (ω Pa s^{-1}) wind, temperature (K) at 200hPa, and geopotential height (m) at 500hPa. The observed

precipitation is obtained from Tropical Rainfall Measuring Mission (TRMM) Multi-satellite Precipitation Analysis (TMPA, 3B42) (Huffman *et al.*, 2007). 3B42 data contains a gridded, satellite-based merged infrared precipitation data (mm/hr), with a 3-hour temporal resolution and a 0.25-degree spatial resolution. We have converted the sub-daily data to daily data.

2.3. Models

The Indian Institute of Tropical Meteorology (IITM) extended range forecast (IITM-ERPAS) runs (Abhilash *et al.*, 2014; Sahai *et al.*, 2019), UKMO (United Kingdom Met Office), and ECMWF (European Centre for Medium-range Weather Forecasts) forecast runs are the S2S reforecast model runs used in this study. All the observed and model data set regridded to 1° ×1° spatial resolution and daily temporal resolution with appropriate pre-processing. Except for IITM-ERPAS (Abhilash *et al.*, 2014), the UKMO and ECMWF forecast data were accessed through the S2S "*instantaneous and accumulated*" database maintained by ECMWF (Vitart *et al.*, 2017). ERPAS data is obtained from the IITM-IMD operational database maintained at IITM. Each S2S model has a control member (using unperturbed initial conditions) and several perturbed members produced for sampling uncertainty in the initial conditions**.** In the present study, the model forecast is taken from the closest available initial condition on 9th June 2013 for ERPAS and UKMO and for 10th June 2013 for ECMWF when the forecast of 16-17 June lies in the synoptic range. Spatial plots are shown for the ensemble mean (IITM-ERPAS-16-

member mean; UKMO-7 member (including one control member); ECMWF-11 member (including one control member) unless stated otherwise.

3.0 A schematic description of the ~~Life Cycle~~life cycle of extratropical intrusion

The extratropical eddies ~~have~~ are associated with colder extratropical air ~~mass~~masses and ~~strong~~stronger westerly momentum ~~at~~in the upper ~~level compared to~~levels than tropical monsoonal flow ~~at upper level.~~. The ~~convergence~~transport of this eddy momentum and heat flux over the Indian region in the presence of low-frequency monsoonal background (monsoon intraseasonal oscillations and low ~~-~~pressure systems ~~(Goswami, 2012)~~(Goswami, 2012)) can significantly impact~~.~~ the local flow as it imparts additional heat and momentum in the local budget terms (cf. eq. one and eq.2 in sec.3.2). The event life cycle can thus ~~can~~ be hypothesized to have three major stages: (i) southward *digging* (or intrusion ~~)~~with amplification) of troughs associated with a meandering of ~~Jetstream,~~(the subtropical jet stream, (ii) transient eddy forcing onto the mean flow, and (iii) reversal of jet stream (or weakening of southward intrusion) position with the restoration of monsoon flow. These are described below.

3.1 Linear Process: Intensification of digging trough over the Indian Region during the monsoon season

Rossby ~~wave~~waves show meridional propagation, but the southward intrusion of the Rossby wave ~~is prohibited to~~in the ~~deep~~ tropical region ~~into the Indian region~~is generally restricted due to the presence of critical latitudes where the phase velocity of the wave approaches the

zonal (westerly) wind speed, ~~below which no zonal propagation of Rossby wave phases is seen.~~and the waves are absorbed along the critical latitudes as it propagates equatorward (Karoly and Hoskins, 1982). Normally Rossby waves break, and mixing of potential vorticity (PV) occurs with the decay of the wave~~.~~ leading to mid-latitude to tropical exchange (Homeyer and Bowman, 2013). However, Rossby waves can dig deep south into the tropical region ~~provided the critical latitudes shifted southward due to~~due to the ducting effect or southward extension of westerlies over a certain region ~~(Webster and Holton, 1982)~~(Webster and Holton, 1982). ~~Southward~~ The southward shifting/meandering of the westerly jet stream ~~southward~~ due to the presence of the blocking high can provide such ducts where Rossby ~~wave~~waves can propagate into the tropics. At the same time, ~~the~~ cyclonic Rossby wave breaking can be prevented, and it can intensify over the Indian region in the presence of monsoonal instabilities. It can be seen as follows:

Consider the conservation of PV~~:~~ $\frac{\zeta + f}{\frac{\partial p}{\partial \theta}} \approx Const$ in the absence of diabatic heating: $\frac{\zeta + f}{\frac{\partial p}{\partial \theta}}$

$$\approx Const$$

If a cyclonic phase Rossby wave (positive vorticity) comes ~~to~~into a region of higher thickness $(\frac{\partial p}{\partial \theta})(\frac{\partial p}{\partial \theta})$ and f decreases, relative vorticity has to increase. For more detailed explanations of the PV aspects of synoptic developments, the reader refers to case studies discussed in ~~(Hoskins, 1997).~~Hoskins (1997). Thus, the cyclonic vorticity induced by the Rossby wave can

intensify (or ~~atleast~~at least its amplitude does not decay) depending on the strength of the denominator, as a southward extension means a decrease in f. Typically such thickness would increase in the presence of strong heating. Hence the Rossby wave would strengthen and not break or weaken in the presence of background instability that modifies $(\frac{\partial p}{\partial \theta})$. Such increased background thickness ~~during some period~~ can be provided by latent heat release associated with ~~the intraseasonal monsoon oscillation~~modes of subseasonal variability when the organized convection stays over the foothills of the Himalayas.

The intruded (or possibly intensified) Rossby wave can create a digging trough, leading to indirect ageostrophic circulation with the high vertical velocity at the jet exit region. ~~The upper-level divergence force lower-level convergence via the indirect circulation~~ (e.g., Chapter 2.3 and ~~if moisture present, it support convection. This forced convection is then enhanced due to indirect circulation.~~

Fig. 2.7 of Lackmann (2012). In addition to such direct effects, the strengthening or weakening of the westerly or the Rossby wave depends on the growth of ~~the~~ eddy instability, which can extract energy from the mean flow (Held and Phillips, 1989). The response of the mean state due to ~~the~~ transient eddy forcing ~~would be~~is essential to control the growth or decay of the Rossby wave. This nonlinear process is discussed next.

3.2 Nonlinear process: the transient eddy forcing of the mean flow and ~~Monsoonal~~ Monsoon time mean background

~~There are numerous studies on empirical evidence of feedback of transient eddies to maintain time mean flow and how eddies extract energy from the mean flow or give energy to the mean flow(Lau and Holopainen, 1984; G. Branstator, 1995; Jin, 2010; Tan *et al.*, 2014). In particular recent study shows transient eddy feedback for Rossby waves over the orographic region is more important than latent heating (Wills and Schneider, 2018). The eddy mean interaction for the horizontal momentum equations assuming zonal wind (u) and meridional wind (v) compartmentalized into mean and transient eddy components~ $(\boldsymbol{\mathcal{V}} = \overline{\boldsymbol{\mathcal{V}}} + \boldsymbol{\mathcal{V}}', \boldsymbol{\mathcal{V}} = (u,v)$ ~~) (Hoskins et al. 1983; James 1994; Williams et al. 2007)is given by:~~

$$\frac{\overline{D}\overline{u}}{Dt} = fv_{am} + \nabla.E \quad \text{----------(1a)}$$

$$\frac{\overline{D}\overline{v}}{Dt} = -fu_{am} - (\overline{u'v'})_x \quad \text{----------(1b)}$$

$\frac{\overline{D}}{Dt} = \overline{u}\frac{\partial}{\partial x} + \overline{v}\frac{\partial}{\partial y}$, ~~$-$~~ $( )_x = \frac{\partial}{\partial x}$, ~~$-\nabla$ is~~There are numerous studies demonstrating empirical evidence of the role of the transient eddies in maintaining the time-mean flow and how eddies extract energy from the mean flow or give energy to the mean flow (Lau and Holopainen, 1984; G. Branstator, 1995; Jin, 2010; Tan *et al.*, 2014). In particular, a recent study (Wills and Schneider, 2018) showed transient eddy feedback for Rossby waves over the orographic region is more important than latent heating. The eddy mean interaction for the horizontal momentum equations, assuming zonal wind *(u)* and meridional wind *(v)* compartmentalized into mean and transient eddy components: $(\boldsymbol{\mathcal{V}} = \overline{\boldsymbol{\mathcal{V}}} + \boldsymbol{\mathcal{V}}', \boldsymbol{\mathcal{V}} = (u,v))$ (Hoskin et al. 1983; James 1994; Williams et al. 2007) is given by:

$$\frac{\overline{D}\overline{u}}{Dt} = f + \nabla.E \text{----------(1a)}$$

$$\frac{\overline{D}\overline{v}}{Dt} = -f u_{am} - (\overline{u'v'})_x \text{----------(1b)}$$

$\frac{\overline{D}}{Dt} = \overline{u}\frac{\partial}{\partial x} + \overline{v}\frac{\partial}{\partial y}$, $(\,)_x = \frac{\partial}{\partial x}$, ∇ is the horizontal gradient operator and f is the Coriolis parameter. $\boldsymbol{V_{am}} = (u_{am}, v_{am})$ $V_{am} = (u_{am}, v_{am})$ is the "*modified ageostrophic*" wind given by $\overline{\boldsymbol{v_{am}}} = \overline{\boldsymbol{v}} - \boldsymbol{f}^{-1}\boldsymbol{k} \times \nabla(\overline{\boldsymbol{\phi}} + \overline{\boldsymbol{v}'^2})$. For more details refer $\overline{v_{am}} = \overline{v} - f^{-1}k \times \nabla(\overline{\phi} + \overline{v'^2})$. Refer to Appendix A of Hoskins et al., (1983) for more details.

$\boldsymbol{E}$ in eqnthe equation. (1a) is the so-called E-vector defined as:

$$\boldsymbol{E} = \left(\overline{\boldsymbol{v}'^2} - \overline{\boldsymbol{u}'^2}, -\overline{\boldsymbol{u}'\boldsymbol{v}'}\right) \text{----------(2)}$$

Where $\overline{v'^2} - \overline{u'^2}$ *= Ex, Eddy anisotropy or asymmetry,* $-\overline{u'v'}$ *= Ey, eddy momentum flux transport (EMF) .*

The E-vector is a generalized form of Eliassen-Palm flux (Andrews and McIntyre, 1976), i.e., and can be used to estimates the local impact of transient eddies (Hoskins *et al.*, 1983; James, 1994; Trenberth, 2002)(Trenberth, 1986).

The E-vector is a generalized form of Eliassen-Palm flux (Andrews and McIntyre, 1976) and can be used to estimate the local impact of transient eddies (Hoskins *et al.*, 1983; Trenberth, 1986; James, 1994).

The above relations suggest that athe E-vector flux divergence can change in mean zonal can be brought by the E vector flux divergencezonal and meridional wind (assuming

other factors like friction are negligible in the upper level~~))~~, i.e~~.~~, eddies can force the mean flow. Divergence of the E-vector can cause acceleration of mean flow, and convergence can decelerate the mean flow. In a monsoonal setting, if we ~~consider~~take the terms in the LHS of Eq.1 as representing the mean monsoonal quasi-stationary background, the second term in the RHS can be interpreted as the eddy forcing term arising due to extratropical intrusions or similar low-pressure systems. Depending on the sign of the eddy convergence, the eddy can either grow (or extract energy from mean flow) or they can dissipate by supplying energy to the monsoonal mean flow~~. To understand and estimate the impact of this eddy forcing, we will use the~~ (also refer to (Held and Phillips, 1989). To understand and estimate the impact of this eddy forcing during the Uttarakhand event, we will use this E-vector formalism.

~~The E-vector is also related to transient eddy vorticity flux convergence and divergence. It can be shown that,~~ $\nabla.\overline{\boldsymbol{u}'\boldsymbol{\zeta}'} \approx \frac{d}{dy}(\nabla.\boldsymbol{E})$ ~~.....(3)~~

~~Then from Eq.1 and Eq.3 we can see that an E-vector framework provides a first-hand idea of the transient eddy forcing and zonal asymmetries imparted by the *transient* eddies (Hoskins *et al.*, 1983; Trenberth, 1986)in the momentum and the vorticity equations. Also plotting of E-vectors, i.e. (Ex,Ey) can give an idea about the direction and location of eddy convergence. The E-vector approach can be used to study both zonally asymmetric tropical (Leroux *et al.*, 2010) and extratropical transport patterns (Novak *et al.*, 2015).~~

The E-vector is also related to transient eddy vorticity flux convergence and divergence. It can be shown (Hoskins *et al.*, 1983) that:

$$\nabla.\overline{u'\zeta'} \approx \frac{d}{dy}(\nabla.\boldsymbol{E}) \quad \ldots\ldots\ldots\ldots\ldots\ldots\ldots\ldots(3)$$

Then, from Eq.1 and Eq.3, we can see that an E-vector framework provides a first-hand idea of the transient eddy forcing and zonal asymmetries imparted by the *transient* eddies (Hoskins *et al.*, 1983; Trenberth, 1986) in the momentum and the vorticity equations. Also, plotting of E-vectors, i.e. (Ex, Ey), can give an idea about the direction and location of eddy convergence. The E-vector approach can be used to study both zonally asymmetric tropical (Leroux *et al.*, 2010) and extratropical transport patterns (Novak *et al.*, 2015). The above discussion is only based on the mechanical effects of eddies. A complete quasigeostrophic discussion including the thermal effects of eddies by defining a third component in E-vector using temperature (T) and meridional wind ($\sim\overline{v'T'}$) can also be made analogously but is beyond the scope of our study.

3.3 *Extratropical ~~Intrusion~~intrusion and ~~extreme~~heavy rainfall events*

The next question is, how are the extratropical intrusions or the eddy forcing are linked to the ~~extreme~~high-intensity rainfall events? ~~Based on~~ We can have two possibilities based on the above two sections (3.1 and 3.2~~), we can have two possibilities.~~). First, a convergence of eddy flux can be interpreted as a positive~~-~~, i.e., cyclonic curl directly introduced in the mean flow (eq.12 and 13 of Williams et al., ~~*2007*).~~(2007). In a monsoon environment, this can invigorate the existing monsoonal convergence directly over a region where the curl is created

(such as when a monsoon trough exists over the foothills of the Himalayas). The second possibility is through an ageostrophic secondary circulation mechanism. The generation of cyclonic (anticyclonic) vorticity ~~at~~in the lower ~~tropospheric region~~troposphere (transverse circulation dynamics) is associated with the formation of surface lows and indirect circulation (e.g~~.~~., Fig.2 of Hoskins 1982). Such circulation will lead to the generation of ageostrophic vertical velocity, and depending on local factors (like orography and moisture), ~~extreme precipitation~~dramatic intensification can occur over the elevated topographies ~~(Uccellini and Johnson, 1979; Vellore *et al.*, 2016a; Hunt *et al.*, 2021)~~(Uccellini and Johnson, 1979; Vellore *et al.*, 2016a; Hunt *et al.*, 2021), ~~such~~leading to extreme precipitation, as ~~over the Himalayan region.~~a result of a jet streak excitation as shown by Hunt *et al.*, (2021). This ageostrophic motion associated with the indirect circulation can extract ~~the~~ kinetic energy ~~of~~from the mean flow in the downstream region of the jet exit, where it is super-geostrophic ~~(Lau, 1979).~~(Lau, 1979). Extreme precipitation can result from strong ageostrophic vertical upward motion restoring ~~the~~ static stability. Based on Orlansky and Sheldon~~(1995)~~ (1995), the quasigeostrophic omega equation can be written as:

$$f_0{}^2\frac{\partial}{\partial z}\left(\frac{1}{\rho}\frac{\partial}{\partial z}\rho w\right) + N^2\nabla^2 w = s_g + s' \quad \text{~~----------(4)~~}$$

$$f_0{}^2\frac{\partial}{\partial z}\left(\frac{1}{\rho}\frac{\partial}{\partial z}\rho w\right) + N^2\nabla^2 w = s_g + s' \quad \text{----------(4)}$$

Where~~,~~ w is the vertical velocity, ρ is the density ~~and~~ f_0, f_0 is the Coriolis parameter ~~and~~ N^2, N^2 is the Brunt-Vaisalla frequency~~,~~ s' and s' is the source term involving friction, diabatic

heating, and meridional gradient of Coriolis parameter. s_g is the source term involving geostrophic quantities, (denoted by ***g*** indicated in the suffix), which Sutcliff Sutcliffe approximated as: $s_g = 2$|:

$$s_g = 2|\mathrm{f}\,\partial \boldsymbol{V}_g/\partial \partial \boldsymbol{V}_g/\partial \mathrm{z}|\frac{\partial \zeta_g}{\partial l}|\frac{\partial \zeta_g}{\partial l}| \text{ ,---------(5)}$$

where ***l*** is a unit coordinate aligned along the thermal wind direction and v_g is the geostrophic wind. From Eq (4), (5), (3)), and (1) ,), it is clear that ζ_g as well as $\partial \boldsymbol{V}_g/\partial \mathrm{z}\zeta_g$ *as well as* $\partial V_g/\partial z$ can be forced/modulated by eddy forcing withthrough the generation of vertical velocities. $\nabla.\boldsymbol{E}\nabla.E$ forces the zonal mean wind, which then changes the vertical shear, subsequently changing the source term s_g. An extremes_g. A large increase in vertical shear due to E--vector divergence would then lead to an extremea proportional increase in vertical velocity, resulting in extreme rainfall. Under the right conditions (e.g., moisture supply), increased vertical velocity can result in an increase in rainfall. The jet will move back to the original position after the Rossby wave has propagated out (or dissipated). The cloud--free conditions restore the horizontal meridional (north-south) gradients of temperature, forcing the jet to move back to its normal position. The mechanisms explained in this section isare summarized in **Fig.2**. The theoretical mechanism as proposed here can be verified through the diagnosis ofby diagnosing the direct (mean flow modification e.g., cf eq. 1) and indirect (transverse circulation) mechanism based on the E-vector field will be explored in the next session.

4.0 The lifecycle of extratropical intrusion during the 2013 Uttarakhand extreme event

In the context of the sequence of events described in sec.3, the following section describes the precipitation and circulation plots to quantify the linear and nonlinear perspectives during this event. To understand the nature of the extratropical intrusion, we plot the first two components of E-Vectors (~~Eddy~~eddy asymmetry term $\left(\overline{u'^2} - \overline{v'^2}\right)\left(\overline{u'^2} - \overline{v'^2}\right)$and the eddy momentum flux transfer term$(\overline{u'v'})$ $(\overline{u'v'})$ or the EMF term) area averaged over a domain north of the Uttarakhand (30°-40°N;75°-82°E) region in **Fig.3a.** The primes are defined with respect to ~~a 3 week~~the monthly mean ~~10-30June~~for June 2013. The plot shows that there is strong eddy asymmetry $\overline{v'^2} \gg \overline{u'^2}$ $\overline{v'^2} \gg \overline{u'^2}$ during 16-17 June 2013 and strong northward transfer of EMF. ~~The mean denotes the monthly mean, and the prime represents the deviation from this mean.~~ Such meridional elongation is significant and consistent with theory in the sense that it indicates southward phase propagation associated with northward momentum transfer~~. This meridional intrusion would be discussed in detail in sec.4.2.~~ (e.g., sec. 3b of (Waterman and Hoskins, 2013) A similar EMF flux but weak eddy asymmetry amplitude are seen during 7-9 June. This implies that both flux transfer and eddy asymmetry could play an essential role during this event. This meridional intrusion will be further discussed in detail in sec.4.2. Next, we will see the synoptic situations during this time.

4.1 Precipitation and circulation during the event: synoptic-scale nature of the event

~~In order~~**Fig.3a** shows the strengthening of the eddy asymmetry and EMF index (first and the second components of the E-vector), which helps to understand the low-frequency intrusion over the Indian region (Kalshetti *et al.*, 2021). To understand the synoptic ~~situations~~situation, we first ~~analyse~~analyze the precipitation during June 2013. **Fig. 3b** shows the northward propagation based on 20-80 days Lanczos-filtered TRMM precipitation data during June 2013. It shows clear intraseasonal northward propagation in this band ~~band~~. Around ~~16-17th~~13-17 June, the rainfall band ~~has~~ strengthened due to the expected monsoon progression after the onset phase ~~and is also seen in Fig.1. Fig.3a shows the strengthening of the EHF and EMF index, which defines the low-frequency intrusion over the Indian region (Kalshetti *et al.*, 2021).~~ (also refer to **Fig.1**). Similarly, **Fig.4** shows the evolution of the rainfall and the 200hPa wind pattern~~, which confirms the~~. The meandering contours confirm the deeper southward movement of the jet stream. staying southward of its climatological mean position during summer (~35°N). The temporal evolution plots in **Fig.4** show how the blob of precipitation evolves and decays over the Uttarakhand region. It is clear from this plot that the rainfall band spans over larger areas spanning a few thousand ~~kilometres~~square kilometers, indicating that the event which caused the ~~extreme~~ high-intensity rainfall is not a purely local extreme event phenomenon and is likely to be correlated with large-scale structures. This large-scale nature is further confirmed from the vorticity plots in **Fig.5**. The temporal evolution on 16th June and 17th June shows cyclonic vorticity advection with strong vorticity bands moving eastward with the additional formation of jet streaks~~. The plot also shows the~~ (on 16th June, the

strongest vorticity shading is in the southward descending branch west of 75°E and on 17th June it is east of 7°5E in the northward ascending branch). The contours of EMF terms ~~shows~~show strong northward (i.e., positive contours) transport of eddy momentum. Thus, cyclonic vorticity advection could be responsible for creating anomalous eddy momentum fluxes, and hence the Uttarakhand region shows ~~stronger~~more substantial eddy forcing ~~over~~ during this period as compared to other days in June 20013.

In addition to the extratropical system, as shown in **Fig. 3**, a low-pressure system ~~is~~was also propagating over the Indian region. The low-level circulation and the sea-level pressure pattern are shown in **Fig.6.** The strong low-level ~~system~~circulation is associated with ~~the~~ strong moisture inflow. Also, the surface pressure shows negative anomalies over northwest India and positive anomalies over the eastern part along the Bay of Bengal. Strong northerlies and anomalous high pressure and low-~~-~~pressure regions are also visible over the Afghanistan region, indicating the existence of upper-~~-~~level waves ~~over this region.~~. How is the moisture ~~transport~~transported in the upper level? We plot the 500-200hPa averaged moisture transport (***uq***, ***vq***~~),~~) and see the strong moisture outflow from the southern side, particularly from the Bay of Bengal low-pressure system towards the Uttarakhand region in **Fig.7a-d**. The north-westerly moisture transport is strong in the upper level, with the dominant source of moisture ~~is~~being the Bay of Bengal ~~taking a north-westerly turn during this period~~. The static stability plots (**Fig.7e-h)** also ~~shows~~show a ~~robust north-south~~strong meridional gradient with ~~the~~ stability decreasing ~~over~~northwest to southeast over the location of the extreme ~~event location~~ rainfall

534 during 16-17th June 2013~~.~~ (blue shading). Thus, ~~Fig~~**Figs.3-7** ~~confirms~~confirm the presence of
535 both the extratropical system and the tropical system during this period with adequate
536 monsoonal and extratropical influence over the Uttarakhand region—. In the next section, we
537 will elaborate on the southward extension of the extratropical intrusion.

538 ***4.2 Southward digging of extratropical troughs***

539 To understand the southward digging of the trough, which faces decreased stability over
540 the Indian region, we plot ***Fig.8***. The plot has multiple variables, all ~~are~~ averaged for the days
541 15-17 June 2013 ~~and~~, which are described below: (a) the shading shows the vertical velocity
542 (***w***) with positive shading ~~means~~indicating upward motion, (b) the magenta curve shows the
543 ~~streamlines~~streamlines at 200hPa, (c) blue contours shows the (positive only) relative vorticity
544 at 200hPa, (d) the black contours ~~shows~~show zonal winds at 200hPa (positive values are
545 contoured) (e) the green curve shows the 1 PVU contour. The black contours show that the
546 mean jet is shifted over the Indian region and is highly meandering. This meandering indicates
547 trough intrusion, confirmed by the blue vorticity contour in the northern part of Pakistan and
548 Indian region over Kashmir and Leh-Ladakh region. The jet is pushed southward with the
549 southward extending intensified Rossby wave trough. ~~The two~~Two anticyclones are formed on
550 the southern side of the jetstream, ~~as~~which is evident ~~from~~by the streamlines (magenta color~~),~~
551 ~~and the~~). The deep cyclonic curvature over the northern flank of India shows that the southward
552 extension is deep with an intense Rossby wave trough. The green-coloured 1PVU curve shows

that the Rossby wave did not break over the Indian region during this period as the breaking of the Rossby wave induces higher PV ~~(>2PVU) over the Indian region(below 30°N). The strong amplitude of anomalous relative vorticity (blue contours showing positive only values), southward curvature of zonal winds in the figure~~(~1-2PVU or higher) over the Indian region (below 30°N(Fadnavis and Chattopadhyay, 2017). The strong amplitude of anomalous relative vorticity (blue contours showing positive only values) indicates that the Rossby wave is intense, with no sign of weakening and breaking with jet pushed southward. At the same time, however, there is ~~substantial~~ upward vertical velocity (red shading)) and rainfall (**Fig.4**) over both the central and the north Indian ~~region~~regions. It is interesting to note that the Rossby wave vorticity structure does not directly reach the region where the ~~extreme~~ heavy rainfall event occurred and does not show much tilt in the zonal vertical direction until 600hPa~~.~~ (plot not shown). Hence, none of the above discussions would indicate the rainfall over the Uttarakhand region occurs as ~~an~~the end product of ~~a~~ simple in-situ linear ~~process~~processes such as Rossby ~~wave~~waves or monsoon low pressure~~-~~-induced local convergence (~~refer **Fig.2**~~e.g., the linear part~~). This~~ in **Fig.2**). Can this widespread rainfall ~~can~~ be explained if we assume that the ageostrophic vertical velocity is generated due to a nonlinear conversion process related to downstream amplification associated with baroclinic conversion ~~(Orlanski and Sheldon, 1995)~~(Orlanski and Sheldon, 1995) or a downstream wave-mean interaction or a combination of both over the Uttarakhand region~~.~~? Such nonlinear conversion processes and wave mean

interaction can lead to the conversion of zonal mean to eddy kinetic energy or vice versa and generate ageostrophic vertical velocity.

To highlight the strong vertical velocity and the ageostrophic component, the vertical velocity over a region including ~~the~~ Uttarakhand is plotted in **Fig. 9** as a height ~~-~~-latitude plot**.** The plot clearly shows ~~extreme~~large vertical velocity developing over the Indian region ~~developing as~~. The development of vertical velocity at this scale can be contributed to by two components, one coming from orographically-forced ascent and the other from wave-induced ascent associated with shears (Teixeira, 2014; Cohen and Boos, 2017). As the upper-level flow is ~~getting~~ predominantly westerly and largely baroclinic (i.e~~. ∂~~., $\partial u/\partial z$~~>0)~~>0), having developed from barotropic easterlies (i.e~~.~~., predominantly easterlies at all levels) before 16th June~~. The~~ , the plot shows the development of strong vertical velocity that is associated with strong vertical shear (zonal wind contours). Such shear development would give rise to unstable waves and vertical velocities (contained in the term sg ~~$and\ s'$~~ $sg\ and\ s'$ in eq.4). We also examine (not shown) the bulk Richardson index (the ratio of Brunt Vaisala frequency to vertical shear). ~~The plot shows that~~This index and also **Fig.7d-f** show troposphere above the southern Himalayas ~~is~~ slowly ~~getting~~becomes unstable as the westerly shear zone develops over the slopes~~ of the Himalayas.~~. This generation of ageostrophic vertical velocity also indicates the conversion of mean flow to eddy kinetic energy, as ~~can be seen~~we demonstrate in the next section.

4.3 Transient Eddy Mean Interaction

Fig.10 shows the E-vector divergence ~~of E-vector~~, i.e. $\nabla.(\overrightarrow{E})$ ~~which is~~ $\nabla.(\overrightarrow{E})$ (shaded) and the E-vectors. The mean is defined as the 21-day average from 9th June to 30th June, and the daily transient is defined accordingly as a departure from this mean. Components of E-vectors and the divergence are computed after that. The divergence plot is averaged for the period 14-~~18June2013~~18 June 2013. Divergence is very strong for the period 15-~~17June~~17 June 2013 (not shown). Also, we superimposed the contour of zonal wind averaged during 15-~~17th~~17 June to show the location of the ~~jet stream~~jetstream during this period. The $\nabla.$ E ~~-~~vector shadings indicate that over the Uttarakhand region, $\nabla.$E is positive, and hence the mean flow gains energy (cf. ~~eqn~~equation 1a). The vector plot shows the convergence pattern of the E vector (Ex, Ey). There are two zones of convergence-divergence patterns around 40°N, which are consistent with the locations of blocking ridges (east and west Asian ridges). This transfer of energy is further confirmed from the plot of the $1/2(u'^2 + v'^2)$, ~~i.e.,~~ local transient eddy kinetic energy (EKE~~)~~ given by $1/2(u'^2 + v'^2)$ in **Fig.11**. The black bar plot from ERA5 shows the growth of EKE during that period ~~and~~, which reduces ~~afterwards~~afterward. The growth of EKE ~~can occur from~~ and the ~~extraction of kinetic energy from the jetstream. The growth of EKE~~increased eddy forcing on the mean can lead to an increase in the upper level zonal flow and vertical shear, as shown in **Fig.8**. This can lead to the development of ~~indirect ageostrophic circulation~~vertical velocity over the ~~Uttarakhand~~forcing region ~~in the presence~~(eq.5), and with the appropriate feedback of moisture supply from monsoon

intraseasonal oscillations (**Fig.7**~~)~~), the condition may ~~explain~~then be more favorable for the ~~vigorous~~ development of ~~extreme events~~heavy rainfall episodes over this region. This analysis demonstrates that the wave-mean ~~to eddy conversion~~flow interaction in the presence of moisture can ~~cause the extreme~~create favorable conditions for high-intensity precipitation ~~event~~events, depending on the potential of wave-mean interaction during the intrusion event ~~forcing the zonal wind at the upper level thereby developing shear source in the omega equation(eqn.5) resulting in localized updrafts and extreme rainfall events~~.

5.0 Operational Model Forecast

It is clear from **Fig.1** that the operational models (IITM-ERPAS, UKMO, and the ECMWF have failed to capture the event. Among the three models, ECMWF performs ~~better~~the best. It is natural to evaluate ~~the~~ model performance in the light of the above discussion and see if the relative success or failure is linked to the inability to capture the intrusion or not. The verification of rainfall is plotted in ***Fig. 12.*** The plot shows that all ~~the~~three models underestimated the rain over the Uttarakhand region. IITM-ERPAS shows low-intensity rainfall over the whole of north India~~,~~; the UKMO rainfall shows a high-intensity rainfall blob over the Pakistan region but ~~missing~~has very little over the Uttarakhand region. The ECMWF model, however, shows some success in capturing the rainfall, but it started one day later than the actual event. Thus, rainfall shows a spatial and temporal shift, which could indicate either improper eddy forcing onto the mean flow resulting in improper vertical velocity or improper

moisture transport or a combination of both. The spatial pattern of moisture transport averaged between 500-200hPa is shown in **Fig. 13,** which shows that the models fail to forecast the low pressure-induced moisture transport. Improper moisture transport means the moisture is not available for conversion to rainfall. During 15-~~16June2013~~ 16 June 2013, IITM-ERPAS ~~shows~~has the cyclonic circulation shifted towards the Bay of Bengal, while for UKMO ~~shows~~, it ~~is~~has shifted more towards the Arabian Sea, both missing the Indian landmass~~.~~, which could cause rainfall over the Pakistan region. The ECMWF model shows two anticlockwise cyclonic circulations over the Arabian Sea and the Bay of Bengal during 15-16 June 2013. Finally, we show ~~the~~ $\nabla.(\overrightarrow{E})$ $\nabla.(\overrightarrow{E})$ in **Fig.14** to ~~show~~determine how well the models have forecasted the eddy ~~means~~mean interaction ~~and compare~~by comparing it with the reanalysis data. The top left panel is shown for reanalysis ~~which is like~~, as in **Fig. 10**. The ~~reanalyses~~reanalysis plots show that $\nabla.(\overrightarrow{E})$ $\nabla.(\overrightarrow{E})$ is positive (red shading) over the Uttarakhand and Kashmir ~~region~~regions, implying acceleration of the zonal mean wind. The hindcast from the models ~~show~~shows weaker E~~-~~-vector divergence (red shades) over the Uttarakhand region. Hence, the plot indicates that the eddy E-vector convergence and divergence are not ~~appropriate~~correctly simulated in the model forecasts over the Uttarakhand region, which is also indicated by the yellow vectors (Ex, Ey~~) in yellow shadings.~~). Also, the isotachs are much less dense with ~~lesser~~a less wavy and intruding pattern over Kashmir, Uttarakhand, and Punjab ~~region~~ (between 25°-35°N and 70°-80°E) in the model than the ~~observation~~reanalysis over the Indian region, implying that the mean flow is also not ~~proper~~correctly simulated in the model. Thus,

the location of eddy-transient forcing is also not ~~appropriate~~correctly simulated in the model. ~~Also, the vector shows weaker amplitude of E-vector divergence in the extratropical region north of 30N, implying inappropriate (lower amplitude) eddy transport in the northern extratropics.~~ Due to inappropriate eddy forcing, the zonal wind height longitude profile also does not show the development of appropriate zonal wind acceleration at the upper level (not shown). Inappropriate zonal wind acceleration at the upper-level ~~weekend~~weakened the vertical shear, thus weakening the ~~Sutcliff~~Sutcliffe term in ~~eqn~~equation (5), indicating weaker ageostrophic vertical velocity, resulting in reduced precipitation amplitude. The result ~~thus suggest~~, therefore, suggests that the model did not capture the Uttarakhand event because of inappropriate moisture transport from the monsoon flow and forecast of the wrong location of eddy transport leading to ~~the~~a spatial phase shift of eddy flux divergence ~~and~~(north and south of Uttarakhand region), resulting in improper eddy forcing over the Uttarakhand region. This is also confirmed from the eddy kinetic energy (EKE) plot in **Fig.11**, which shows EKE plots for the model forecasts. From ~~**fig**~~**Fig.11**, it may be ~~noted~~seen that the ECMWF~~, though,~~ model captured this time sequence of EKE evolution more effectively ~~compared to~~than either the IITM-ERPAS ~~and~~or the UKMO ~~model~~models. Thus, the analysis suggests that inappropriate eddy forcing and improper representation of EKE in the model could be a reason for erroneous rainfall forecast in the model.

6.0 Discussion and Conclusion

This case study examines the life cycle of the extratropical intrusion event over Uttarakhand (India) during June 2013 to understand the role of anisotropic shape, meridional propagation of extratropical eddies, and their feedback onto the monsoon mean flow during the 2013 Uttarakhand ~~extreme~~ event. Previous studies of extreme events such as those over the Uttarakhand region during June 2013 neglect the role of eddy-mean interaction in the monsoonal region**.** The study reveals a potential role of underlying eddy dynamics and the inadequacy in the operational forecast models to capture the eddy dynamics. The E-vector-based approach that is adopted here gives a first-hand idea about the eddy forcing mechanism, both in the observation and in the model forecast for the 2013 Uttarakhand ~~extreme~~heavy rainfall event.

On the synoptic scale, extratropical Rossby wave intrusion influenced the ~~2013~~ June 2013 heavy rainfall event over the Uttarakhand ~~extreme event~~region through the southward extension of troughs and associated southward shift in the subtropical jet pattern. Such synergistic evolutions are documented earlier also ~~(Raman and Rao, 1981; Kalshetti *et al.*, 2021)~~(Raman and Rao, 1981; Kalshetti *et al.*, 2021). At a local scale, along with western Himalayan orography and moisture convergence associated with monsoon lows during this time, the upper-level extratropical trough intrusion imparted a strong eddy forcing, which is evident through the existence of E-vector divergence (**Fig. 10**) and the conversion of mean

kinetic energy to eddy kinetic energy (**Fig.11**). Thus, on 16-17 June, upper-level eddy forcing accelerated the eddy circulation dynamics~~,~~ and developed an additional shear flow that leads to the ~~extreme~~high-intensity rainfall event by ~~amplification of~~amplifying the Sutcliff source term~~(eqn 5).~~ (equation 5). In some locations, the mesoscale circulation can develop through feedback from the large-scale flow. It can lead to cloudburst-type situations by forming a super-convective system, as discussed in Houze et al. (2000). However, we have not focused on this large scale to mesoscale connection in this study as we emphasized the quantification of eddy forcing. The current analysis, unlike earlier studies, differentiates the eddy and ~~means~~mean flow over the monsoonal region during this period. Our analysis only assumes the mean flow and background instability associated with extratropical modes and does not assume tropical depressions as a precondition. During the intrusion event, if there is background instability (which can be provided by eddies of extratropical origin), wave-mean interaction can develop ageostrophic velocity leading to ~~extreme~~high-intensity rainfall events.

~~The above explanation based on the E-vector approach is then verified in operational model forecasts. Result suggests that ECMWF, ERPAS, and UKMO simulated upper-level circulation patterns, but E-vector divergent field and their impact on underlying atmospheric states seems to be not in order. E-vector divergence and local eddy kinetic energy is captured in varying degrees of~~The analysis presented here is based on a single extreme event. Does every extreme event over the north Indian region require extratropical intrusion? It is found that high-intensity rainfall events over northern India (along the Himalayan belt and adjoining

foothills and plains) can occur in the absence of extratropical eddy forcing. Extreme events can occur purely due to monsoon flow over the Indian region and are common during monsoon season over different areas of India. Is there any apparent difference in the spatial pattern of rainfall when an extratropical intrusion occurs? We have checked for two situations when the standardized anomaly of rainfall over the north Indian region (area averaged over a box of 25°-40°N & 65°-90°E) is more than two standard deviations (i.e., the rainfall is high intensity). In the first situation, we computed rainfall, 200-hPa wind vectors, and eddy flux divergence composites in the presence of strong low frequency southward EMF transfer, and in the second situation, when there is negligible EMF transfer. The low-frequency eddy transfer band is defined by taking a 30-60 day filtered EMF index (F_L) area averaged over a box (30°-45°N & 70°-95°E) which is then standardized. Strong southward transfer cases are selected by identifying days when the standardized anomaly is less than -1. This plot is shown in **Fig.15.** The figure compares the rainfall, wind vector at 200hPa, the divergence of E vector, and E-vector components for the two extreme rainfall scenarios: with or without eddy forcing. The composite is based on 24 selected cases. The plot shows that there are indeed certain regions in the Himalayas and the foothills of the Himalayas, starting from Uttarakhand and extending towards the east, where high-intensity rainfall occurs when there is southward momentum transfer (**Fig.15a**). High-intensity precipitation also occurs when there is negligible eddy transfer (**Fig.15b**). The rainfall bias plot (**Fig.15c**) in the last row shows a positive rainfall anomaly in Uttarakhand. Although there are regional variations, many locations over the

foothills of the Himalayas in the eastern side of Uttarakhand show positive rainfall anomalies. The wind vector plot shows that the cyclone-anticyclone pattern is much closer and stronger over the north Indian region in the strong low-frequency eddy transfer case. The E-vector and its divergence $\nabla.(\overrightarrow{E})$ are shown for the two corresponding scenarios in **Fig.15d** and **Fig.15e**. Strong positive values of $\nabla.(\overrightarrow{E})$ indicate substantial divergence in the low-frequency band and strong forcing on the zonal wind over the Indian region (in the Kashmir region). The bias plot for divergence in **Fig.15(f)** also shows that these extreme events associated with momentum flux transfer require strong E-vector divergence above the Kashmir region. Although we have highlighted the role of EMF and its southward transfer in the low-frequency mode only, all E-vector components can generate extreme events. A detailed analysis for all the bands is required to understand the full implications and it will be reported in a later study. Our initial results based on a case study and a composite analysis in the low-frequency band suggests the usefulness of the E-vector approach in understanding extratropical intrusion event.

The above explanation, based on the E-vector approach, was then verified in operational model forecasts. Results suggest that ECMWF, ERPAS, and UKMO operational models simulated upper-level circulation patterns but that the E-vector divergent field and their impact on underlying atmospheric states were not correctly simulated. E-vector divergence and local eddy kinetic energy are captured with varying accuracy, suggesting improper eddy forcing in S2S forecast models. Also, the moisture transport in the upper level is also not captured adequately (**Fig.13**). Thus, inappropriate eddy forcing leads to ~~inappropriate~~improper

ageostrophic and mean flow adjustment in the forecast, and inappropriate moisture transport weakens ~~the support of~~ moisture support, leading to a lack ~~in~~of skill in the model forecast. Although previous analyses provided a description of the event as a Rossby wave intrusion process, the exact role of Rossby wave dynamics and the eddy-mean interaction was not very clear. Our analysis uncovers a series of dynamic steps to understand the reason ~~on~~ why the rainfall is underestimated in operational models during the Uttarakhand ~~extreme~~heavy rainfall event. Our ~~analysis~~study also provides a diagnostic basis for evaluating the model skill using the E-vector approach and can be used for model skill evaluation.

Acknowledgments

MK acknowledges ~~PhD~~Ph.D. research fellowship from the Indian Institute of Tropical Meteorology, Pune (IITM), an autonomous Institute under the Ministry of Earth Sciences, Govt. of India. The authors acknowledge the research and funding support from IITM and India Meteorological Department(IMD). All the computations and plots are carried out using the freely available NCL-NCAR software and XmGRACE. The forecast data for the UKMO and ECMWF models are downloaded from the S2S project website hosted by ECMWF (https://apps.ecmwf.int/datasets/data/s2s/levtype=sfc/type=cf/). S2S, a sub-seasonal to seasonal prediction project, is a WWRP/THORPEX-WCRP joint research project established to improve forecast skill and understanding on the sub-seasonal to seasonal time scale and promote its uptake by operational ~~centres~~centers and exploitation by the applications

community. IITM CFS model extended forecast runs are available in the IITM data server and would be made available on request (https://www.tropmet.res.in/monsoon/). ~~KH~~KMRH is funded through Weather and Climate Science for Service Partnership (WCSSP) India, a collaborative initiative between the Met Office, supported by the UK Government's Newton Fund, and the Indian Ministry of Earth Sciences (MoES). ~~Authors~~The authors would like to acknowledge Dr. Gill Martin, UKMO, Program Manager Indo-UK WCSSP India project (UK side~~))~~, for providing detailed comments and suggestions in this version of the manuscript.

References

Abhilash S, Sahai AK, Pattnaik S, Goswami BN, Kumar A. 2014. Extended range prediction of active-break spells of Indian summer monsoon rainfall using an ensemble prediction system in NCEP Climate Forecast System. *International Journal of Climatology*, 34(1): 98–113. https://doi.org/10.1002/joc.3668.

Andrews DG, McIntyre ME. 1976. Planetary Waves in Horizontal and Vertical Shear: The Generalized Eliassen-Palm Relation and the Mean Zonal Acceleration. *Journal of the Atmospheric Sciences*, 33(11): 2031–2048. https://doi.org/10.1175/1520-0469(1976)033<2031:PWIHAV>2.0.CO;2.

Bohlinger P, Sorteberg A, Liu C, Rasmussen R, Sodemann H, Ogawa F. 2019. Multiscale characteristics of an extreme precipitation event over Nepal. *Quarterly Journal of the Royal Meteorological Society*. John Wiley & Sons, Ltd, 145(718): 179–196. https://doi.org/10.1002/qj.3418.

Charney JG. 1969. A Further Note on Large-Scale Motions in the Tropics. *Journal of Atmospheric Sciences*. American Meteorological Society: Boston MA, USA, 26(1): 182–185. https://doi.org/10.1175/1520-0469(1969)026<0182:AFNOLS>2.0.CO;2.

Chevuturi A, Dimri AP. 2016. Investigation of Uttarakhand (India) disaster-2013 using weather research and forecasting model. *Natural Hazards*. Springer Netherlands, 82(3): 1703–1726. https://doi.org/10.1007/s11069-016-2264-6.

Cohen NY, Boos WR. 2017. The influence of orographic Rossby and gravity waves on rainfall. *Quarterly Journal of the Royal Meteorological Society*. John Wiley & Sons, Ltd, 143(703): 845–851. https://doi.org/10.1002/qj.2969.

Dube A, Ashrit R, Ashish A, Sharma K, Iyengar GR, Rajagopal EN, Basu S. 2014. Forecasting the heavy rainfall during Himalayan flooding-June 2013. *Weather and Climate Extremes*. Elsevier, 4(June 2013): 22–34. https://doi.org/10.1016/j.wace.2014.03.004.

Edmon HJ, Hoskins BJ, McIntyre ME. 1980. Eliassen-Palm Cross Sections for the Troposphere. *Journal of the Atmospheric Sciences*. American Meteorological Society, 37(12): 2600–2616. https://doi.org/10.1175/1520-0469(1980)037<2600:EPCSFT>2.0.CO;2.

Fadnavis S, Chattopadhyay R. 2017. Linkages of ~~subtropical stratospheric intraseasonal intrusions~~Subtropical Stratospheric Intraseasonal Intrusions with Indian ~~summer monsoon deficit rainfall~~Summer Monsoon Deficit Rainfall. *Journal of Climate*, 30(13): 5083–5095. https://doi.org/10.1175/JCLI-D-16-0463.1.

G. Branstator. 1995. Organization of storm track anomalies by recurring low-frequency circulation anomalies. , 52: 207–226.

Goswami BN. 2012. South Asian monsoon. *Intraseasonal Variability in the Atmosphere-Ocean Climate System*. Springer, Berlin, Heidelberg, 21–71.

Hanley D, Molinari J, Keyser D. 2001. A Composite Study of the Interactions between Tropical Cyclones and Upper-Tropospheric Troughs. *Monthly Weather Review*. American Meteorological Society: Boston MA, USA, 129(10): 2570–2584. https://doi.org/10.1175/1520-0493(2001)129<2570:ACSOTI>2.0.CO;2.

Held IM, Phillips PJ. 1989. A Barotropic Model of the Interaction between the Hadley Cell and a Rossby Wave. *Journal of the Atmospheric Sciences*, 47(7): 856–869. https://doi.org/10.1175/1520-0469(1990)047<0856:ABMOTI>2.0.CO;2.

Hersbach H, Bell B, Berrisford P, Hirahara S, Horányi A, Muñoz-Sabater J, Nicolas J, Peubey C, Radu R, Schepers D, Simmons A, Soci C, Abdalla S, Abellan X, Balsamo G, Bechtold P, Biavati G, Bidlot J, Bonavita M, De Chiara G, Dahlgren P, Dee D, Diamantakis M, Dragani R, Flemming J, Forbes R, Fuentes M, Geer A, Haimberger L, Healy S, Hogan RJ, Hólm E, Janisková M, Keeley S, Laloyaux P, Lopez P, Lupu C, Radnoti G, de Rosnay P, Rozum I, Vamborg F, Villaume S, Thépaut ~~JN, Huffman GJ, Adler RF, Bolvin DT, Gu G, Nelkin EJ, Bowman KP, Hong Y, Stocker EF, Wolff DB.~~J-N. 2020. The ERA5 global reanalysis. *Quarterly Journal of ~~Hydrometeorology~~the Royal Meteorological Society*. John Wiley & Sons, Ltd, 146(~~1~~730): 1999–2049. https://doi.org/10.~~1175/JHM560.1~~1002/qj.3803.

Homeyer CR, Bowman KP. 2013. Rossby Wave Breaking and Transport between the Tropics and Extratropics above the Subtropical Jet. *Journal of the Atmospheric Sciences*. American Meteorological Society: Boston MA, USA, 70(2): 607–626. https://doi.org/10.1175/JAS-D-12-0198.1.

Hong CC, Hsu HH, Lin NH, Chiu H. 2011. Roles of European blocking and tropical - extratropical interaction in the 2010 Pakistan flooding. , 38(May): 1–6. https://doi.org/10.1029/2011GL047583.

Hoskins B. 1997. A potential vorticity view of synoptic development. *Meteorological Applications*. John Wiley & Sons, Ltd, 4(4): 325–334. https://doi.org/10.1017/S1350482797000716.

Hoskins BJ. 1982. The Mathematical Theory of Frontogenesis. *Annual Review of Fluid Mechanics*. Annual Reviews, 14(1): 131–151. https://doi.org/10.1146/annurev.fl.14.010182.001023.

Hoskins BJ, James IN, White GH. 1983. The Shape, Propagation and Mean-Flow Interaction of Large-Scale Weather Systems. *Journal of the Atmospheric Sciences*. American Meteorological Society: Boston MA, USA, 40(7): 1595–1612. https://doi.org/10.1175/1520-0469(1983)040<1595:TSPAMF>2.0.CO;2.

Hoskins BJ, Karoly DJ. 1981. The Steady Linear Response of a Spherical Atmosphere to Thermal and Orographic Forcing. *Journal of the Atmospheric Sciences*, 38(6): 1179–1196. https://doi.org/10.1175/1520-0469(1981)038<1179:TSLROA>2.0.CO;2.

Houze RA, Chen SS, Kingsmill DE, Serra Y, Yuter SE. 2000. Convection over the Pacific Warm Pool in relation to the Atmospheric Kelvin-Rossby Wave. *Journal of the Atmospheric Sciences*. American Meteorological Society: Boston MA, USA, 57(18): 3058–3089. https://doi.org/10.1175/1520-0469(2000)057<3058:COTPWP>2.0.CO;2.

Huffman GJ, Adler RF, Bolvin DT, Gu G, Nelkin EJ, Bowman KP, Hong Y, Stocker EF, Wolff DB. 2007. The TRMM Multisatellite Precipitation Analysis (TMPA): Quasi-global, multiyear, combined-sensor precipitation estimates at fine scales. *Journal of Hydrometeorology*, 8(1): 38–55. https://doi.org/10.1175/JHM560.1.

Hunt KMR, Turner AG, Schiemann RKH. 2021. How Interactions between Tropical Depressions and Western Disturbances Affect Heavy Precipitation in South Asia. *Monthly Weather Review*. American

Meteorological Society: Boston MA, USA, 149(6): 1801–1825. https://doi.org/10.1175/MWR-D-20-0373.1.

Hunt KMR, Turner AG, Shaffrey LC. 2018a. The evolution, seasonality and impacts of western disturbances. *Quarterly Journal of the Royal Meteorological Society*, 144(710): 278–290. https://doi.org/10.1002/qj.3200.

Hunt KMR, Turner AG, Shaffrey LC. 2018b. Extreme Daily Rainfall in Pakistan and North India: Scale Interactions, Mechanisms, and Precursors. *Monthly Weather Review*, 146(4): 1005–1022. https://doi.org/10.1175/MWR-D-17-0258.1.

James IN. 1994. *Introduction to Circulating Atmospheres*. *Cambridge Atmospheric and Space Science Series*. Cambridge University Press: Cambridge.

Jin F-F. 2010. Eddy-Induced Instability for Low-Frequency Variability. *Journal of the Atmospheric Sciences*. American Meteorological Society: Boston MA, USA, 67(6): 1947–1964. https://doi.org/10.1175/2009JAS3185.1.

Joseph S, Sahai AK, Sharmila S, Abhilash S, Borah N, Chattopadhyay R, Pillai PA, Rajeevan M, Kumar A. 2015. North Indian heavy rainfall event during June 2013: diagnostics and extended range prediction. *Climate Dynamics*, 44(7–8): 2049–2065. https://doi.org/10.1007/s00382-014-2291-5.

Kalshetti M, Chattopadhyay R, Phani R, Joseph S, Sahai AK. 2020. Climatological patterns of subseasonal eddy flux transfer based on the co-spectral analysis over the Indian region and the derivation of an index of eddy transfer for operational tracking. *International Journal of Climatology*. John Wiley & Sons, Ltd, 41 (Suppl. 1)(n/a): E1906–E1925. https://doi.org/10.1002/joc.6821.

Kalshetti M, Chattopadhyay R, Phani R, Joseph S, Sahai AK. 2021. Climatological patterns of subseasonal eddy flux transfer based on the <scp>co-spectral</scp> analysis over the Indian region and the derivation of an index of eddy transfer for operational tracking. *International Journal of Climatology*, 41(S1): E1906–E1925. https://doi.org/10.1002/joc.6821.

Karoly DJ, Hoskins BJ. 1982. Three Dimensional Propagation of Planetary Waves. *Journal of the Meteorological Society of Japan. Ser. II*, 60(1): 109–123. https://doi.org/10.2151/jmsj1965.60.1_109.

Kaur S, Gupta PK. 2017. Devastating rainstorm of June-2013 in Uttarakhand. *Mausam*, 68(4): 633–642.

Kiladis GN. 1998. Observations of Rossby Waves Linked to Convection over the Eastern Tropical Pacific. *Journal of the Atmospheric Sciences*. American Meteorological Society: Boston MA, USA, 55(3): 321–339. https://doi.org/10.1175/1520-0469(1998)055<0321:OORWLT>2.0.CO;2.

Krishnan R, Kumar V, Sugi M, Yoshimura J. 2009. Internal Feedbacks from Monsoon–Midlatitude Interactions during Droughts in the Indian Summer Monsoon. *Journal of the Atmospheric Sciences*, 66(3): 553–578. https://doi.org/10.1175/2008JAS2723.1.

Lackmann G. 2012. *Midlatitude Synoptic Meteorology Dynamics, Analysis, and Forecasting*. American Meteorological Society: Boston (US).

Lau N-C. 1979. The Structure and Energetics of Transient Disturbances in the Northern Hemisphere Wintertime Circulation. *Journal of Atmospheric Sciences*. American Meteorological Society: Boston MA, USA, 36(6): 982–995. https://doi.org/10.1175/1520-0469(1979)036<0982:TSAEOT>2.0.CO;2.

Lau N-C, Holopainen EO. 1984. Transient Eddy Forcing of the Time-Mean Flow as Identified by Geopotential Tendencies. *Journal of the Atmospheric Sciences*, 41(3): 313–328. https://doi.org/10.1175/1520-0469(1984)041<0313:TEFOTT>2.0.CO;2.

Lau WKM, Kim K-M. 2011. The 2010 Pakistan Flood and Russian Heat Wave: Teleconnection of Hydrometeorological Extremes. *Journal of Hydrometeorology*, 13(1): 392–403. https://doi.org/10.1175/jhm-d-11-016.1.

Leroux S, Hall NMJ, Kiladis GN. 2010. A climatological study of transient-mean-flow interactions over West Africa. *Quarterly Journal of the Royal Meteorological Society*, 136(SUPPL. 1): 397–410. https://doi.org/10.1002/qj.474.

Lillo SP, Parsons DB. 2017. Investigating the dynamics of error growth in ECMWF medium-range forecast busts. *Quarterly Journal of the Royal Meteorological Society*. John Wiley & Sons, Ltd, 143(704): 1211–1226. https://doi.org/10.1002/qj.2938.

Novak L, Ambaum MHP, Tailleux R. 2015. The life cycle of the North Atlantic storm track. *Journal of the Atmospheric Sciences*, 72(2): 821–833. https://doi.org/10.1175/JAS-D-14-0082.1.

Orlanski I, Sheldon JP. 1995. Stages in the energetics of baroclinic systems. *Tellus A: Dynamic Meteorology and Oceanography*. Taylor & Francis, 47(5): 605–628. https://doi.org/10.3402/tellusa.v47i5.11553.

Parida BR, Behera SN, Bakimchandra O, Pandey AC, Singh N. 2017. Evaluation of satellite-derived rainfall estimates for an extreme rainfall event over Uttarakhand, Western Himalayas. *Hydrology*, 4(2): 1–18. https://doi.org/10.3390/hydrology4020022.

Parsons DB, Lillo SP, Rattray CP, Bechtold P, Rodwell MJ, Bruce CM. 2019. The Role of Continental Mesoscale Convective Systems in Forecast Busts within Global Weather Prediction Systems. *Atmosphere*, 10(11). https://doi.org/10.3390/atmos10110681.

Pattanaik DR, Pai DS, Mukhopadhyay B. 2015. Rapid northward progress of monsoon over India and associated heavy rainfall over Uttarakhand: A diagnostic study and real time extended range forecast. *Mausam*, 66(3): 551–568.

Raman CR V, Rao YP. 1981. Blocking highs over Asia and monsoon droughts over India. *Nature*. Nature Publishing Group, 289: 271.

~~RAMASWAMY~~Ramaswamy C. 1962. Breaks in the Indian summer monsoon as a phenomenon of interaction between the easterly and the sub-tropical westerly jet streams. *Tellus*. Taylor & Francis, 14(3): 337–349. https://doi.org/10.~~1111/j.2153-3490.1962.tb01346.x~~3402/tellusa.v14i3.9560.

Sahai AK, Chattopadhyay R, Joseph S, Krishna PM, Pattanaik DR, Abhilash S. 2019. Chapter 20 - Seamless Prediction of Monsoon Onset and Active/Break Phases. In: Robertson AW and Vitart F (eds) *Sub-Seasonal to Seasonal Prediction*. Elsevier, 421–438.

Singh C, Chand R. 2015. Exceptionally heavy rainfall over Uttarakhand during 15-18 June, 2013 - A case study. *Mausam*, 66(4): 741–750.

Sooraj K, Terray P, Shilin A, Mujumdar M. 2020. Dynamics of rainfall extremes over India: A new perspective. *International Journal of Climatology*, (February): joc.6516. https://doi.org/10.1002/joc.6516.

Tan G-R, Jin F-F, Ren H-L, Sun Z-B. 2014. The role of eddy feedback in the excitation of the NAO. *Meteorological Applications*. John Wiley & Sons, Ltd, 21(3): 768–776. https://doi.org/10.1002/met.1415.

Teixeira MAC. 2014. The physics of orographic gravity wave drag. *Frontiers in Physics*, 2: 43. https://doi.org/10.3389/fphy.2014.00043.

Trenberth KE. 1986. An Assessment of the Impact of Transient Eddies on the Zonal Flow during a Blocking Episode Using Localized Eliassen-Palm Flux Diagnostics. *Journal of the Atmospheric Sciences*, 43(19): 2070–2087. https://doi.org/10.1175/1520-0469(1986)043<2070:AAOTIO>2.0.CO;2.

~~Trenberth KE. 2002. An Assessment of the Impact of Transient Eddies on the Zonal Flow during a Blocking Episode Using Localized Eliassen-Palm Flux Diagnostics. *Journal of the Atmospheric Sciences*, 2070–2087.~~

Trenberth KE, Fasullo JT. 2012. Climate extremes and climate change: The Russian heat wave and other climate extremes of 2010. *Journal of Geophysical Research: Atmospheres*. John Wiley & Sons, Ltd, 117(D17). https://doi.org/10.1029/2012JD018020.

Uccellini LW, Johnson DR. 1979. The Coupling of Upper and Lower Tropospheric Jet Streaks and Implications for the Development of Severe Convective Storms. *Monthly Weather Review*, 107(6): 682–703. https://doi.org/10.1175/1520-0493(1979)107<0682:TCOUAL>2.0.CO;2.

Vellore RK, Jayant RK. 2014. On the anomalous precipitation enhancement over the Himalayan foothills during monsoon breaks. , 2009–2031. https://doi.org/10.1007/s00382-013-2024-1.

Vellore RK, Kaplan ML, Krishnan R, Lewis JM, Sabade S, Deshpande N, Singh BB, Madhura RK, Rama Rao MVS. 2016a. Monsoon-extratropical circulation interactions in Himalayan extreme rainfall. *Climate Dynamics*. Springer Berlin Heidelberg, 46(11–12): 3517–3546. https://doi.org/10.1007/s00382-015-2784-x.

Vellore RK, Kaplan ML, Krishnan R, Lewis JM, Sabade S, Deshpande N, Singh BB, Madhura RK, Rama Rao MVS. 2016b. Monsoon-extratropical circulation interactions in Himalayan extreme rainfall. *Climate Dynamics*, 46(11): 3517–3546. https://doi.org/10.1007/s00382-015-2784-x.

Vitart F, Ardilouze C, Bonet A, Brookshaw A, Chen M, Codorean C, Déqué M, Ferranti L, Fucile E, Fuentes M, Hendon H, Hodgson J, Kang HS, Kumar A, Lin H, Liu G, Liu X, Malguzzi P, Mallas I, Manoussakis M, Mastrangelo D, MacLachlan C, McLean P, Minami A, Mladek R, Nakazawa T, Najm S, Nie Y, Rixen M, Robertson AW, Ruti P, Sun C, Takaya Y, Tolstykh M, Venuti F, Waliser D, Woolnough S, Wu T, Won DJ, Xiao H, Zaripov R, Zhang L. 2017. The subseasonal to seasonal (S2S) prediction project database. *Bulletin of the American Meteorological Society*, 98(1): 163–173. https://doi.org/10.1175/BAMS-D-16-0017.1.

Waterman S, Hoskins BJ. 2013. Eddy Shape, Orientation, Propagation, and Mean Flow Feedback in Western Boundary Current Jets. *Journal of Physical Oceanography*. American Meteorological Society: Boston MA, USA, 43(8): 1666–1690. https://doi.org/10.1175/JPO-D-12-0152.1.

Webster PJ, Holton JR. 1982. Cross-Equatorial Response to Middle-Latitude Forcing in a Zonally Varying Basic State. *Journal of Atmospheric Sciences*. American Meteorological Society: Boston MA, USA, 39(4): 722–733. https://doi.org/10.1175/1520-0469(1982)039<0722:CERTML>2.0.CO;2.

970 Williams RG, Wilson C, Hughes CW. 2007. Ocean and Atmosphere Storm Tracks: The Role of Eddy
971 Vorticity Forcing. *Journal of Physical Oceanography*. American Meteorological Society: Boston MA,
972 USA, 37(9): 2267–2289. https://doi.org/10.1175/JPO3120.1.

973 Wills RCJ, Schneider T. 2018. Mechanisms Setting the Strength of Orographic Rossby Waves across a
974 Wide Range of Climates in a Moist Idealized GCM. *Journal of Climate*. American Meteorological
975 Society: Boston MA, USA, 31(18): 7679–7700. https://doi.org/10.1175/JCLI-D-17-0700.1.

977 *6.0 **Table***

978 **Table 1 The important configuration of three S2S operational models used in the**
979 **study. The range stands for forecast lead time in days, resolution represented in**
980 **degrees of latitude versus longitude; letter "L" stands for vertical resolution, ens**
981 **size for ensemble size of the run, frequency of forecast suggests operational run**
982 **scheduled, forecast are past run using output from the actual forecast for**
983 **calibration purpose, ocean, and ice coupled through their respect to the**

Model	Range	Resolution	Frequency	Ens Size	Reforeca	
					Frequency	Period
ERPAS: Extended Range Prediction For Application to Society	Days 0-33	T382 & T126, L64	Weekly	16	On the fly	2003-201
UKMO: United Kingdom Meteorological Office	Days 0-60	~0.5° × 0.8°, L85	Weekly	4	On the fly	1996-200
EMWF: European Centre for Medium-range Weather Forecasts	Days 0-46	0.25° × 0.25° days 0-10 0.5° × 0.5° After day 10, L85	Twice in week	51	On the fly	Last 20 ye

984 **dynamical core.**

985

986

Graphical Abstract

Eddy transport, Wave-mean flow interaction, and Eddy forcing during the 2013 Uttarakhand Extreme Event in the Reanalysis and S2S Retrospective Forecast Data

Mahesh Kalshetti[1,3], Rajib Chattopadhyay[1,2], Kieran M R Hunt[4], R Phani[1], Susmitha Joseph[1], DR Pattanaik[2], AK Sahai[1]

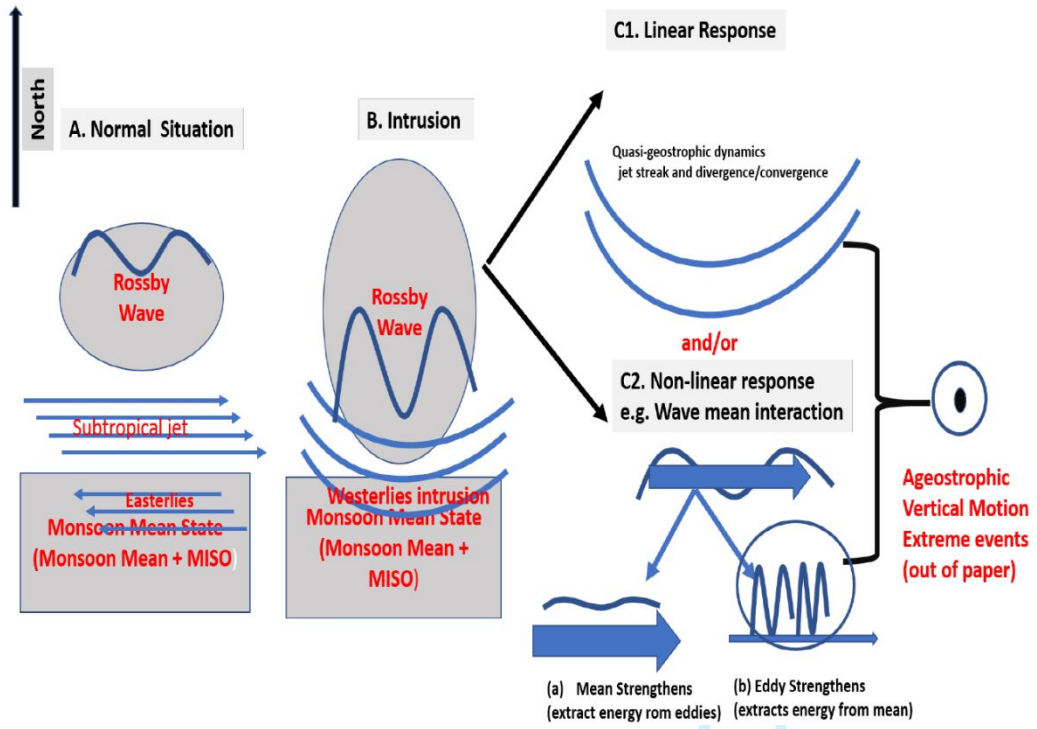

Keywords

Extreme events; Extratropical-Tropical teleconnection; Indian monsoon, S2S subseasonal forecasts.

Caption: The study proposes a diagnostic framework using E-vectors to analyze and understand the extratropical transient eddy forcing over Indian Region during the monsoon season. The framework can be used both in observation/reanalysis data and operational forecast models. The analysis is based on a case study of the 2013 Uttarakhand (India) extreme rainfall event over the Himalayan region. The study indicates that the transient eddy forcing can force extreme rainfall events in addition to other forcings.